NASA CR-159,210

3 1176 00162 2738

NASA Contractor Report 159210

FOR REFERENCE

NASA-CR-159210
1980 0017894

Advanced Risk Assessment of the Effects of Graphite Fibers on Electronic and Electric Equipment

L. Pocinki, M. Cornell and
L. Kaplan

ORI, Inc.

JUN 17 1980

CONTRACT NAS1-15379
MAY 1980

NASA
National Aeronautics and
Space Administration

Langley Research Center
Hampton, Virginia 23665

PREFACE

This report summarizes the work performed by a team of ORI scientific staff members who are recognized as authors of the report. In addition, Messrs. Fred Zusman and Ralph Ottey made significant contributions to the effort in the development of the computer model; they were ably assisted by Ms. Elizabeth Battino.

The authors wish to recognize Israel Taback of Bionetics Corporation for his contributions to all aspects of the work.

We also wish to thank the Project Officers, Dr. Wolf Elber and Mr. Robert J. Huston, of the National Aeronautics and Space Administration, Langley Research Center, for their interest and suggestions during the course of this work.

N80-26393 #

EXECUTIVE SUMMARY

BACKGROUND

Carbon fibers bonded in epoxy constitute one of today's "miracle" structural materials. For particular applications structural components can be designed with great strength, while being considerably lighter than the conventional parts they replace. Carbon fiber composite material has been used to date in sporting goods and military aircraft primarily. Limited near-term use in civil aircraft is expected to grow considerably in the future. The material is also expected to be used in automobiles. In view of the many potential applications of carbon-fiber composites considerable concern was engendered as the result of evidence that individual fiber segments could cause electrical and electronic equipment to fail under certain operating conditions. Such individual fiber segments could be released, for example, in a fire involving the composite material. As a result of this concern a national multi-agency program was established under the aegis of the Office of Science and Technology Policy. In this program the National Aeronautics and Space Administration was assigned the responsibility of examing the risk due to possible accidents and fire involving civil aircraft, with carbon fiber composite structural components.

The scenario envisaged in the NASA-funded ORI investigation is:

- A commercial jet aircraft in an accident with fire leading to ...

- Release of substantial numbers of individual carbon fiber segments which ...
- Are carried far from the accident scene by prevailing winds and ...
- Enter buildings and parked aircraft in their path causing ...
- Failures of electrical and electronic equipment resulting in ..
- Economic impact

In order to examine the potential magnitude of the omerall effect ORI, Inc developed a computer simulation model which replicates these events as far as possible. In its final Phase I Report, published in May 1979 ORI described its initial modeling effort and presented the results obtained from a large number of simulation runs for nine major airports in the United States, using the best estimates available for all required input data. The airport results were combined statistically to obtain an estimate of the total national risk.

In Phase II the ORI airport risk assessment model was extended in several respects, principally to increase the variance -- i.e. improve the likelihood that extreme values would be generated. Additional experimental data made available by other NASA-sponsored efforts were used in the new calculations. A new national risk model was developed; it was designed to be more useful for estimating the statistical confidence that can be assigned to the results. An essentially independent study was mounted to assess the risk to the electric power distribution system.

SINGLE AIRPORT RISK ASSESSMENT

Method

The method used to estimate the risk associated with accidents involving aircraft with carbon fiber composite structural components is essentially a Monte Carlo simulation model. The method requires the generation of many aircraft accidents, with variables used in the calculation drawn at random from defined probability instructions. The impact of each accident is calculated and saved; after many accidents have been simulated the model computes several statistical measures from the results of all the accidents. The method is illustrated schematically in Figure 1.

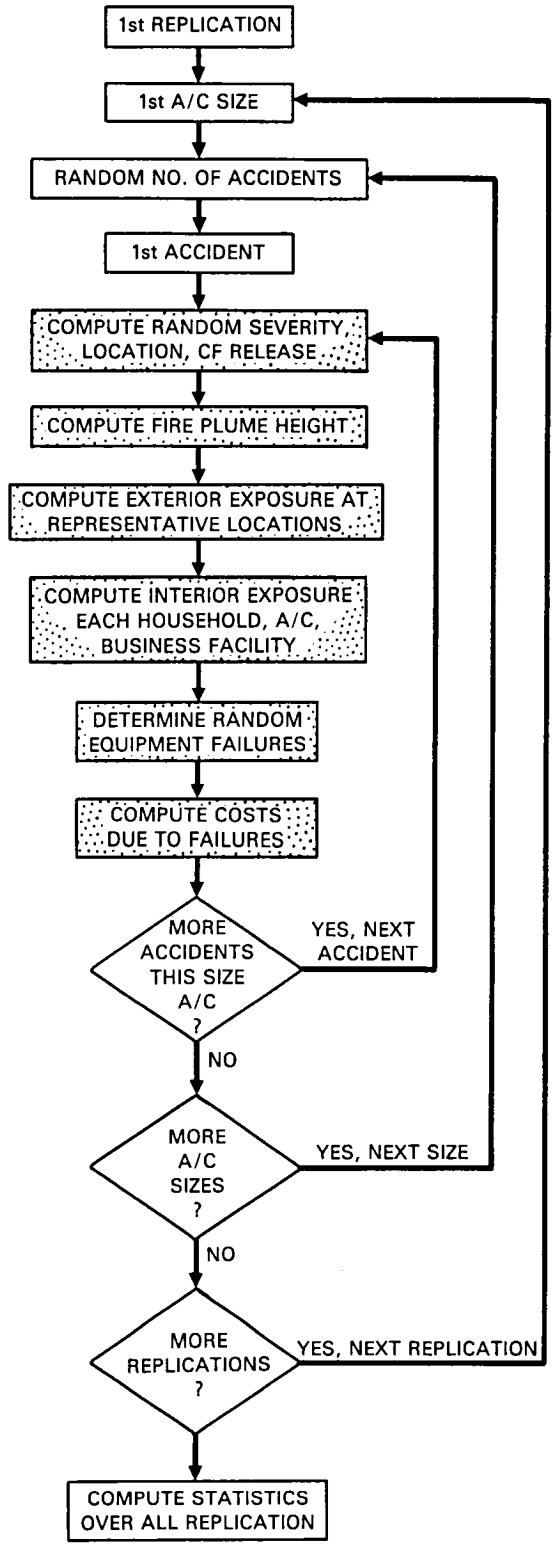

FIGURE 1. SCHEMATIC REPRESENTATION OF ORI AIRPORT CF RISK ASSESSMENT MODEL. SHADED BOXES REPRESENT SINGLE ACCIDENT SCENARIO.

The principal elements or submodels in the improved ORI Phase II Risk Assessment Model are:

- Random accident generation. For each replication, comprising a year's accidents, the model first determines, using appropriate stochastic methods, the actual number of accidents for each size aircraft. The mean annual fire-accident rate is based on the analysis of historical accident data conducted by the major airframers. This submodel makes use of aircraft manufacturers' projections of increased use of carbon fiber composite material in individual aircraft, and the changes in the fleet mix between now and 1993, the target year for the risk assessment. The airframers also prepared a detailed analysis of historical jet aircraft accidents involving fires, which provided critical inputs describing accident impact. This submodel randomly selects the aircraft involved in each simulated accident, based on the projected fleet mix - and randomly determines the extent of damage to the aircraft. The location is also determined by drawing a random sample from a distribution obtained from the historical data.

- For the specific accident characteristic the resulting fire plume is modelled using standard methods. This determines the height to which the fibers are carried.

- An improved Phase II transport and diffusion calculation determines the concentration of individual fibers at selected representative points downwind from the accident scene. Weather variables used in the calculation are selected at random from historical data for each airport.

- County-based data are used to describe the numbers of each type of vulnerable business and industrial facility, and housing patterns within a 50-mile range of the airport in all directions.

- Each household, and each size and type of business facility is characterized by a specific type of building or other structure. A transfer submodel determines the fraction of fibers outside the building, determined in the transport and diffusion calculation, that gets inside the building.

- For each type and size of business at risk a production model describes the power flow for that type of business. This production model is used with the interior dosage and equipment failure inputs, based on current experimental data, to determine which equipments fail, and the resulting impact on each business. A similar calculation is made for each class of vulnerable aircraft at the airport itself.

- Repair costs are computed for each piece of equipment that fails in the parked aircraft, and in each business and industrial facility. In addition, we determine on a stochastic basis those business establishments that close as a result of the cumulative effects of individual equipment failures. The economic impact of such closings is determined by allocating to each business establishment its share, based on payroll, of the Gross Domestic Product for the particular type of business represented by that establishment.

The methods briefly described above are applied repetitively to a large number of randomly generated accidents at one airport. The result is the development of a set of accident impact costs for many replications of the year 1993 at each airport. These results are then examined to provide statistical measures of the risk. Sample results are described below.

Results

The average annual impact (in 1976 dollars) and the average impact per accident for each of the airports analyzed in the standard 1993 scenario, are summarized in Table 1. The average impact over all simulated accidents (about 2250) at all airports is $5 for household equipment damage, $172 for business and industry equipment repair and business dislocation, and less than one dollar for repair of damaged avionics equipment. In addition to the mean values, the analysis of the simulation results provides considerable statistical insight into the results. For example, the most costly accidents generated at any of the airports, for each of the major impact categories were:

$2,665 in household damage: Kennedy Airport, New York

$274,000 in business/industrial impact: Logan Airport, Boston

TABLE 1

SUMMARY OF INDIVIDUAL AIRPORT RISK ASSESSMENT RESULTS - 1993

Airport	Mean Impact per Accident ($)	Mean Annual Impact ($)
O'Hare/Chicago	169	17
John F. Kennedy/New York City	212	15
Washington National Airport/Washington, D.C.	315	12
Lambert/St. Louis	69	3
LaGuardia/New York City	384	24
Logan/Boston	153	9
Hartsfield/Atlanta	73	8
Miami International/Miami	31	2
Philadelphia International/Philadelphia.	200	8

$3,910 in avionics equipment damage: Kennedy Airport, New York.

These results are from a total of approximately 2500 simulated accidents at each of the airports, or from a total of more than 22,500 accidents simulated at all airports.

A risk profile prepared from the computer-generated results for Washington National Airport appears in Figure 2. It shows that, although the average annual cost resulting from these accidents is $12, there is some chance of exceeding this figure by a considerable amount. However, the probability that the annual impact will exceed $100,000 is only .00003 (3 in 100,000). Expressed another way this implies that costs of this magnitude might be incurred once every 33,333 years, on the average.* The computed statistical confidence limits applied to these results indicate that we can be quite confident that the statistical uncertainties inherent in the computer simulation method would not cause us to raise these probabilities significantly.

In addition to the purely statistical uncertainty involved, the model was also used to examine the sensitivity of the results to possible input data errors. This can be done relatively easily by changing particular input data elements and rerunning the model. Several such sensitivity tests were conducted; none indicate that the impact of input errors or changes in assumptions would require us to significantly change our conclusions regarding the nature of the risk. An example of one rather drastic sensitivity calculation is the one conducted for O'Hare Airport. In this case we changed the inputs to reflect an assumption that all aircraft with composite operating at O'Hare were loaded -- that is: they were all heavy jets with 15,619 kilograms of composite material onboard. In our standard 1993 fleet this aircraft only comprises about a half of one percent of the aircraft with carbon fiber composite components. The average amount of composite on the 'standard' 1993 aircraft with carbon fiber composite aboard is about 2800 kilograms. This worst-case O'Hare Airport risk profile is compared with the standard case in Figure 3. The result shows that, even in this "worst case", the probability of exceeding an annual impact of $100,000 is approximately .003 (3 in 1000) at the nation's

*Since the likelihood of more than one accident at the airport in one year is very small, this may be safely paraphrased as: "one such accident might occur every 33,333 years, on the average."

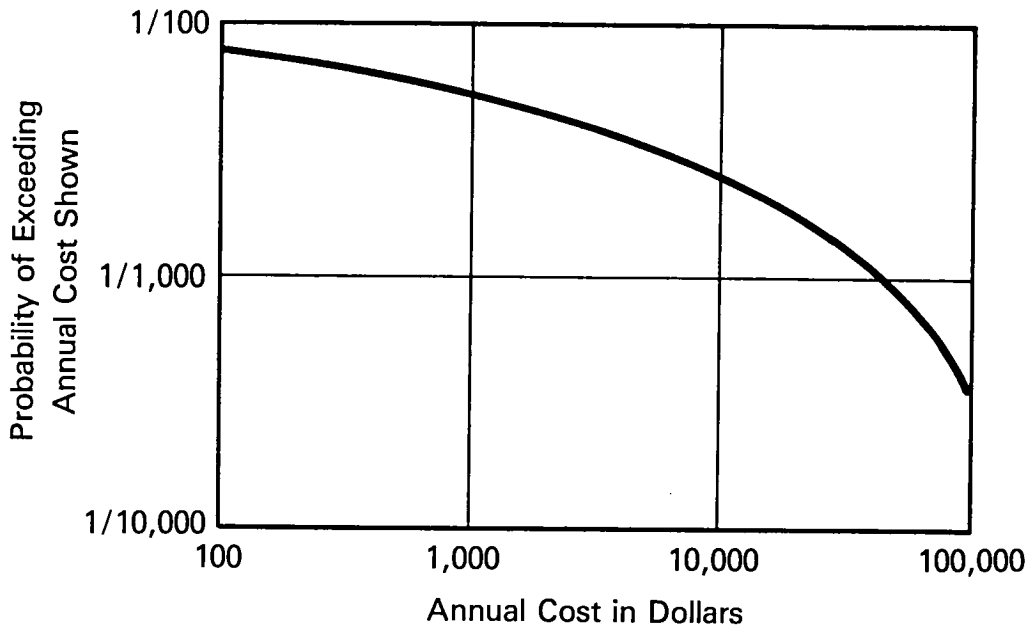

FIGURE 2. 1993 WASHINGTON NATIONAL AIRPORT ANNUAL RISK PROFILE

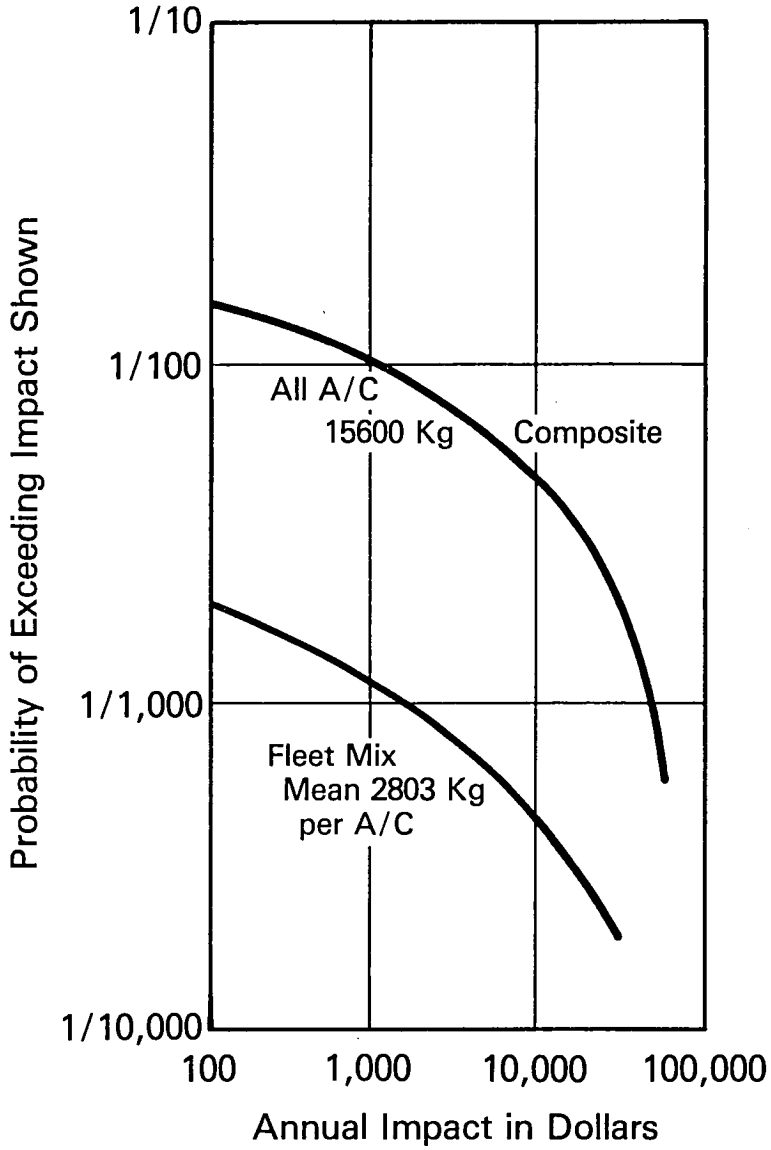

FIGURE 3. COMPARISON OF ANNUAL 1993 O'HARE AIRPORT RISK PROFILES: STANDARD AIRCRAFT MIX AND ALL CF AIRCRAFT WITH MAXIMUM AMOUNT OF COMPOSITE

busiest airport. The results also show that the mean annual impact increased by a factor of ten from $17 for the standard aircraft mix to $172 for all aircraft "loaded" with CF.

NATIONAL RISK

In order to estimate the total national risk due to release of CF in an aircraft fire-accident, and the subsequent damage to electric and electronic equipment, we assumed that the nine airports encompassed all of the commercial aircraft activity in the United States. This greatly overestimates the risk since these tend to be busy airports with considerable surrounding busi-business and industry. The model generates a random number of accidents with fire occuring in the entire United States, based on the mean values determined in the previously-referred to airframers' analysis of historical accidents. The individual accidents are assigned to one of the airports previously analyzed according to the relative traffic level at that airport. The impact of that accident is obtained by randomly drawing one of the accidents that was previously simulated at that airport. The result is a conservative estimate (that is -- on the high side) of the national risk, in that accidents will not be allocated to other low-risk airports. The resulting national annual risk profile is shown in Figure 4. A summary of the results also appears in Table 2, where we have separated out the avionics equipment impact because of special interest in that aspect of the risk assessment. The risk profile may be interpreted as showing that the probability of exceeding $100,000 in annual impact is approximately .00015; the estimated probability of exceeding an economic impact of $1,000,000 is less that than .00001. (one year out of a hundred thousand) The tests of statistical confidence and the sensitivity tests conducted during the study indicate that we may be confident that these results are statistically valid and conservative, in that they tend to overestimate the actual risk.

IMPACT ON ELECTRIC UTILITY SYSTEMS

Parallel efforts, primarily under the sponsorship of the Department of Energy, investigated the vulnerability of electrical transmission equipment to carbon fiber incursion. These indicated some vulnerability of individual components in the electrical distribution system, but tend to show that high high voltage (above 38 kilovolts) and low voltage systems (below 2.4 kilovolts)

TABLE 2

NATIONAL RISK IMPACT RESULTS

Type of Cost	Mean	Worst Case
Business, Industry, and Household Impact	$466	$275,000
Avionics Equipment Failures	$2	$3,900

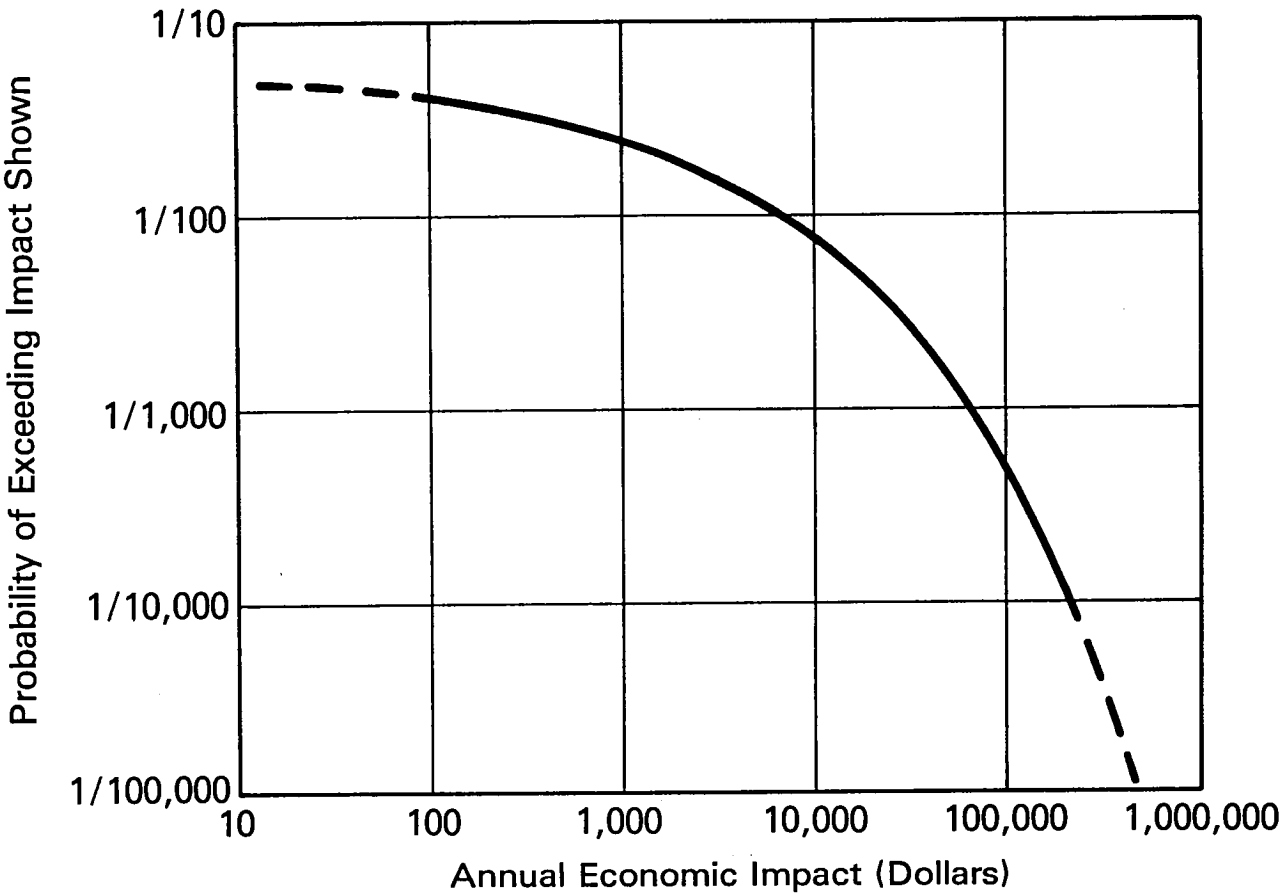

FIGURE 4. 1993 ANNUAL NATIONAL RISK PROFILE

are both essentially invulnerable. In the risk assessment model described above, the vulnerability of equipment in the intermediate range was accounted for in specific cases by examining the probability of failure of stepdown transformers for specific industrial facilities. At NASA's request ORI conducted a separate analysis to estimate the impact of possible aircraft-fire accident on the total national electric power distribution system; this was conducted in parallel with a historical review of electrical power outage data.

In order to conduct the analysis, typical and actual distribution systems operating in the vulnerable voltage range were defined. Estimates of the effects of carbon fibers on the circuits were based on experimental data made available to ORI by the Department of Energy team under NASA auspices. In order to be conservative this calculation assumed a downwind pattern of carbon fiber exposure based on a combination of parameters defined as the worst possible case. Individual insulator and bushing failure probabilities are based on these worst case exposure values and experimental failure data for these components.

The results were obtained for several sets of conditions. The circuits examined include a typical (textbook) electrical distribution circuit operating in the 7.5 KV range, and an actual suburban system provided by an operating electric utility system in the 23 KV range. For the typical circuit, failures were computed based on published component reliability data, and the worst-case carbon fiber scenario. For the 23 KV circuit we obtained actual reported outages, and also computed the worst-case carbon fiber scenario failures. In all cases the failures were extrapolated to a national base, assuming that all users were served by the system under examination, and using the national average annual number of carbon fiber aircraft-fire accidents for 1993. The results are summarized in Table 3. As a further comparision we note that annual bulk outages reported to the Federal Energy Regulatory Commision indicate that, typically, 3,000,000 (3×10^6) customers suffer an outage in one year for an annual average of about 0.05 outages per utility customer. Such bulk outages comprise an interruption occuring at 69KV and above and resulting in a loss of at least 100 megawatts for at least 15 minutes, or a loss of more than one half of a small system's annual peak load. These outages clearly comprise only a fraction of the total outages in the nation.

TABLE 3

COMPARISON OF ANNUAL ACTUAL AND "NORMAL" ELECTRIC POWER DISTRIBUTION SYSTEM OUTAGES WITH WORST-CASE CARBON FIBER RELATED OUTAGES

Measure	Distribution Circuit			
	Typical: 7.5 Kv		Actual: 23 Kv	
	"Normal"	Worst-Case CF	Reported	Worst-Case CF
Total National Outages per Year	22×10^6	23	140×10^6	3300
Annual Outages per Customer	0.32	10^{-6}	2.1	5×10^{-5}

All of the carbon-fiber related outage results are based on assumptions that are all on the conservative side; that is, they overestimate the resulting number of expected power outages. The result is that we can expect less than one civil aircraft fire-accident carbon fiber release related power outage for about every 200,000 to million outages that occur for a variety of other reasons.

Clearly, then, we conclude that the carbon fibers potentially released in a civil aircraft accident with fire represent a relatively insignificant threat to the electric power distribution network.

TABLE OF CONTENTS

		Page
	EXECUTIVE SUMMARY	i
	LIST OF FIGURES	xvi
	LIST OF TABLES	xviii
I.	INTRODUCTION	1-1
II.	ACCIDENT/RELEASE	2-1
	1993 FLEET COMPOSITION	2-1
	ACCIDENT RATE	2-3
	AMOUNT OF CARBON FIBER RELEASED	2-5
III.	PLUME HEIGHT CALCULATION	3-1
	GENERAL METHOD	3-1
	HEAT EMISSION RATE	3-2
IV.	DOWNWIND TRANSPORT AND DIFFUSION OF FIBERS	4-1
	BASIC CONCEPTS	4-1
	ORI TRANSPORT AND DIFFUSION EQUATIONS	4-2
	INPUTS TO TRANSPORT CALCULATIONS	4-5
	TRANSPORT AND DIFFUSION MODEL SENSITIVITY TESTS	4-7
	GEOGRAPHICAL INPUTS	4-7
V.	TRANSFER OF FIBERS INTO INTERIOR OF STRUCTURES	5-1
	METHOD	5-1
	IMPLEMENTATION	5-2

VI. EQUIPMENT FAILURES 6-1
FAILURE MODEL 6-1
EQUIPMENT CONFIGURATIONS 6-3
COMPUTER IMPLEMENTATION 6-9
VII. COSTS DUE TO EQUIPMENT FAILURES 7-1
BUSINESS/INDUSTRY REPAIR COSTS 7-2
FACILITY CLEAN-UP COSTS 7-4
DISLOCATION COST 7-4
HOUSEHOLD IMPACT 7-12
AIRCRAFT VULNERABILITY 7-13
COSTING SUMMARY 7-21
VIII. INDIVIDUAL AIRPORT RESULTS 8-1
SAMPLE ACCIDENT 8-1
SIMULATION OUTPUTS 8-3
COMPARISON OF DIFFERENT AIRPORTS 8-6
STATISTICAL CONFIDENCE LIMITS 8-8
ADEQUACY OF SAMPLE SIZE 8-11
SENSITIVITY TESTS 8-11
IX. NATIONAL RISK 9-1
METHOD 9-1
RESULTS 9-2
X. SUMMARY AND CONCLUSIONS 10-1
APPENDIX A: THE EFFECTS OF CARBON FIBER EXPOSURE ON ELECTRIC UTILITY SYSTEMS A-1
APPENDIX B: TOTAL AIRCRAFT ACCIDENT COSTS B-1

LIST OF FIGURES

		Page
1.1	ORI Risk Assessment Model Flowchart	1-4
4.1	Downwind Exposure Pattern; Singles, Stability Class 6	4-9
4.2	Downwind Exposure Pattern; Clumps, Stability Class 6	4-10
4.3	Downwind Exposure Pattern; Singles, Stability Class 1	4-11
4.4	Downwind Exposure Pattern; Clumps, Stability Class 1	4-12
4.5	Schematic Method of Modelling an Individual County	4-14
4.6	Definition of Areas at Risk for Washington National Airport	4-15
6.1	Generalized Business/Industry Equipment Configuration	6-4
7.1	Flowchart for Computing Repair Costs due to Equipment Failure	7-5
7.2	Schematic Plant Failure Decision Tree	7-7
7.3	Flowchart for Computing Business/Industry Facility Closings	7-9
7.4	Flowchart for Computing Avionics Failures and Associated Costs	7-20
8.1	Random Accident at Kennedy Airport	8-2
8.2	Annual Output for 34,000 Replications; Kennedy Airport, 1993	8-4
8.3	Annual Risk Profiles for Kennedy Airport, 1993	8-5
8.4	Annual Risk Profiles for Selected Airports, 1993	8-9
8.5	Accident Risk Profiles for Selected Airports, 1993	8-10
8.6	1993 Washington National Airport Annual Risk Profile with Statistical Confidence Limits	8-12

8.7 1993 Washington National Airport Annual Risk Profiles for Different Inversion Height Assumptions 8-16

8.8 O'Hare Airport Annual Risk Profiles for Standard and Worst Case, 1993 8-19

9.1 Flowchart for National Risk Assessment Model 9-3

9.2 Conceptual Results of Single Airport Simulations 9-4

9.3 National Risk Profile, 1993, With Statistical Confidence Limits 9-5

9.4 Comparison of Phase I and Phase II National Risk Profiles . . . 9-6

LIST OF TABLES

		Page
2.1	Definition of Aircraft in 1993 Commercial Fleet	2-2
2.2	1993 Commercial Aircraft Fleet Projection	2-4
2.3	Amount of Composite Involved in Fire for 1993 Aircraft . . .	2-6
3.1	Estimated Fuel Burn Rates	3-4
4.1	Wind Profile Exponent	4-3
4.2	Input Conditions for Transport Model Tests	4-8
5.1	Design Factors for ORI Standard Enclosures	5-4
5.2	Transfer Functions for Standard Enclosures	5-5
6.1	Generic Equipment Failure Parameters	6-5
6.2	Equipment Configurations for Manufacturing Facilities . . .	6-7
6.3	Enclosure Types by SIC/Size Category	6-10
7.1	Input Repair Costs for ORI Standard Equipments	7-3
7.2	Estimated Number of Aircraft Exposed on the Ground, 1993 . .	7-14
7.3	Examples of Vulnerable Equipment Aboard L-1011 TRISTAR . . .	7-16
7.4	Aircraft Avionics Equipment: Failure and Cost Inputs	7-18
7.5	Ventilation Factors and Probabilities for Avionics Equipment	7-19
7.6	Summary: Business/Industry Cost Model Input Requirements . .	7-22
8.1	1993 Results for Simulated Accidents at Nine Airports . . .	8-7
8.2	Comparison of Different Numbers of Simulations; O'Hare, 1993	8-13
8.3	Comparison of Best-Estimate and Worst-Case Results; O'Hare Airport, 1993	8-18

I. INTRODUCTION

This is the Final ORI Report on Phase II of its Civil Aviation Carbon Fiber Risk Assessment study performed for the National Aeronautics and Space Agency under Contract No. NAS1-15379. The NASA-funded effort is part of a major national program directed toward estimating the potential risk of increased use of carbon fiber composite material in a variety of applications. This program was initiated as the result of evidence that electrical and electronic equipment may fail as the result of the deposit of carbon fibers released by burning of the composite material. Carbon fiber - expoy composite materials offer considerable advantage over more conventional material due to the ability to engineer in superior strength while achieving a considerable weight saving. The national program was established to investigate the nature of this potential hazard in the light of projected increased use of these materials. The NASA program, of which the ORI investigation reported here is a small part, is directed particularly at the possible risk associated with the use of carbon fiber composite materials in civil aviation.

In Phase I of its investigation ORI developed a computer simulation model that was used to generate risk statistics for accidents at several airports, which were later combined to estimate the national risk. The Phase I model, although using many Monte Carlo - or stochastic - submodels, did compute the business-industry impact on an expected value basis. This may have tended to limit the variance of the final results and thus reduced the likelihood of

generating extreme values on the "tails" of the accident cost distribution. In the Phase II model this computation has been made stochastic, and several other subroutines in the complete model have similarly been made to operate in a random rather than an expected value mode.

The calculation is essentially "input driven"; that is, the results depend on a host of input data, many of which are from sources not directly linked to the problem at hand (for example, national economic data). Other input data elements, such as the amount of carbon fiber composite on an airplane, and the fraction of carbon that would be released if that airplane were to crash and burn, are documented for the Phase I calculation. For Phase II additional experimental data were available, and were used. Thus the results presented in this report are based on the use of a computer model that is more sophisticated than the one used in Phase I, operating on a much more solid data base. In addition ORI was requested to investigate the potential risk to the electric utility subdistribution system.

The basic technical approach to the risk assessment problem is to simulate many aircraft accidents with fire, each one characterized by many random variables, and then compile statistics based on the analysis of the computed impact of the series of accidents. The availability of high-speed digital computing techniques makes this approach feasible. This is an application of the so-called Monte Carlo simulation technique. The principal elements in the scenario that is simulated are:

- Aircraft accident with fire
- Release of carbon fiber material
- Entrainment of the carbon fibers in a smoke plume
- Transport of the carbon fiber material downwind
- Transfer of some of the fibers into the interior of buildings
- Failures of electrical and electronic equipment
- Economic impact of these failures

In addition to the simulation of these events per se the complete model must perform many other functions related to the selection of appropriate random

variables, as well as what may be termed "housekeeping" functions. A simplified form of the complete airport risk assessment model is illustrated in the flowchart appearing in Figures 1.1a and 1.1b.

The simulation of one accident requires the random selection of the accident location. This selection depends on input data that is the result of a detailed analysis of all historical jet aircraft accidents in which fires were involved, performed under NASA sponsorship by the principal airframe manufacturers. The estimate of the amount of fibermaterial released depends on inputs that define the mix of aircraft in the fleet for the target year of 1993. The fraction of the material that is released as fibers in the size range of interest is based on recent experimental results. The computer program models the behavior of the resulting fire plume that carries the released fibers aloft. The downwind transport and diffusion processes are then modelled using methods that are somewhat more general and refined compared to those used in Phase I. The necessary meteorological inputs for this calculation are drawn at random from a body of data for each of the airports for which the calculations are made.

The transport and diffusion calculation provides the exposure or dosage at predefined points. These points are selected in advance to be representative of the area at risk surrounding the airport. In all cases these extend to a range of at least 50 miles from the airport at which the simulated accidents occur. The points are selected to represent concentrations of businesses, industry, and private residences in individual counties, in order to make use of readily available county-based economic and other census data. All types of vulnerable businesses and industry, as well as households, are characterized by particular types of buildings at the representative points. The definition of the building types includes a set of ventilation parameters, obtained from standard engineering sources modified by particular experimental data appropriate to the carbon fibers. These parameters are used in the calculating the fraction of the fibers outside each building that would get inside, termed the transfer function. In this way the risk assessment model determines the exposure or dosage to which vulnerable equipment is subjected.

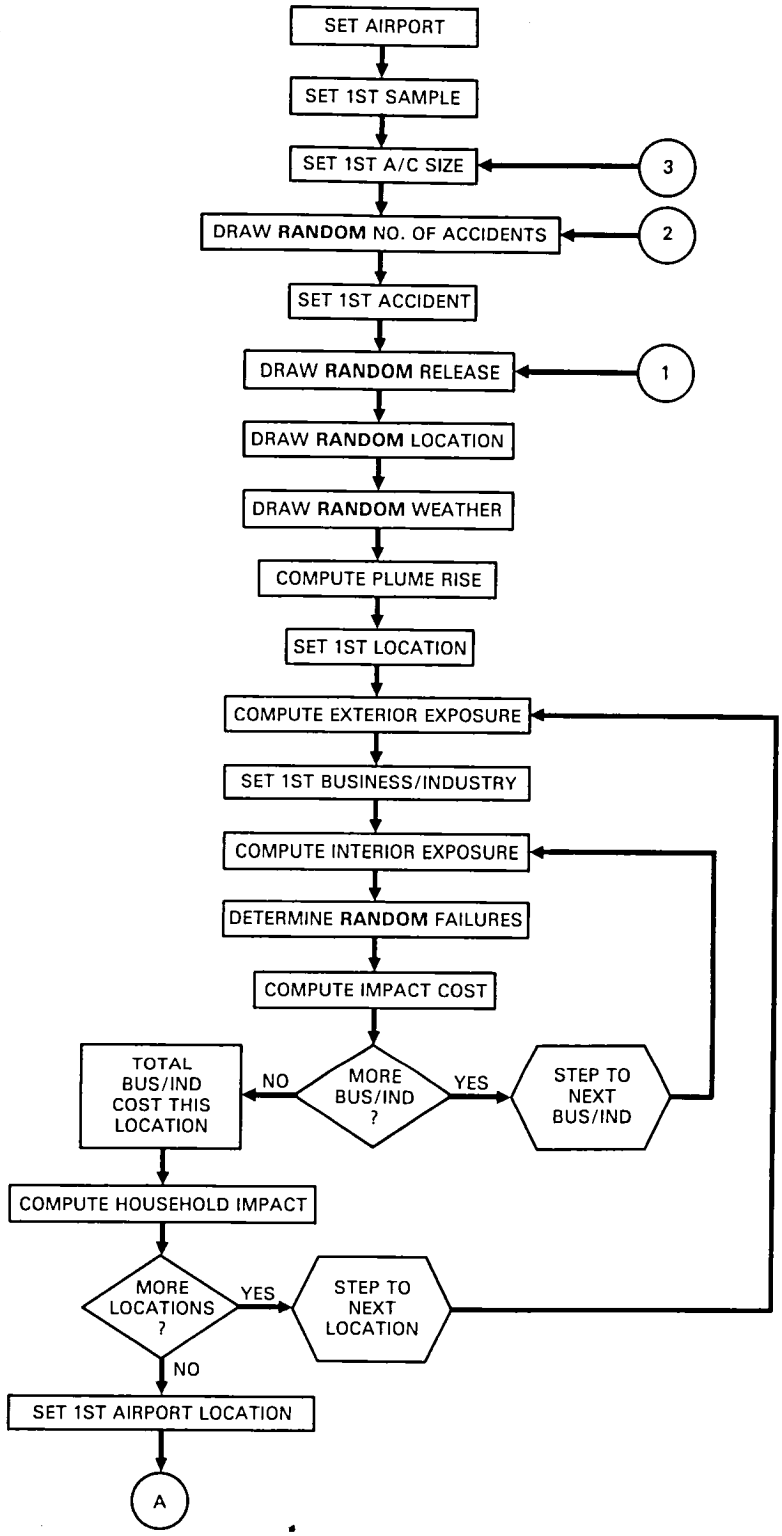

FIGURE 1.1 a. ORI RISK ASSESSMENT MODEL FLOWCHART

(continued)

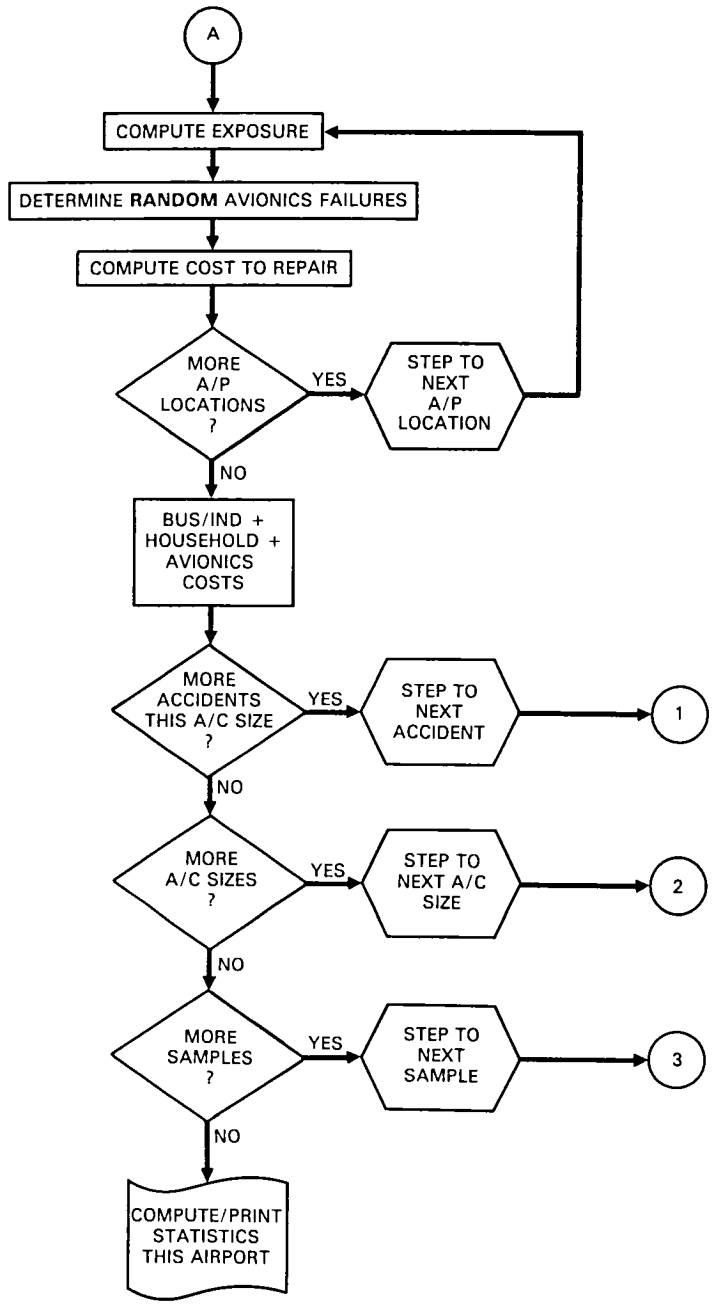

FIGURE 1.1 b. ORI RISK ASSESSMENT MODEL FLOWCHART (concluded)

With the interior exposure available we can then compute the probability of failure for specific classes of vulnerable equipment, previously defined for each type of business, industry, and household in the airport environs. The failures of individual equipments are then determined using randomized or Monte Carlo methods. The impact of these failures is then assessed in several ways. First all equipment failures are totalled to estimate the required cost to repair the damaged equipment. The likelihood that the equipment failure would be severe enough to cause a place of business to close is then examined. This is based on the assumption that the business facility would close if electric power were lost, if its principal control systems were knocked out, or if half of its production equipment fails. These events are also determined on a random basis for essentially each place of business in the downwind path of the plume resulting from the and accident and fire. The financial impact of such closings is estimated by allocating to each place of business its estimated share of the Gross Domestic Product for that class of business or industry. If a place of business is determined to have closed as a result of the carbon fiber release incident, a clean up cost is also assessed. The household equipment impact, because of the large number of essentially identical equipments at risk in very similar environments is treated on an expected-value basis.

The vulnerability of avionics equipment aboard aircraft parked at the airport is also examined in the risk assessment calculation. The number of aircraft in a potentially vulnerable state at the airport is determined from data provided by the aircraft manufacturers via NASA. For each aircraft the calculation determines the number of each class of equipment in each of several at-risk states. The number of failures is then determined on a random basis, and the input repair costs are used to determine the total impact of such failures.

After all business facilities and households at risk, and all parked aircraft have been examined, the model has generated an estimate of the total impact of one accident, in 1976 dollars. These results are available for the three principal impact categories: business/industry, household, and avionics equipment in parked aircraft. The computer program management module then returns to the "front end" to generate the details associated with the next accident in the sample year being replicated, if there are any more. Once all

accidents in a sample year have been simulated the model generates another sample year, with its aircraft accidents, simulates the details of each accident, then does the next sample. This process continues until the preset number of annual replications has been completed. At this point we have the impact for many sample years and compute the statistics over all samples. These include such measures as the mean annual impact, and the mean impact per accident, as well as the risk profiles. The risk profile shows graphically the probability that the annual impact will exceed any value.

The method described briefly above has been applied to a sample of nine airports. These were selected as reasonably representative of U.S. airports in Phase I, although they were purposely chosen to be a conservative group, in the sense of representing the "high side" of the risk. In order to compute the total risk at the national level, this set of airports was assumed to represent the entire United States. The national risk model generates random accidents during a sample year and determines, on a random basis, which of the nine airports that each accident would have taken place. A previously simulated accident at that airport is selected at random, and its computed impact added to the running total for the current replication's national impact. By repeating this process many times the national model generates the statistics necessary to produce the national risk profile.

The methods outlined here are described in detail in the remainder of this report. The accident details, including extrapolation of the 1993 commercial aircraft fleet mix, and other necessary inputs are described in Section II which follows immediately. The fire plume calculation is described in detail in Section III.

The improved Phase II methods for computing the downwind transport and diffusion of the material contained in the plume are described in Section IV. The methods used to compute the transfer of the diffused material into the interior of buildings and other structures, including the use of new Phase II data, appears in Section V. The following part of the report, Section VI, discusses the methods of treating equipment failures. At this point in the logic flow of the simulation we are ready to calculate failures and need to convert those failures into dollar measures of impact. The required methods are described in detail in Section VII; this part of the methodology comprises

the major Phase II improvement over Phase I. The required data bases for the economic inputs are also detailed in that section. Results of the single airport simulations are presented in Section VIII, including several sensitivity tests, which examine the impact on the risk results of significant changes in input data and associated assumptions. The national model and the results it generated are presented in Section IX. The ORI conclusions appear in Section X. The analysis of failures in the electrical power distribution system is described in Appendix A.

II. ACCIDENT/RELEASE

In this section of the report we describe the method used to "generate" an accident and determine the amount of fiber released in the accident. The model is applied to a single airport at a time. The generation of an accident with fire involving an aircraft with CF composite in its structure is the first step in the scenario simulated by the ORI risk assessment model.

1993 FLEET COMPOSITION

In order to estimate the amount of carbon fiber that might be released in an accident with fire it was first necessary to estimate the amount of carbon fiber that would be on particular aircraft, as well as the mix of aircraft in the 1993 fleet. The principal aircraft manufacturers, working with NASA, and in consultation with ORI, prepared descriptions of the different aircraft configurations to be introduced from now until 1993. These are defined by the amount of composite material in all structural components; each of the aircraft types is defined in Table 2.1. Several aircraft, defined early in Phase II, were later dropped when it was determined that it was unlikely that they would be in the 1993 fleet. For this reason no aircraft of types 3 and 4 appear in Table 2.1. Several different aircraft defined by the airframe manufacturers that were essentially identical from the composite distribution viewpoint were combined in preparing the table. Retirement schedules were developed, and

TABLE 2.1
DEFINITION OF TYPES OF AIRCRAFT EXPECTED TO BE IN THE 1993 COMMERCIAL FLEET BY SIZE AND AMOUNT OF COMPOSITE (KILOGRAMS)

	Aircraft Size and Identification Number																
	Small		Medium				Large										
Component	1	2	5	6	7	8	9	10	11	12	13	14	15	16	17	18	19
1. Rudder and Tab	0	0	73	73	73	250	0	0	0	50	50	341	98	98	98	98	98
2. Vertical Stab.	0	0	0	0	0	12	0	0	0	17	17	17	0	212	212	212	212
3. Elev. and Tab	0	0	107	107	107	170	0	0	0	0	0	237	199	116	116	116	116
4. Hor. Stab.	0	0	0	0	0	129	0	0	0	180	180	180	593	741	741	741	741
5. Wing Flap T.E.	0	0	0	0	462	156	0	0	0	219	219	219	0	593	593	593	593
6. Spoiler	54	54	68	68	68	98	0	0	0	137	137	137	0	0	0	0	0
7. Ailerons	0	0	24	24	24	171	0	0	103	0	0	239	103	103	103	103	103
8. Wing T.E. Sup.	0	0	0	0	461	0	0	0	0	0	0	0	0	0	410	410	410
9. L.E. Flap	0	0	0	0	0	0	0	0	0	0	0	0	0	0	0	0	0
10. Wing L.E. Sup.	0	0	0	0	0	0	0	0	0	0	0	0	0	0	553	553	553
11. Wing Box	0	0	0	0	0	0	0	0	0	0	0	0	0	0	0	0	10206
12. Nacelle	0	0	45	45	45	1852	0	131	131	0	3107	3107	132	307	611	1391	1391
13. Fan Blade	0	0	0	0	0	0	0	0	0	0	0	0	0	0	0	0	0
14. Wing Fairing	11	11	16	16	16	361	0	0	0	506	506	506	0	0	328	328	328
15. Wheel Doors	0	0	34	34	34	29	0	0	0	0	0	179	157	157	157	157	157
16. Fuselage	0	127	0	215	215	0	155	155	1000	0	0	0	0	0	0	0	0
17. Floor Beams	0	0	0	0	0	558	0	0	0	909	909	909	0	711	711	711	711
18. Cockpit Window Sup.	0	0	0	0	0	0	0	0	0	0	0	0	0	0	0	0	0
Composite	65	192	367	582	1505	3786	155	286	1234	2018	5125	6071	1282	3038	4633	5413	15,619

Note: Types 3 and 4 defined early in Phase II were later dropped. Types 20, 21, 22 not shown in table are aircraft with no CF.

introduction of new aircraft "played" for each year. This straightforward calculation led to the development of an estimate of the 1993 fleet mix. The result is shown in Table 2.2.

ACCIDENT RATE

In Phase I, ORI conducted a limited analysis of individual aircraft accident reports and summary data available through the National Transportation Safety Board. In Phase II, under NASA auspices, the major aircraft manufacturers completed detailed analyses of approximately 100 jet aircraft accidents in which fire played a part. These analyses provided estimates of the damage to each major aircraft structural component. Based on this data base, it was determined that the annual fire-accident rate pertinent to the risk assessment was 3.8 per year; this has been accepted as the best estimate available for the 1993 scenario. For the risk assessment calculation we are only concerned with aircraft containing composite material, estimated to be about 70 percent (cf. Tables 2.1, 2.2) of the 1993 fleet, for a resulting national mean number of carbon-fiber aircraft accidents with fire of 2.6 per year.

The simulation model treats one aircraft size at a time. Accordingly, for airport A and aircraft of size S, we estimate the annual accident-with-fire rate by:

$$\lambda(A,S) = \frac{N_{A,S} \times 2.6}{\sum_A \sum_S N_{A,S}}$$

where $N_{A,S}$ is the number of operations of aircraft of size S at airport A; thus the sum

$$\sum_A \sum_S N_{A,S}$$

comprises all operations in the U.S. In any one replication (a random year) the number of accidents is assumed to fit a Poisson distribution. The

TABLE 2.2

1993 COMMERCIAL AIRCRAFT FLEET PROJECTION

Aircraft Size	ORI Identification Number	Number in Fleet	Composite per aircraft (kilograms)
Small	1	71	65
	2	80	192
	20	409	0
Medium	5	125	367
	6	37	582
	7	255	1,505
	8	329	3,786
	21	34	0
Large	9	7	155
	10	5	286
	11	326	1,234
	12	54	2,018
	13	80	5,125
	14	192	6,071
	15	53	1,282
	16	53	3,038
	17	143	4,633
	18	79	5,413
	19	11	15,619
	22	396	0

probability of exactly n accidents with fire involving aircraft of size S at airport A is given by [1]:

$$P(n; \lambda(A,S)) = e^{-\lambda(A,S)} \frac{\lambda^n(A,S)}{n!}$$

The Monte Carlo simulation model makes a random draw from this distribution during each replication for one airport, and one size aircraft. Because the number of accidents in any one replication is very small the computer model actually uses a double precision sampling technique.

AMOUNT OF CARBON FIBER RELEASED

The airframer accident analysis generated estimates of the amount of each major aircraft component that was involved in each accident. These output results were combined with the characterization of each aircraft--amount of composite in each component--to provide an estimate of the amount of composite that would have been involved in each of the historical fire accidents. For each projected 1993 aircraft type identified in Table 2.1 the ORI risk assessment team computed the sum:

$$\text{Composite Consumed} = \sum_c (\text{Fraction Consumed})_c \times (\text{Amount of Composite})_c$$

for all accidents in the airframers' analysis, where the index c refers to an aircraft component. Thus, for one aircraft type, defined by a distribution of composite material, we estimated the total amount of composite material that would have been consumed in each of the analyzed historical accidents. The results, a sample of which are shown in Table 2.3, comprise one of the major input data sets for the risk calculation. In each simulated accident involving an aircraft in a particular size category, the specific aircraft type is determined in a random draw. The probability that the aircraft is of type k is determined by the ratio of the number of aircraft of type k in the fleet to the total number of aircraft in the size category. The simulation model then determines the amount of composite material involved in the fire by randomly selecting, on an equally likely basis, one of the accidents, i.e., an amount of composite from the appropriate column of the complete form of Table 2.3.

---

1) W. Feller, 1950. An Introduction to Probability Theory and Its Applications, Vol I, John Wiley, New York. Page 158 et seq.

Table 2-3

AMOUNT OF COMPOSITE INVOLVED IN FIRE (KILOGRAMS) FOR

1993 COMMERCIAL AIRCRAFT IN SELECTED ACCIDENTS

Accident No.	Op Phase	Severity	Aircraft Type																
			1	2	5	6	7	8	9	10	11	12	13	14	15	16	17	18	19
1	Takeoff	Severe	49	164	209	403	1141	1699	139	152	985	1763	2074	2682	687	1993	3122	3200	13406
4	Takeoff	Moderate	2	2	10	10	195	141	0	0	0	189	189	224	31	269	334	334	334
22	Landing	Moderate	14	52	36	101	285	423	46	59	313	317	628	699	76	212	655	733	733
23	Landing	Severe	49	160	135	322	958	2170	135	200	997	1686	3239	3561	285	1558	2561	2951	8054

To actually determine the amount of carbon fiber released, it is assumed that one percent of the carbon fiber involved is actually released as 3-mm single fibers. Analysis of the accident data indicated that approximately 1 out of 30 accidents during landings and takeoffs involved explosions. The model uses this value as the appropriate probability to randomly determine whether an explosion occurred in the simulated accident. If an explosion did occur, an additional two-and-a-half percent of the carbon fiber is released due to the agitation of the composite material. This input is based on experimental evidence obtained after completion of Phase I, and is in marked contrast to the input used then. In Phase I the fraction of carbon fiber released as single fibers was assumed to be 0.20.

Each accident in the historical file is also characterized by the operational phase during which the accident occurred and the degree of severity. The accidents were analyzed to obtain a distribution of locations for landing and takeoff accidents. The generalized distribution was applied to each of the airports for which the risk calculations were made. In each simulated accident the location distribution is sampled to draw an actual location to be used in the calculation. The severity measure associated with each accident is used later in determining the plume height. It should be noted that the methods described here represent a great increase in the amount of variance permitted in the calculation over those employed in the Phase I risk assessment.

III. PLUME HEIGHT CALCULATION

The simulated release of graphite fibers starts with the aircraft accident and resulting fire. In the preceding section we described the methods used to estimate the fraction of the aircraft consumed in the fire and the calculation of the amount of fiber released. The next step in the simulation is described in this section.

As a result of the fire a hot buoyant plume is formed that rises to a "stabilization" height which is a function of the energy available, the wind speed, and the atmospheric stability. The graphite fibers enter the buoyant plume and are lifted to the stabilization height.

GENERAL METHOD

As in Phase I, calculation of the plume rise (or elevation), H, at stabilization from an open fire follows the work of Briggs[1)], since no improved approach has been located in Phase II. In the Briggs model, as adapted, the height of the plume, in meters, is given by:

$$H = 2.9\ (F/us)^{1/3}$$

1/ G.A. Briggs: "Some Recent Analyses of Plume Rise Observations." Paper presented at the 1970 International Air Pollution Conference of the International Union of Air Pollution Prevention Associations.

for stable conditions, and

$$H = 1.6F^{1/3}u^{-1}x^{2/3}, \text{ when } x < 3.5x^* \quad (3.1\ b)$$

$$H - 1.6F^{1/3}u^{-1}(3.5X^*)^{2/3}, \text{ when } x < 3.5x^* \quad (3.1\ c)$$

for neutral or unstable conditions, where u is the mean wind speed in meters per second and:

$$x^* = 14F^{5/8}, \text{ when } F<55 \quad (3.2\ a)$$

$$x^* = 34F^{2/5}, \text{ when } F>55 \quad (3.2\ b)$$

The buoyancy flux parameter, F, appearing in the above equation, is given by

$$F = \frac{gQ_R}{\pi C_p \rho T}$$

where:

G = acceleration of gravity, 9.8 m/sec^2

Q_R = heat emission rate, kcal/sec

C_p = specific heat of air at constant pressure, .2391 kcal/kg^{o}K.

ρ = atmospheric density, 1.239 kg/m^3

T = ambient temperature, ^{o}K.

The atmospheric stability parameter, s, is defined by:

$$s = \frac{g\partial\theta}{T\ z}$$

where:

$\frac{\partial\theta}{\partial z}$ = gradient of potential temperature, 0.35^o/km for stable conditions.

HEAT EMISSION RATE

In order to use the Briggs formulas, it is necessary to specify Q_R, the heat emission rate for a burning aircraft; this is, in turn, the product of the rate measured in gallons per unit time, and the fuel heat content per gallon. In Phase I a standard burn rate was used, based on the experimental data available at that time. In Phase II we were able to turn to the detailed fire-accident analysis previously referred to. In this case, it was possible to estimate the fuel burn rate for accidents occuring during different operational phases, as well as accidents of different severity. The reported accidents involved small jet aircraft almost exclusively, so a scaling factor

proportional to the relative volume of the aircraft fuel tanks, as reported in Janes'[2/] was used to estimate the burn rates for other size aircraft. The results are summarized in Table 3.1.

Another major input, or modelling assumption, concerns the behavior of the plume at an inversion. In the ORI Phase I Final Report this matter was discussed at some length. On the basis of the evidence available then, and not significantly increased during Phase II, we continued to model the plume so that it does not penetrate the inversion. In subsequent sections of this report we examine the impact of this assumption on the final results.

With the inputs described here, and the above decision regarding behavior of the plume at an inversion, the computer model implementing Equations (3.1) and (3.2), can determine the stabilization height for the plume resulting from the simulated accident involving any of the projected 1993 aircraft for any combination of wind speed and stability conditions.

2/ Janes' All The Worlds Aircraft—1977-78, J. Taylor.

TABLE 3.1

ESTIMATED FUEL BURN RATES (Liters/Minute)

Operational Phase	Damage Severity	Aircraft Size		
		Small	Medium	Large
Takeoff	Minor	238	397	794
	Substantial	1590	2650	5300
Landing	Minor	719	1192	2385
	Substantial	1590	2650	5300
Static	-	19	19	19

IV. DOWNWIND TRANSPORT AND DIFFUSION OF FIBERS

After a simulated accident, fire, and release of carbon fibers, a buoyant plume carries the fibers aloft, as described in the preceding section of this report. The plume at its stabilization height may be considered a point source; meteorological transport and diffusion methods are then applied to determine the downwind dosage (or exposure) at points of interest.

BASIC CONCEPTS

In Phase I, ORI adapted an essentially standard EPA Gaussian plume transport and diffusion model to the needs of the risk assessment study. The model provides for downwind transport and diffusion of material in the form of a plume that diffuses simultaneously in the crosswind and vertical directions. The emitting source can be elevated at any specified height. The atmosphere is characterized as being in one of several stability classes. Dispersion parameters that govern the rate of crosswind and downwind diffusion are associated with each stability class. The plume rise calculations, described previously, give the source height which is used explicitly in the transport and diffusion model.

In Phase II further extensions were made to the ORI transport and diffusion model. These allow for multiple reflections of the diffusing particles and provide an improved mechanism for accounting for particle fallout at downwind distances that are so large that the cloud is uniformly dispersed in the vertical.

The wind speed at plume height is treated as representative of the layer in which the carbon fibers are dispersing. The standard power law for the variation of wind speed with height may be written:

$$U = u_0 \, (H/7)^p \tag{4.1}$$

where H is the height in meters. In the cases presented in this report, then, H is typically assigned a value equal to the stabilization height of the plume resulting from the fire following the aircraft accident. The exponent "p" is assigned specific values for different atmospheric stability conditions, as shown in Table 4.1.

In most cases rather stringent physical conditions must be met for the plume to "punch through" an inversion. Observations indicate that this typically does not occur. It was therefore considered reasonable to assume that if the computed plume height is greater than the height of the inversion, it can be set equal to the inversion height. The impact of relaxing this condition and permitting the plume to penetrate the inversion is examined in Section VII below.

ORI TRANSPORT AND DIFFUSION EQUATIONS

General Case

The Phase I meteorological transport and diffusion equations were modified to include the direct component and five reflected components at downwind locations. The method of treating the multiple reflections follows that presented by Cramer, et al.[1/] generalized for additional reflections in accordance with the concepts presented by the Environmental Protection Agency[2/]. The general result for the dosage (exposure) at a point on the surface at a location (x,y) in units of particle-seconds per cubic meter is:

$$E\,(x,y,0,H') = \frac{Q}{\pi \sigma_y \, \sigma_z u} \exp\left[-\frac{1}{2}\left(\frac{y}{\sigma_y}\right)^2\right] \left\{ \exp\left[-\frac{1}{2}\left(\frac{H'}{\sigma z}\right)^2\right] + \right.$$

1/ H.E. Cramer, et al. 1972: Development of Dosage Models and Concepts, U.S. Army Dugaway Proving Ground, Dugway, Utah. AD893 341 L.

2/ User's Manual for Single-Source (CRSTER) Model, EPA, July 1977, EPA-450/2-77-013.

TABLE 4.1

WIND PROFILE EXPONENT

Pasquill-Gifford Stability Class	Exponent, p
A - Most Unstable	0.10
B	0.15
C	0.20
D - Neutral	0.25
E	0.30
F - Most Stable	0.30

$$+ r\exp\left[-\frac{1}{2}\frac{(H' + 2H_m)^2}{\sigma_z}\right] + \left[\exp -\frac{1}{2}\frac{(-H' + 2H_m)^2}{\sigma_z}\right] \tag{4.2}$$

$$+ r^2 \exp\left[-\frac{1}{2}\frac{(H' + 4H_m)^2}{\sigma_z}\right] + r\exp\left[-\frac{1}{2}\frac{(-H' + 4H_m)^2}{\sigma_z}\right]$$

$$+ r^2 \exp\left[-\frac{1}{2}\frac{(-H' + 6H_m)^2}{\sigma_z}\right]\Bigg\}$$

where:

- x = downwind distance from source to receptor,
- y = crosswind distance from source to receptor,
- u = mean wind speed, m/sec,
- Q = number of particles released
- σ_y = standard deviation of the wind speed in the crosswind direction, as a function of x and the stability class
- σ_z = standard deviation of the wind speed in the vertical, as a function of x and the stability class
- r = reflection coefficient, the fraction of particles that are reflected from the ground surface. The corresponding coefficient for reflections from the base of the inversion is assumed to be unity.

In order to incorporate the effect of particle fallout into our calculations we adopted the tilted-plume method presented by Van der Hoven,[3/] and also used by Cramer[4/]. Equation (4.2) makes use of the effective plume height, H', given by:

$$H' = H - (v_s/u)\,x, \tag{4.3}$$

where v_s is the particle fall rate. This is essentially the method previously used in Phase I to account for particles falling out of the cloud.

3/ Meteorology and Atomic Energy 1968, David H. Slade, Editor, AEC, July 1968.

4/ Cramer, et al. op. cit.

Modification for Large Distance Downwind

When the vertical range over which the plume is mixed becomes equal to the depth of the mixed layer (below the inversion), we can assume that a relatively uniform distribution of particles in the vertical exists. The model therefore makes the distribution of graphite fibers uniform in the vertical, from the ground surface to the base of the inversion, when σ_z becomes larger than 1.6 H_m, and where H_m is the height of the base of the inversion.

At distances far enough downwind ($\sigma_z > 1.6\ H_m$) that mixing results in an essentially uniform distribution of the fibers in the vertical, we therefore use:

$$E(x,y,0,H') = \frac{Q}{2.5066\sigma_y H_m u}\left[\exp -\frac{1}{2}\left(\frac{y}{\sigma_y}\right)^2\right] \exp\left[-\frac{v_s\ x\ (1-r)}{u_{H_m}}\right] \quad (4.4)$$

The general form of this expression follows Turner [5/], except for the final term, which accounts for the fallout of the particles due to gravitational settling. This result may be derived by considering the change in the number of particles in a uniformly distributed layer during a small time interval of length dt:

$$dN = -(N/H_m)\ v_s(1-r)dt$$

where N is the number of particles, and the other variables have been defined previously. Upon integration we obtain

$$N = N(0)\ \exp\left[-(v_s/H_m)\ (1-r)\ t\right] \quad (4.5)$$

where N(0) is the number of particles present at time t=0. Since t may be estimated by the ratio x/u, we obtain the final term appearing in Equation (4.4).

INPUTS TO TRANSPORT CALCULATIONS

Actual mixing height values were developed, as in Phase I, from climatological mean values reported by Holzworth[6/], modified for different

---

[5/] D. Bruce Turner, Workbook of Atmospheric Dispersion Estimates, EPA, 1970. Publication No. AP-26.

[6/] Holzworth, Mixing Heights, Wind Speeds, and Potential for Urban Air Pollution Throughout the Contiguous United States, EPA, January 1972.

stability conditions as suggested by Calder [7]. Sensitivity tests to determine the impact of changes in mixing height values are presented later in this report.

In many diffusion problems it is customary to determine the location of an upwind virtual point source from which a diffusing plume would have grown to the size computed at plume stabilization. In view of the large uncertainties in other phases of the risk calculation, and our concern with effects some miles downwind from the accident site, we have set the virtual point source directly over the accident - fire site.

The reflection coefficient has been set equal to 1 at the inversion and to 0.7 at the ground. These values were developed in consultation with Messrs. Cramer and Tretheway at a meeting convened by the NASA Graphite Fiber Risk Assessment Program Office. The general association between the 2 centimeter-per-second fall rate of the fiber particles and the reflection coefficient at the ground has been demonstrated by Dumbauld, Rafferty, and Cramer.

The diffusion calculation requires input values of the dispersion parameters, σ_y and σ_z, as functions of the downwind distance, x, and the prevailing stability conditions. The standard in this case is provided by the well-known Pasquill-Gifford curves [8]. Several invesigators have questioned their universal applicability; the reader is referred to Pasquill's recent work on this subject [9]. In view of the fact that no generally accepted modification of the Pasquill-Gifford curves exists, we adopted these curves for the Phase I calculations and continued to use them in Phase II. For present purposes there were most conveniently used in the form of a computer program made available by EPA.

The basic weather inputs required, surface wind speed and direction, and stability class, are drawn from historical data. These data were obtained

---

[7] K. L. Calder, "A Climatological Model for Multiple Source Urban Air Pollution," Appendix D to A. D. Buse and J. R. Zimmerman, User's Guide for the Climatological Dispersion Model, EPA-71-024, December 1973.

[8] See Turner, op cit, for example.

[9] F. Pasquill, Atmospheric Dispersion Parameters in Gaussian Plume Modeling, Part II, "Possible Requirements for Change in the Turner Workbook Values," EPA-600/4-76-0306.

from the National Weather Records Center for the airports we studied; the data provide the frequency for each combination of the three weather parameters. The simulation model makes a random draw of one of these combinations weighted by the input frequency.

TRANSPORT AND DIFFUSION MODEL SENSITIVITY TESTS

ORI, Inc. was required by the Phase II contract to test the model results' sensitivity to different particle sizes. For this purpose the transport and diffusion calculations were performed independently of the complete risk assessment model. Figures 4.1 to 4.4 compare the downwind "foot-prints" for 200 kilograms of carbon released as single fibers and as brush-clumps in different meteorological conditions. The input conditions for these results are summarized in Table 4.2.

In order to normalize the comparison, the amount of carbon release in the two forms is kept constant in the different calculations. The combination of the reduced number of particles — 10^8 clumps versus 10^{12} singles — and the higher fall rate of the clumps results in a greatly reduced footprint for the clumps. The maximum exposures for the clump calculations are lower than for the singles by at least two orders of magnitude. The dominant factor in these comparisons is the difference in the number of particles per kilogram.

GEOGRAPHICAL INPUTS

The methods described to this point permit the computer model to generate an accident, determine a release amount of CF, the height to which the carbon fibers are lofted, and the downwind transport end diffusion of these fibers. All of these events are randomized using appropriate Monte Carlo methods. The transport and diffusion calculation provides the dosage or exposure at particular points defined by their by x, y coordinates. It is appropriate to define these points here, although much of the underlying motivation comes from the methods used in the cost calculations, described later. Briefly, it is pointed out here that much of the required economic data is county based. For this reason the focus of our interest is on counties surrounding the airport at or near which simulated accidents may occur.

TABLE 4.2

SUMMARY OF INPUT CONDITIONS
AND RESULTS OBTAINED
IN TEST OF TRANSPORT/DIFFUSION
MODEL FOR DIFFERENT FIBER
PARTICLE SIZES

(Release = 200 kilograms)

Meteorology	Output	Particle Size			
		Single		Clump	
		No.	Fall Rate (M/sec)	No.	Fall Rate (M/sec)
		10^{12}	.02	10^{8}	1.0
Stability Class 6 Plume Height 100 m Mean Wind 5-5 m/sec	Fig. No.	4.1		4.2	
	Max Exp. (FSec/m^3)	$2x10^6$		$2x10^4$	
Stability Class 1 Plume Height 1900m	Fig. No.	4.3		4.4	
Mean wind 3.5 M/sec	Max Exp. (FSec/m^3)	$1.6x10^5$		20	

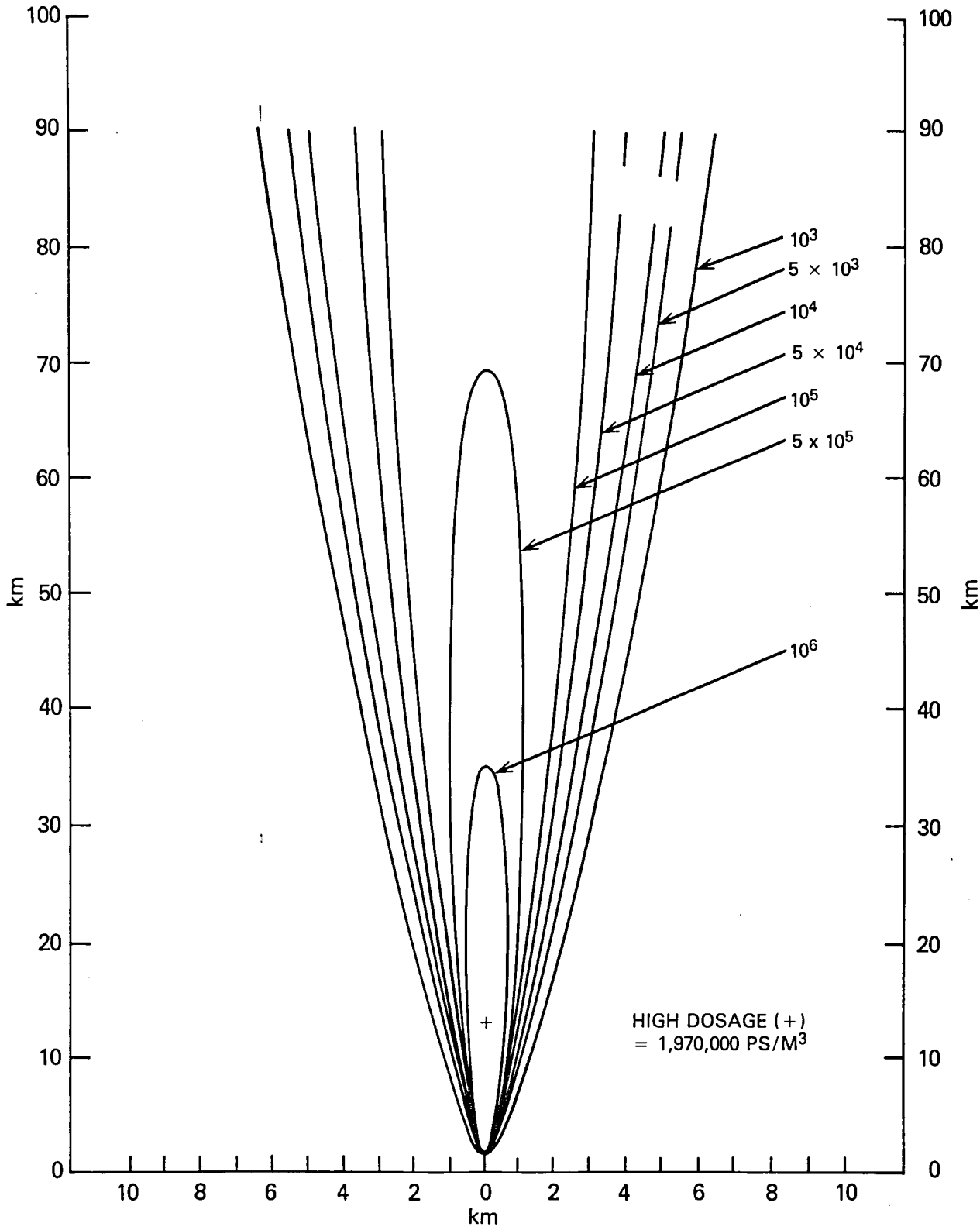

FIGURE 4.1. DOWNWIND EXPOSURE PATTERN (Fiber-seconds/cubic meter); SINGLES, STABILITY CLASS 6.

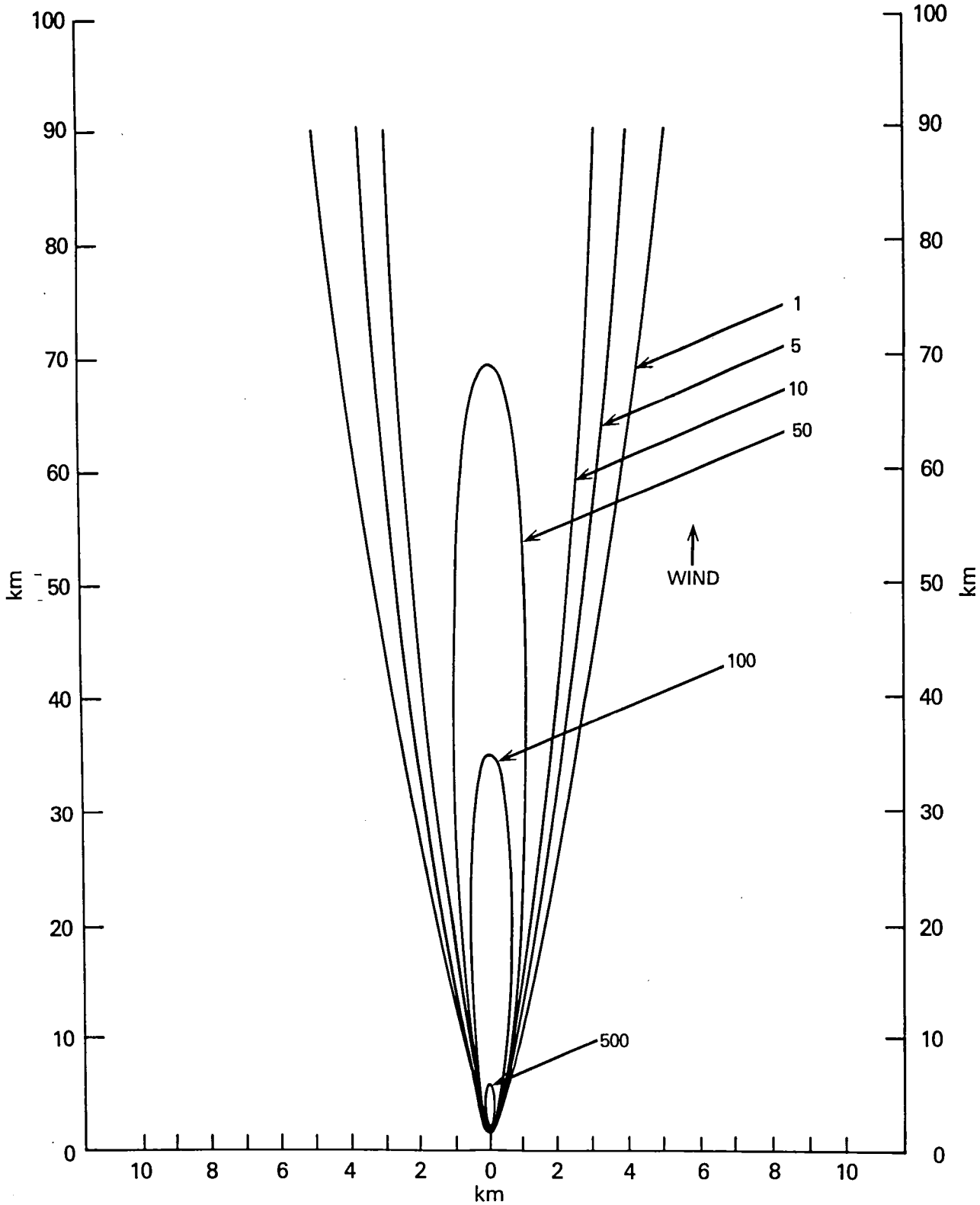

FIGURE 4.2. DOWNWIND EXPOSURE PATTERN (Fiber-seconds/cubic meter); CLUMPS, STABILITY CLASS 6.

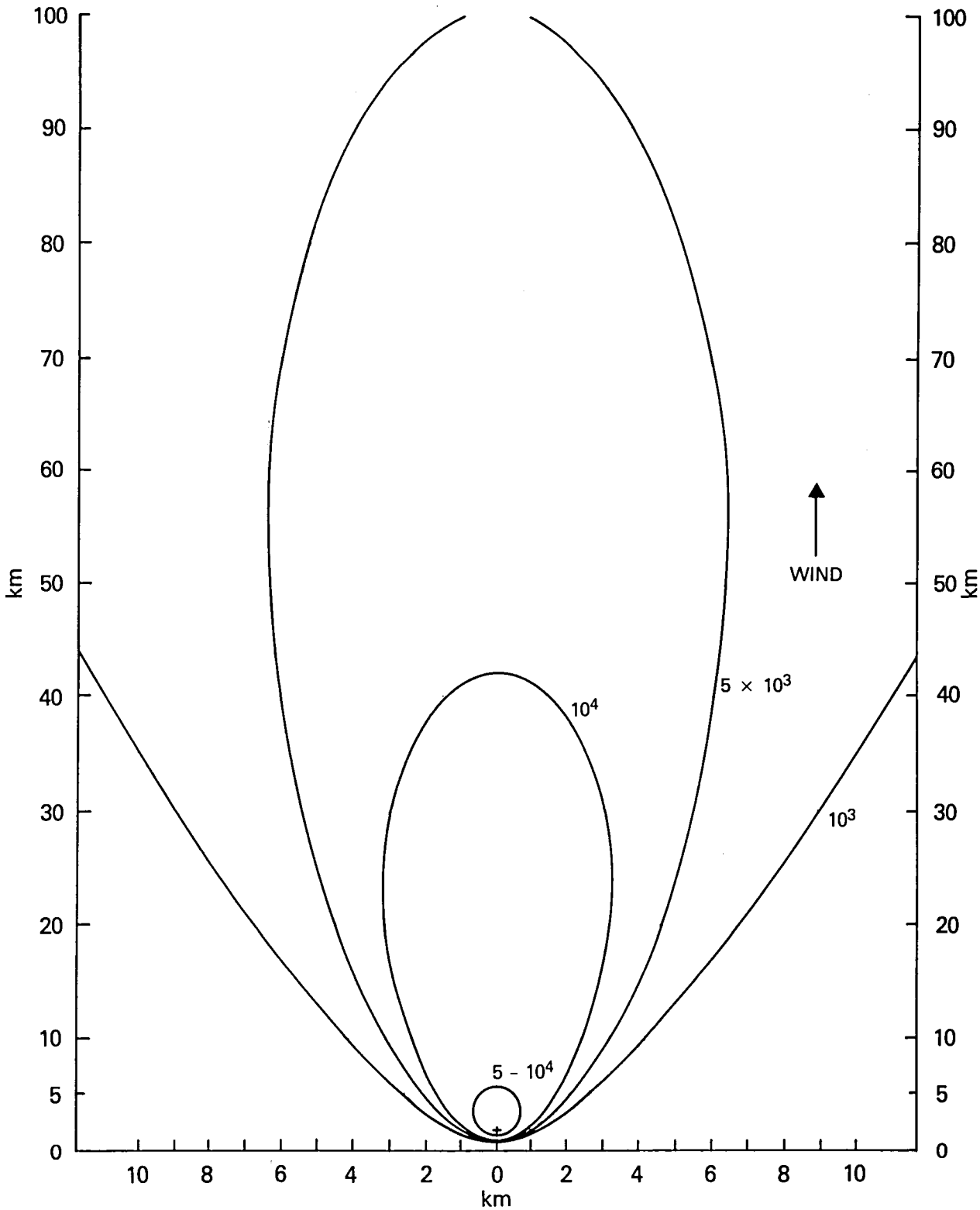

FIGURE 4.3. DOWNWIND EXPOSURE PATTERN (Fiber-second/cubic meter); SINGLES, STABILITY CLASS 1.

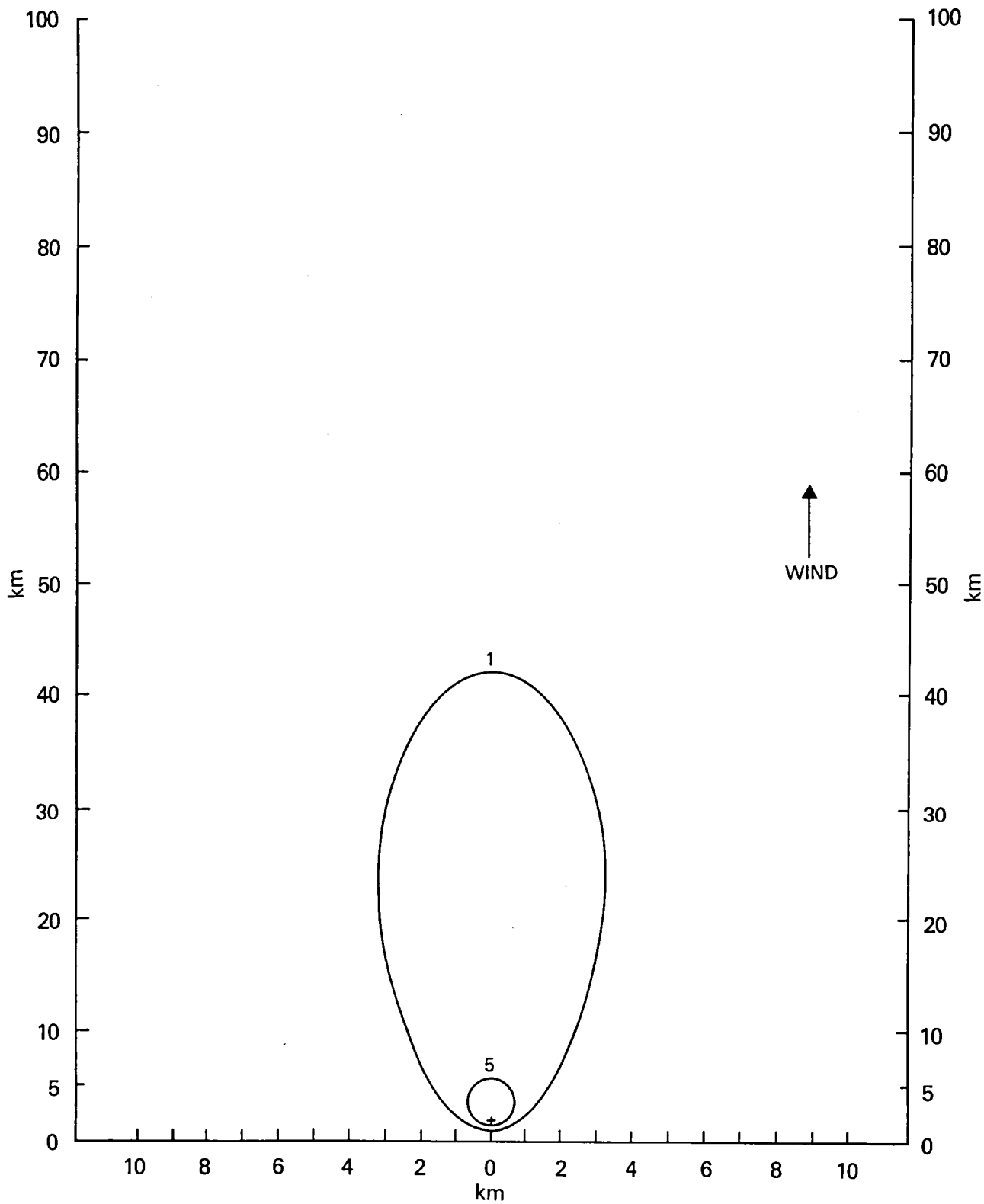

FIGURE 4.4 DOWNWIND EXPOSURE PATTERN (Fiber-seconds/cubic meter); CLUMPS, STABILITY CLASS 1.

As in Phase I, then, county-based economic data were adopted for computer input; in many cases counties were divided into smaller, homogeneous geographical units. In each case the center of the county or sub-county geographical unit was selected and a representative circle inscribed within that area. The input data set includes the coordinates of the center and the associated radius. The exposure and resulting impact calculations are made at the center and points a distance equal to two-thirds of the radius to the east, west, north, and south of the center.

Figure 4.5 shows this geometrical pattern schematically. This method was adopted to provide area-sensitivity in the resulting impact calculation. The use of the two-thirds radius mesh interval was selected so that representative points selected in neighboring circles could not be colocated. The resulting mesh, if all circles were equal in size, would be square with all points equidistant from one another.

In each case the county-based business/industry sites are uniformly distributed over these five points. The concept is illustrated in Figure 4.6, as it was applied to <u>one</u> county for the Washington National Airport risk calculations. In all cases this method was applied to the area around each airport to a distance of 50 miles or more.

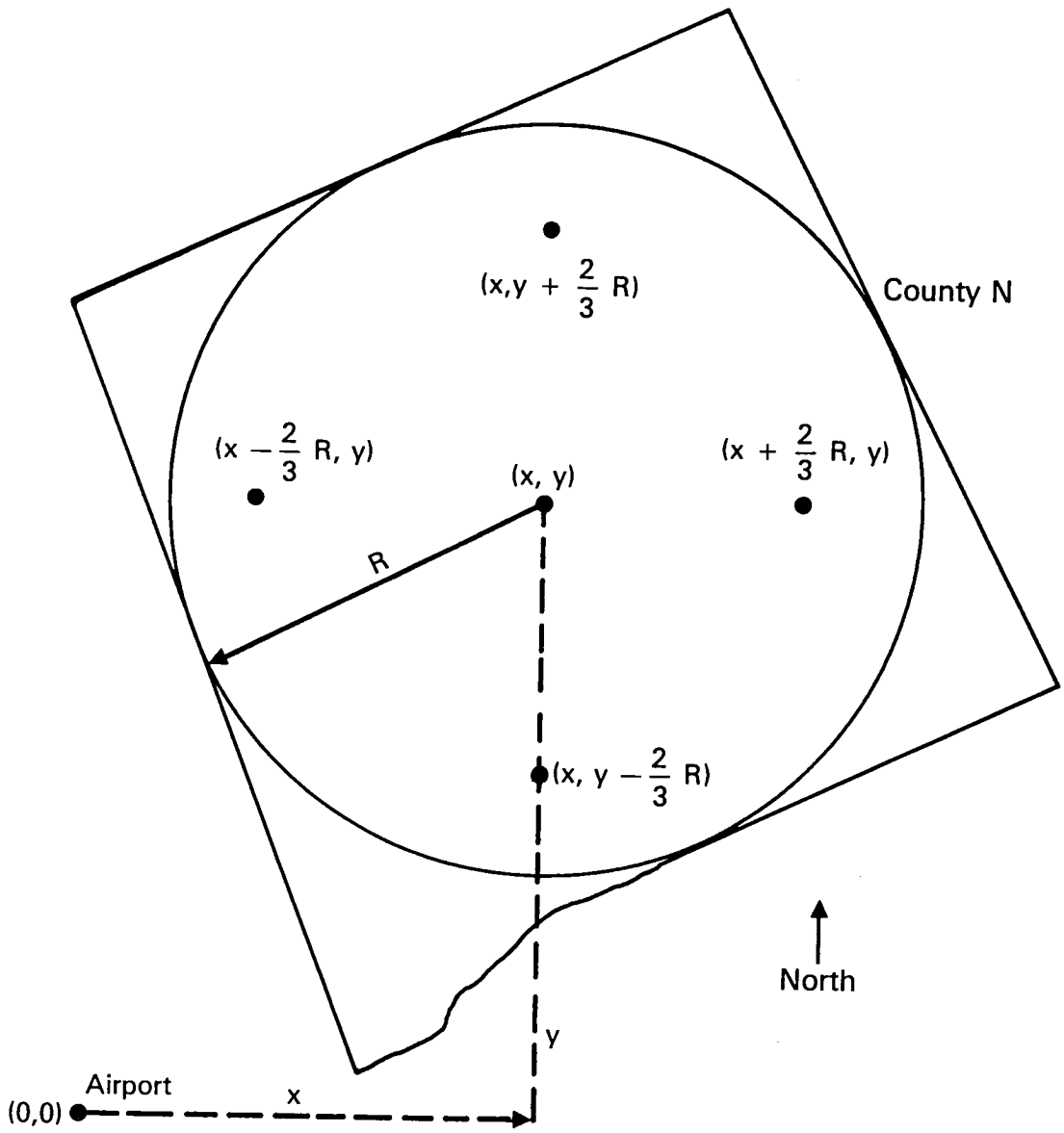

FIGURE 4.5. SCHEMATIC METHOD OF MODELLING AN INDIVIDUAL COUNTY, SHOWING REPRESENTATIVE POINTS AT WHICH EXPOSURE AND IMPACTS ARE COMPUTED.

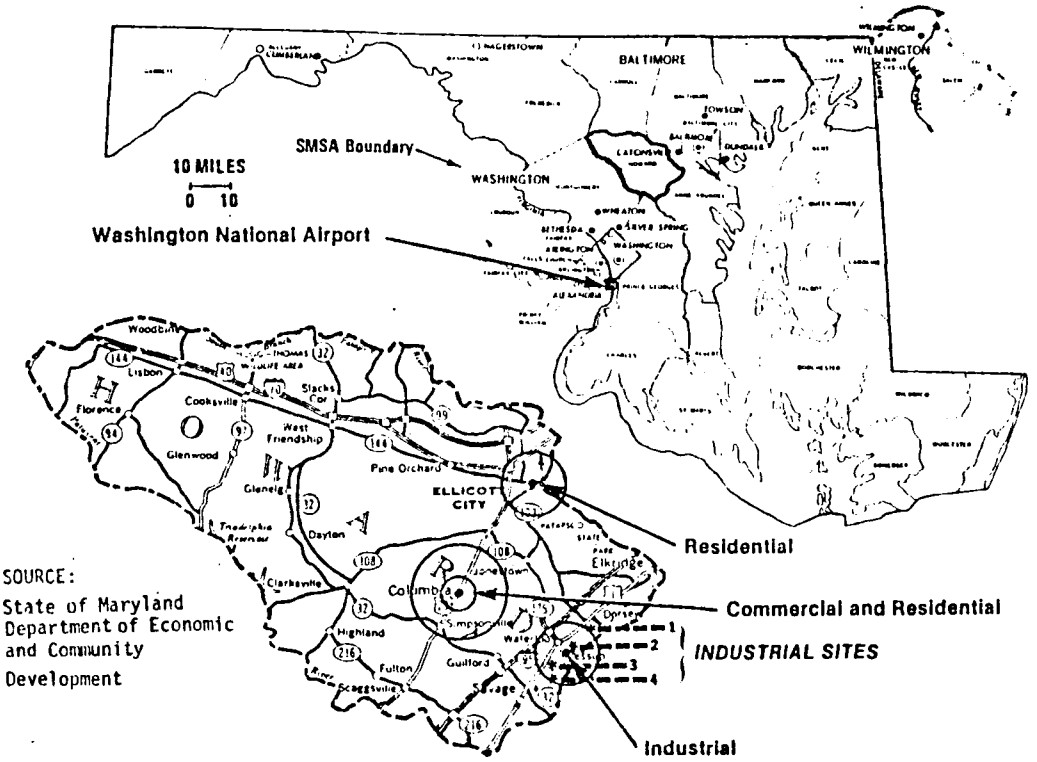

FIGURE 4.6. Definition of Areas at Risk for Washington National Airport. Howard County, Maryland, Outlined in Upper Map, Shown in Detail in Lower Map. Circles Represent Concentrations of Business, Industry, and Residences. Method was Applied to all Counties Within 50 Miles of Airport.

V. TRANSFER OF FIBERS INTO INTERIOR OF STRUCTURES

In computing the impact on electrical and electronic equipment of exposure to carbon fibers we are principally concerned with equipment inside buildings. It is therefore necessary to compute the exposure inside a building resulting from a known value of the exposure outside. This section of the report describes the methods developed by ORI to accomplish this. In the logic flow of the risk assessment simulation model the transfer calculation follows the computation of exterior exposure values.

METHOD

When a building is impinged on by a plume of carbon fibers, some of the fibers may enter the building through air conditioning or other ventilation systems and by various leakage paths. Once inside the building or enclosure, fibers will be removed by fallout and through leakage paths back to the outside. If inside air is recirculated and filtered, additional fibers will be removed. The concentration of fibers that produce failure stresses on equipments in a building or enclosure at any time may be determined from equations describing the net flow. These have been developed in a relatively simple form by Slade.[1)]

1/ David H. Slade, Editor, Meteorology and Atomic Energy, AEC, July 1968.

In Phase I, ORI was able to show that the "transfer function" or ratio of interior to exterior exposure can be expressed as:

$$\frac{E}{E_o} = \frac{v_i}{v_o + av_s + v_r} \tag{5.1}$$

where:

v_i = rate at which fiber-borne air enters the building, or enclosure through the air conditioning system and all leakage paths

v_o = rate at which fiber-borne air leaves the building, including that removed by recirculation

v_s = fall rate of carbon fibers

v_r = rate at which fibers are removed by recirculation filtering

s = volume of building or enclosure

a = area of space subject to fallout.

IMPLEMENTATION

As in the earlier Phase I effort, Equation (5.1) provided the basis for calculating interior exposure values. In Phase I, ORI, Inc. defined several types of buildings and other enclosures; each was characterized by size, types of doors and windows and ventilating equipment. These basic enclosure types were used with some minor revisions in Phase II. It was no longer necessary to treat equipment enclosures explicitly since all equipment failure tests (see Section VI below) included the effect of typical enclosures. The following principal building/enclosure categories were defined in Phase II:

1. Small Equipment Building or Van
2. Medium Equipment Building
3. Large Equipment Building or Factory
4. Equipment Room in Building
5. Utility Room
   a) filtered
   b) unfiltered
6. Residence
   a) air conditioned
   b) not air conditioned
7. Retail/Wholesale Establishments.

Generalized design factors are associated with each of these building/enclosure types in Table 5.1.

It was shown in Phase I, that, as long as basic architectural relationships are maintained, the ventilation mode of a building is essentially independent of the actual size of the building. These design factors are used to determine the air conditioning flow rates, filter efficiencies, and air leakage rates used in Equation (5.1). Ventilation rates were based on published industry standards[2,3]. The values of filter efficiency used in Phase I were changed to incorporate new experimental results. It was also shown in Phase I that, although ventilation rates are a function of wind speed, the "fallout term" in Equation (5.1) tends to be dominant. Accordingly, transfer functions were computed for a nominal 10 meter-per-second wind speed. The resulting transfer functions, shown in Table 5.2, were used in all Phase II calculations. Specific building types were associated with different categories of business and industry, as described in Section VI, below.

2/ Carrier Air Conditioning C., Handbook of Air Conditioning System Design, McGraw-Hill Book Co., 1965

3/ Baumeister & Marks, Standard Handbook for Mechanical Engineers, McGraw-Hill Book Co., 1967.

TABLE 5.1
DESIGN FACTORS FOR ORI STANDARD ENCLOSURES

Enclosure Category	Size W x L x H (feet)	Doors Facing Wind			Windows Facing Wind			Ventilation Rate (CFM)
		No.	Size	Type	No.	Size	Type	
1. Small Equipment Building or Van	15 x 30 x 15	1	3' x 7'	Industrial/ Weatherstrip	0			300
2. Medium Equipment Building	30 x 60 x 10	2	3' x 7'	Industrial/ Weatherstrip	2	3' x 5'	Industrial Casement 1/64" Crack	1000
3. Large Equipment Building or Factory Building (per floor)	100 x 300 x 10'	3	3' x 7'	Industrial/ Weatherstrip	20	3' x 5'	Industrial Casement 1/64" Crack	3000
4. Equipment Room in Building (one exterior wall)	30 x 60 x 10	2	3' x 7' Interior/ Exterior Vestibule	Factory Type Interior and Exterior	5	3' x 5'	Industrial Casement 1/64" Crack	1000
5. Utility Room	30 x 60 x 10	1	3' x 7'	Factory Type Exterior/ 1/8" Crack	0	- -	- -	500
6. Residences	40 x 30 x 8	1	3' x 7'	Glass - Avg. Fit 3/16" Crack	4	4' x 7'	Residential Casement 1/32" Crack	a - 300 / b - None
7. Retail/Wholesale Establishments	60 x 40 x 10	1	3' x 7'	Swinging	All Windows Sealed			500

TABLE 5.2 - TRANSFER FUNCTIONS FOR STANDARD ENCLOSURES

Enclosure Category		Transfer Function
1. Small Equipment Building or Van		.012
2. Medium Equipment Building		.010
3. Large Equipment Building or Factory Building (per floor)		.004
4. Equipment Room in Building (one exterior wall)		.010
5. Utility Room	Filtered	.023
	Non-Filtered	.094
6. Residence	Air Conditioned	.058
	Not air Conditioned	.004
7. Retail/Wholesale Establishment		.004

VI. EQUIPMENT FAILURES

FAILURE MODEL

The probability of failure of equipment which is exposed to carbon fibers is obtained from the exponential expression:

$$P_F = 1 - \exp(-E/\overline{E}) \tag{6.1}$$

where:

P_F = probability of equipment failure

E = exposure level in the immediate vicinity of the vulnerable equipment, in fiber-seconds per cubic meter

$\overline{E}$ = average exposure causing a failure.

During Phase I, the U.S. Army Ballistics Research Laboratory (BRL) at Aberdeen, Maryland, determined that experimental failure data for many classes of equipment fit an exponential failure law[1,2/]. Later, it was shown that certain failures were mutliple-fiber events. It appeared that the generalized Weibull distribution provided a better fit to failure data for those equipments. In Phase II it has been shown that, even for those equipments whose

---

1/ Shelton and Moore, Have Name Vulnerability of the Improved Hawk System, BRL Report No. 1964, February 1977.

2/ ORI discussions with BRL, August 15, 1978.

failures do not obey the exponential law, it is conservative to use the exponential law in estimating failures. The exponential relationship gives a higher value of the failure probability for low values of the exposure than the Weibull distribution, thus overestimating failures, and providing the desired conservatism in estimating the overall risk. Typical values of the exponential failure parameter for generic equipment types are shown below in Table 6.1. It should be noted that the failure concepts developed here apply only to equipment when it is energized.

The exposure used in Equation (6.1) is that directly impinging on the vulnerable equipment. When this equipment is inside a building, the interior exposure may be obtained from the exterior exposure by multiplying the exterior exposure by the appropriate transfer function (TF), as described in Section V, above. Since the transfer function and the mean exposure to failure, $\overline{E}$, are constants for a particular piece of equipment in a particular building, we define a failure parameter:

$$K_{ij} = (TF)_j/\overline{E}_i \qquad (6.2)$$

where:

K_{ij} = overall failure parameter for equipment of type i in a building of type j

$(TF)_j$ = penetration factor (transfer function) for a building of type j

$\overline{E}_i$ = mean exposure to failure for equipment of type i.

In subsequent applications, the parameter K_{ij} is substituted into Equation (6.1) to give the probability of failure for equipment of type i in a building of type j for any exterior exposure:

$$P_{F,ij} = 1 - \exp(-K_{ij}E_o) \qquad (6.3)$$

Thus, although the exterior-to-interior transfer process has been discussed as a separate entity in the preceding section, we were able to combine the failure and transfer calculations in one procedural step by defining specific equipments in specific types of buildings. These methods are described in more detail below.

EQUIPMENT CONFIGURATIONS

In treating typical equipment configurations it is convenient to develop expressions for the collective probability of failure of the complete configuration. In particular, if n identical equipments are in series so that a failure of one causes the entire "line" to fail, the probability that the line fails is:

$$P_F\ (\text{LINE}) = 1 - (1 - P_{F,ij})^n$$

$$= 1 - e^{-nK_{ij}E_o} \qquad (6.4)$$

Similarly if n like equipments are in parallel, so that the operation fails only if all equipments fail, the aggregate probability of failure is:

$$P_F(\text{Operation}) = P_{F,ij}^n \qquad (6.5)$$

The computer program that determines the impact of each simulated aircraft accident and associated release of graphite fibers uses Equations (6.3)-(6.5) to estimate the probability that each business or industry in the geographical area of interest is affected.

One of the major efforts in Phase I was the characterization of each business-industry sector, defined by an SIC (Standard Industrial Classification) number, by a specific set of equipments installed in a specific type of building. This effort was extended and made more detailed in Phase II. The generalized business/industry equipment configuration showing the electric power flow appears in Figure 6.1; in any one class of business or industry portions of this configuration may not be present. Typical individual equipments in each of the modules shown in Figure 6.1 are defined in Table 6.1, with their estimated values of mean exposure to failure.

The equipment configuration was made specific to plants of different size (small, medium, and large) in each pertinent SIC - number category. An example will illustrate the method. A large plant in Category 28A (comprising all 3-digit SIC code numbers under 28, basically chemical and allied products) has an internal power interface characterized by one set of input power service equipment, one distribution panel, and an auxiliary generator. Its common module consists of two computers in parallel and two keyboard display units in parallel. The plant has 25 lines in its distributed module. Each line

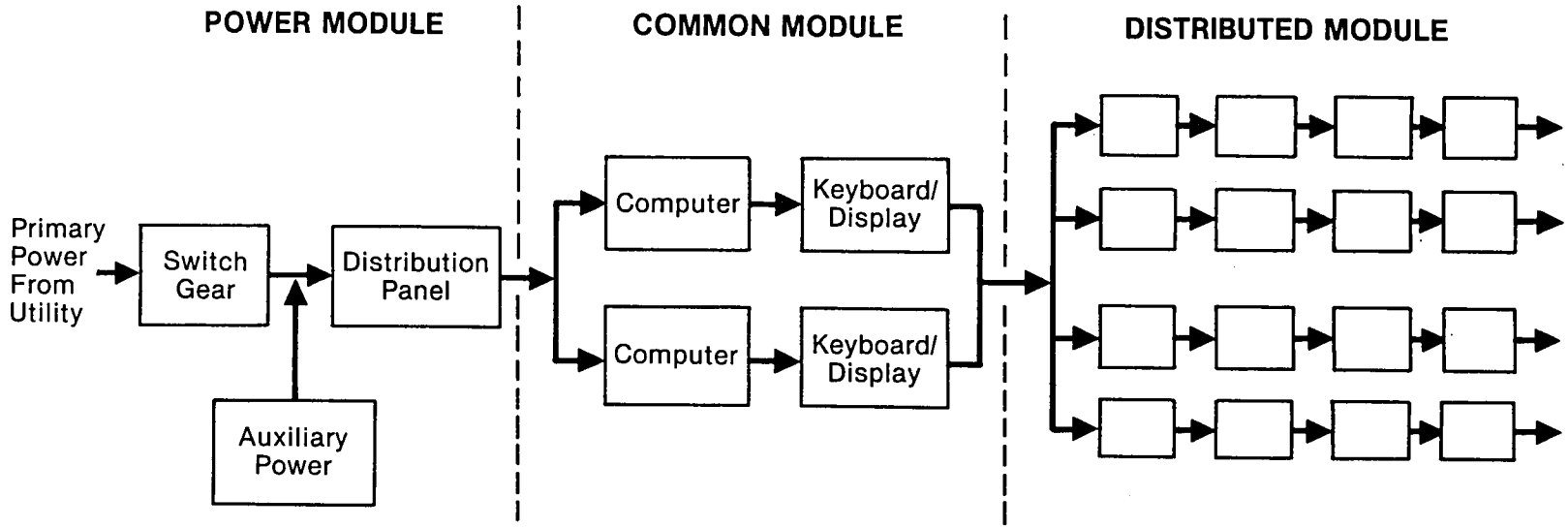

FIGURE 6.1. GENERALIZED BUSINESS/INDUSTRY EQUIPMENT CONFIGURATION AND POWER FLOW

TABLE 6.1

GENERIC BUSINESS/INDUSTRY EQUIPMENTS WITH MEAN EXPOSURE TO FAILURE VALUES ($\bar{E}$ IN FIBER SECONDS/METER^3)

Module	Equipment		Failure Parameter ($\bar{E}$)
	Code	Definition	
Power	SW	Input power service equipment - transformers, breakers, switchgear	10^8
	DIST	Power distribution buses and panels	10^8
	AUX	Auxiliary power supply in parallel with power input	10^6
Common	COMP	Standard-size computer used as a central facility controller	10^7
	K/D	Keyboard-display unit	10^8
Distributed	PS	High-voltage power supply at a machine station	10^8
	INT	Interface unit used to buffer central computers to line controllers	10^8
	MC	Manual controller, associated with each electrically-operated machine	10^8
	MPC	Mini-computer used as a programmable controller	10^8
	μPC	Microprocessor used as a controller	10^8
	MM	High-voltage motor controller	10^8
	MS	Machine station servo-mechanism	10^8
	MH	Heater or oven control	10^8
	SENSOR	Device to measure temperature, thickness, weight, position, motion, etc.	10^7

consists of:

- 5 high-voltage power supply units
- 5 interface units
- 5 manual controllers
- 5 minicomputers, used as controllers
- 2 high-voltage motor controllers
- 2 machine station servo-mechanisms
- 1 heater control unit
- 5 sensor units.

Similar configurations were defined for all vulnerable categories of business and industry. The data was developed as a result of an extensive literature search, augmented by site visits during Phases I and II.

The data collection effort during ORI's risk assessment contract included visits to one or more plants in each of the following major categories:

- 2011 - Meatpacking
- 2331 - Womens Blouses
- 262 - Paper Mills
- 2721 - Periodicals
- 2732 - Book Printing
- 3519 - Internal Combustion Engine Manufacturing
- 3661 - Telephone and Telegraph Equipment
- 3662 - Electronic Equipment
- 458 - Air Transportation Services
- 481 - Radio and Television Broadcasting
- 491 - Electric Services
- 806 - Hospitals

The results of these site visits, conferences with NASA personnel, and the earlier literature surveys are summarized in Table 6.2. Typically, a large factory has more than 250 employees, a medium size factory 50 to 249 employees, and a small factory 20 to 49 employees.

TABLE 6.2
EQUIPMENT CONFIGURATIONS FOR MANUFACTURING FACILITIES BY SIC GROUP AND SIZE (NO. OF EQUIPMENTS)

SIC GROUP/ SIZE		POWER MODULE			COMMON MODULE		DISTRIBUTED MODULE										
		SW	DIST	K/D	COMP	K/D	NO. OF LINES	PS	INT	MC	MPC	μPC	K/D	MM	MS	MH	SENSOR
20A	L	1	1	1	0	0	25	0	0	5	0	0	0	0	0	0	0
	M	1	1	0	0	0	10	0	0	5	0	0	0	0	0	0	0
	S	0	1	0	0	0	1	0	0	5	0	0	0	0	0	0	0
20B	L	1	1	1	(2)	(2)	5	1	12	12	12	0	0	0	0	0	0
	M	1	1	0	0	0	3	1	1	12	1	12	1	0	5	1	12
	S	0	1	0	0	0	1	0	0	12	0	0	0	0	0	0	0
21A	L	1	1	1	0	0	25	0	0	5	0	1	0	0	1	0	1
	M	1	1	0	0	0	10	0	0	5	0	0	0	0	0	0	0
	S	0	1	0	0	0	1	0	0	5	0	0	0	0	0	0	0
22A	L	1	1	1	(2)	(2)	50	1	6	6	6	0	0	1	3	0	6
	M	1	1	0	0	0	10	1	1	6	1	6	1	1	3	0	6
	S	0	1	0	0	0	5	0	0	6	0	0	0	1	0	0	0
23A	L	1	1	1	0	0	75	0	0	4	0	2	0	0	0	0	2
	M	0	1	0	0	0	25	0	0	4	0	2	0	0	0	0	2
	S	0	1	0	0	0	5	0	0	4	0	0	0	0	0	0	0
24A	L	1	1	1	0	0	10	0	0	6	0	0	0	0	0	0	0
	M	1	1	0	0	0	5	0	0	6	0	0	0	0	0	0	0
	S	0	1	0	0	0	1	0	0	6	0	0	0	0	0	0	0
25A	L	1	1	1	0	0	10	0	0	6	0	0	0	0	0	0	0
	M	1	1	0	0	0	5	0	0	6	0	0	0	0	0	0	0
	S	0	1	0	0	0	1	0	0	6	0	0	0	0	0	0	0
26A	L	1	1	1	(2)	(2)	3	4	8	8	8	3	0	4	3	1	4
	M	1	1	0	0	0	3	2	0	6	1	5	1	3	3	0	2
28A	L	1	1	1	(2)	(2)	25	5	5	5	5	0	0	2	2	1	5
	M	1	1	0	0	0	10	5	1	5	1	5	1	2	2	1	5
	S	0	1	0	0	0	1	0	0	5	0	0	0	2	0	0	0
29A	L	1	1	1	(2)	(2)	10	5	1	8	1	8	0	8	0	0	5
30A	L	1	1	1	(2)	(2)	25	5	5	5	5	0	0	2	2	1	5
	M	1	1	0	0	0	10	5	1	5	1	5	1	2	2	1	5
	S	0	1	0	0	0	1	0	0	5	0	0	0	2	0	0	0
32A	L	1	1	1	0	0	5	2	1	8	6	0	1	0	5	2	5
33A	L	1	1	1	(2)	(2)	5	2	1	8	1	6	1	5	0	0	5
35A	L	1	1	1	(2)	(2)	50	1	1	5	1	5	1	0	5	0	2
	M	1	1	0	0	0	20	1	0	5	0	5	0	0	5	0	2
	S	0	1	0	0	0	5	0	0	5	0	0	0	0	0	0	0
35B	L	1	1	0	0	0	5	0	0	0	0	1	0	0	0	0	0
36A	L	1	1	1	(2)	(2)	50	1	1	5	1	5	0	2	2	0	2
	M	1	1	0	0	0	20	1	0	5	0	5	0	2	2	0	2
	S	0	1	0	0	0	5	0	0	5	0	0	0	2	0	0	0
36B	L	1	1	1	(2)	(2)	50	1	1	5	1	5	0	0	3	1	2
	M	1	1	0	0	0	20	1	0	5	0	5	0	0	3	1	2
	S	0	1	0	0	0	5	0	0	5	0	0	0	0	0	0	0
36C	L	1	1	0	0	0	6	0	0	0	0	1	0	0	0	0	0
37A	L	1	1	1	(2)	(2)	50	2	1	8	1	8	1	2	4	1	5
38A	L	1	1	1	0	0	25	1	1	5	1	5	1	0	4	1	5
	M	1	1	0	0	0	10	1	0	5	0	5	0	0	4	1	5
	S	0	1	0	0	0	5	0	0	5	0	0	0	0	0	0	0

( ) DENOTES EQUIPMENTS IN PARALLEL
SIC GROUPS ARE DEFINED IN NOTES FOLLOWING

Notes to Table 6.2

ORI Code	SIC Numbers Included	Types of Business/Industry
20 A	201, 202, 209	Meat, Dairy, Misc. Food and Kindred Products
20 B	203, 204, 205, 206, 208	Preserved Fruits and Vegitables, Grainmill, Bakery, Sugar, Fruits, Oils and Beverages
21 A	21 X	Tobacco Manufacturers
22 A	22 X	Textile Mill Products
23 A	23 X	Apparel and Other Textile Mill Products
24 A	24 X	Lumber and Wood Products
25 A	25 X	Furniture and Fixtures
26 A	26 X	Papers and Allied Products
27 A	27 X	Printing and Publishing
28 A	28 X	Chemicals and Allied Products
29 A	29 X	Petroleum and Coal Products
30 A	30 X	Rubber and Misc. Plastics Products
32 A	321, 322	Glass and Glassware
33 A	331, 332, 335	Blast Furnaces and Basic Steel Products, Iron and Steel Foundries, Non-ferrous Rolling and Drawing
35 A	35 X	Machinery, Except Electrical
36 A	361, 362, 363	Electric Equipment and Household Appliances
36 B	364, 365, 366, 367	Electric Lighting and Wiring, Radio and TV Receiving, Communication Equipment and Electronic Components and Assessories
36C	3662	Radio and TV Communication Equipment
37 A	37 X	Transportation Equipment
38 A	38 X	Instruments and Related Products

The description above provides the linkage from SIC number and size to equipment configuration, then to specific equipments and their associated failure parameters. It was also necessary, as described above in Section V, to relate specific building types to each vulnerable class of business and industry. These results are summarized in Table 6.3. The table associates the different building types defined in Table 5.1 (with transfer functions in Table 5.2) with each of the major sections (modules) of plants of different sizes in different SIC groups.

COMPUTER IMPLEMENTATION

The mean exposure-to-failure values for the generic equipments defined above were summarized in Table 6.1. In using these inputs the equipment-specific value of $\bar{E}$ was combined with the building-specific transfer function, in accordance with Equation (6.2). In order to estimate the impact on specific business and industrial complexes it was assumed that the plant is down if electric power is lost inside the plant, if the common module fails, or if more than one half of the "lines" in the distributed module fail. The implementation of these modeling concepts is described in more detail in the following section of the report.

Phase II results reported by other investigators indicated that the high-voltage power supply system is essentially invulnerable; it was assumed that an equivalent piece of equipment representing the bushings and bus of a step-down transformer could be used to represent the possibility of an exterior power supply failure.

TABLE 6.3
ENCLOSURE TYPES BY SIC/SIZE CATEGORY

SIC Group	Plant Size	Power Module			Common Module	Distributed Module
		SW	Dist.	Aux.		
20A	L	5b	3	5b	-	3
	M	5b	3	-	-	3
	S	-	2	-	-	2
20B	L	5b	3	5b	4	3
	M	5b	3	-	-	3
	S	-	2	-	-	2
21A	L	5b	3	5b	-	3
	M	5b	3	-	-	3
	S	-	2	-	-	2
22A	L	5b	3	5b	4	3
	M	5b	3	-	-	3
	S	-	2	-	-	2
23A	L	5b	3	5b	-	3
	M	-	3	-	-	3
	S	-	2	-	-	2
24A	L	5b	3	5b	-	3
	M	5b	3	-	-	3
	S	-	2	-	-	2
25A	L	5b	3	5b	-	3
	M	5b	3	-	-	3
	S	-	2	-	-	2
26A	L	5b	3	5b	4	3
	M	5b	3	-	-	3
27A	L	5b	3	5b	4	3
	M	5b	3	-	-	3
	S	-	2	-	-	2
28A	L	5b	3	5b	4	3
	M	5b	3	-	-	3
	S	-	2	-	-	2

TABLE 6.3 (CONTINUED)

SIC Group	Plant Size	Power Module			Common Module	Distributed Module
		SW	Dist.	Aux.		
29A	L	5b	3	5b	4	3
30A	L	5b	3	5b	4	3
	M	5b	3	-	-	3
	S	-	2	-	-	2
32A	L	5b	3	5b	-	3
33A	L	5b	3	5b	4	3
34A	L	5b	3	5b	-	3
	M	5b	3	-	-	3
	S	-	2	-	-	2
34B	L	5b	3	5b	-	3
	M	5b	3	-	-	3
	S	-	2	-	-	2
35A	L	5b	3	5b	4	3
	M	5b	3	-	-	3
	S	-	2	-	-	2
35B	L	5a	3	-	-	3
35C	L	5a	3	5a	-	3
36A	L	5b	3	5b	4	3
	M	5b	3	-	-	3
	S	-	2	-	-	2
36B	L	5b	3	5b	4	3
	M	5b	3	-	-	3
	S	-	2	-	-	2
37A	L	5b	3	5b	4	3
38A	L	5b	3	5b	-	3
	M	5b	3	-	-	3
	S	-	2	-	-	2

VII. COSTS DUE TO EQUIPMENT FAILURES

This section of the report presents ORI's Phase II methodology for determining the costs associated with equipment failures. The most significant changes to the Phase I methodology were introduced in this part of the risk assessment calculation. Three categories of cost were considered for business and industry impacts:

- Repair of damaged electrical equipment
- Facility cleanup
- Business/industry disruption.

In the Phase I risk assessment, attention was focussed on the latter cost category using an expected value technique. In Phase II the model has been expanded to treat all the above categories explicitly, while disruption costs are now computed using a Monte Carlo random process. Household equipment failures are treated as in Phase I, using an expected-value algorithm. A completely new submodel has been developed to compute the cost incurred as a result of failures of avionics equipment aboard commercial aircraft on the ground.

BUSINESS/INDUSTRY REPAIR COSTS

For each of the generic types of equipment defined previously (cf. Table 6.1) a repair cost was estimated, using data provided by the Ballistics Research Laboratory, information gained on the industrial site visits, and other sources. Equipment repair cost inputs are summarized in Table 7.1. In many cases it would be expected that repairs could be effected by the simple act of vacuum cleaning the equipment that failed. It was assumed, however, that a minimum repair cost would still be incurred to cover trouble-shooting and repair time on the basis that equipment users would not usually be aware of this fact.

As shown in the preceding section each business or industrial facility defined by SIC number and size has a defined equipment "suit" (cf. Table 6.2). The computer model treats all the equipments of one type at one geographical location collectively. It first computes

$$N(i) = \sum_{\text{SIC}} \sum_{S} (\text{Equipments of Type } i) \text{ SIC } S \qquad (7.1)$$

to obtain the total number of equipment of type i at the location. At its most straightforward the simulation would have been written to test each of the N(i) equipments, and determine whether each failed using a procedure that compares a random number with the computed failure probability $P_F(i)$. This procedure is easy to program, but is somewhat inefficient and wastes computer time if there are many pieces of equipment. Since each piece of equipment either fails or not the process is an example of a Bernoulli trial. The probability that exactly k equipments fail is given by [1/]:

$$b[k;\ N(i),\ P_F(i)] = \binom{N(i)}{k} P_F^k(i)\ [1-P_F(i)]^{N(i)-k} \qquad (7.2)$$

Further, if N(i) is relatively large, and $P_F(i)$ is small, which is true for the cases of interest here, and we define

$$N_F(i) = N(i)P_F(i), \qquad (7.3)$$

the expected number of failures of equipment of type i at the particular location, then is[1/]:

$$b\left[k;\ N(i),\ P_F(i)\right] \approx e^{-\overline{N}_F(i)}\ \frac{\overline{N}^k{}_F(i)}{k!}\ . \qquad (7.4)$$

[1/] W. Feller, op. cit., p. 148 et seq.

Table 7.1

INPUT REPAIR COSTS FOR ORI STANDARD EQUIPMENTS

Equipment		Repair Cost ($)
CODE	Definition	
POW	Exterior Step-Down Transformer	300
SW	Input power service equipment - transformers, breakers, switchgear	3,000
DIST	Power distribution buses and panels	2,600
AUX	Auxiliary power supply in parallel with power input	5,000
COMP	Standard-size computer used as a central facility controller	50,000
K/D	Keyboard-display unit	3,000
PS	High-voltage power supply at a machine station	2,000
INT	Interface unit used to buffer central computers to line controllers	600
MC	Manual controller, associated with each electrically-operated machine	2,500
MPC	Mini-computer used as a programmable controller	10,000
μPC	Microprocessor used as a controller	7,000
MM	High-voltage motor controller	5,600
MS	Machine station servo-mechanism	1,000
MH	Heater or oven control	1,000
SENSOR	Device to measure temperature, thickness, weight, position, motion, etc.	6,000

Equation (7.4) is the Poisson distribution with mean equal to the expected number of failures. In performing the simulation the model computes the expected number of failures for each class of equipment in turn. The number of failures is then obtained by drawing a random sample from the appropriate Poisson distribution. This method is essentially equivalent to "playing" the failure of each equipment individually but is much more economical.

The procedure described above is used in several places in the calculation, because of the simplification and economy it introduces into the calculation, with only very little loss in generality. In cases where the same class of equipment is located in facilities with different transfer functions they are treated as different equipments types for computational purposes. Once the number of failures, $N_F(i)$, is obtained by sampling the Poisson distribution, the total repair cost for that equipment type is the product of the repair cost per equipment (Table 7.1) and $N_F(i)$. This is repeated for all types of equipment at a given location in the downwind path of the plume. The computer program logic is illustrated in Figure 7.1, which is a schematic flow chart for this calculation.

FACILITY CLEAN-UP COSTS

Estimates of facility cleanup costs were made for different businesses and industries on the basis of type of business and size of plant. Using information gained during the Phase II site visits it was estimated that the decision to institute a special plant-wide cleanup would be made on the basis of evidence of major impact of the presence of carbon fibers. Accordingly, it is assumed that an intensive plant cleanup is implemented whenever the plant is shut down due to equipment failures, as described below. For each plant or other facility that is shut down the model looks up the input cleanup cost for a plant of that SIC number-size combination. The calculation of plant shut down is described below.

DISLOCATION COST

It was assumed that a plant or place of business would be shut down if power were lost, the common module failed, or more than half of the production lines failed. Figure 7.2 illustrates this concept in a decision tree formulation. The computation is done for all plants in one SIC-code number

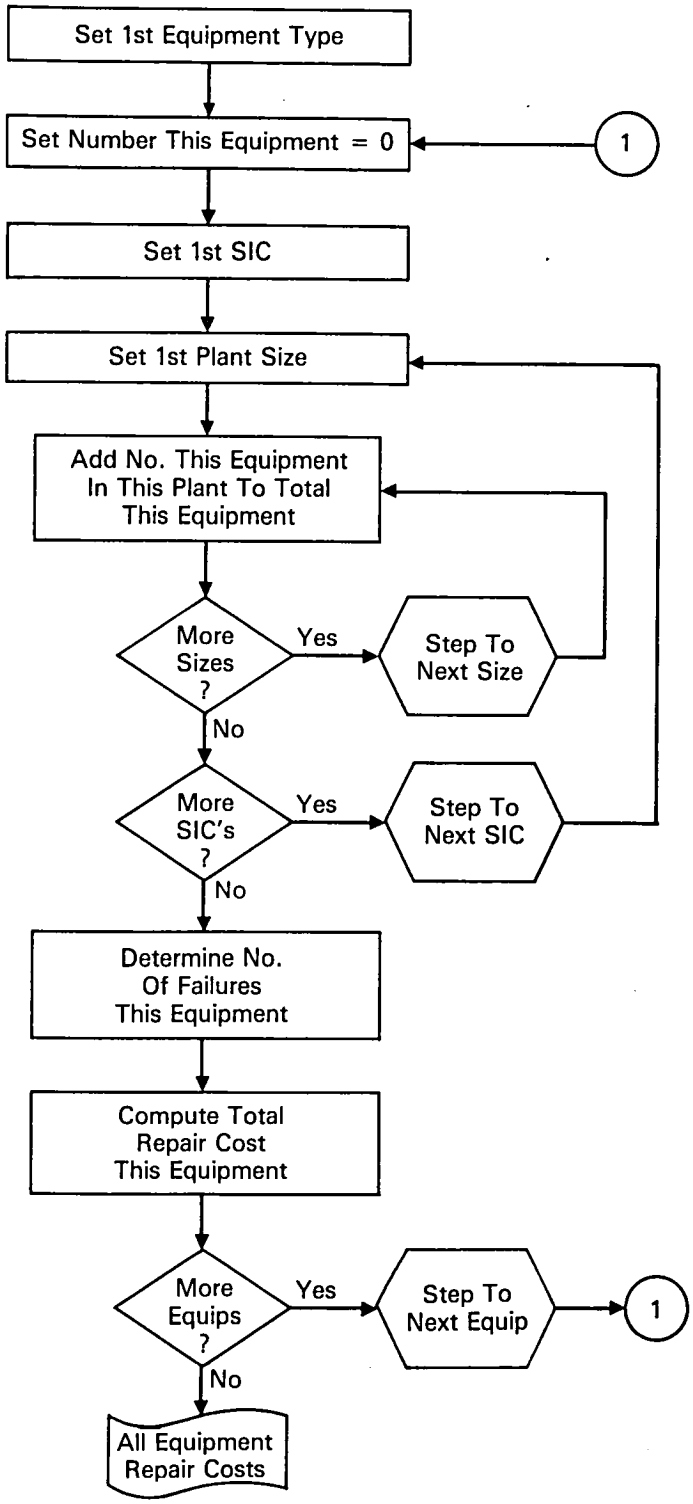

FIGURE 7.1 FLOWCHART FOR COMPUTING REPAIR COSTS DUE TO EQUIPMENT FAILURE

group at one location. In contrast to Phase I, then, we determined plant closings on a stochastic basis, rather than employing an expected-value algorithm. The shutdown calculation proceeds through each SIC number and each size group with that SIC number at each geographical location.

Individual Module Failures

The probability that the power module fails is determined by computing the probability of failure of the primary power input, the switch gear, the distribution panel, and auxiliary power, if present. The probability of a power failure ahead of the distribution panel may be expressed as

$$P_F(\text{Power In}) = \{1-\{1-P_F(\text{POW})\}\ \{1-P_F(\text{SW})\}\}\ P_F(\text{AUX}) \qquad (7.5)$$

where $P_F(\text{POW})$, $P_F(\text{SW})$, and $P_F(\text{AUX})$ are the computed failure probabilities for the primary power source, the switch gear, and the auxiliary power system, respectively. The probability that the plant is without power is then estimated by:

$$P_F(\text{Power}) = P_F(\text{Power In}) + \{1-P_F(\text{Power In})\}\ P_F(\text{DIST}) \qquad (7.6)$$

where $P_F(\text{DIST})$ is the probability of a failure at the distribution panel.

The probability that the common module fails is estimated by:

$$P_F(\text{Common}) = 1 - \{1-P_F^n(\text{COMP})\}\ \{1-P_F^m(\text{K/D})\} \qquad (7.7)$$

where $P_F(\text{COMP})$ and $P_F(\text{K/D})$ are the failure probabilities for the computer and keyboard displays respectively, and n and m are the numbers of each in parallel.

The probability that one line in the distributed module fails is given by:

$$P_F(\text{Line}) = 1 - \{1-P_F(i)\}^{n(i)}\ \ \{1-P_F(j)\}^{n(j)}\ \ldots\ldots \qquad (7.8)$$

where $P_F(i)$ is the probability of failure for equipment of type i, and n(i) is the number of units of type i in series in the line. Equation (7.8) indicates that the line fails if at least one unit in series in the line fails; in the equation we have indicated that there are n units of type i and m units of type j in the line.

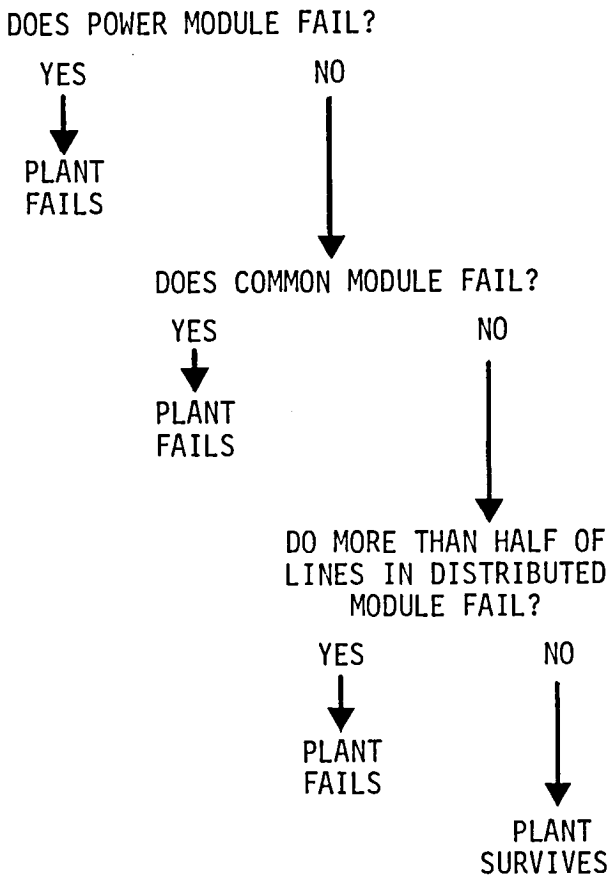

FIGURE 7.2. SCHEMATIC PLANT FAILURE DECISION TREE

Computational Method

Rather than examine each plant individually, the model examines the group of plants in the SIC number-size group. The logic is illustrated schematically in a flow chart appearing as Figure 7.3. We first determine the expected number of power module failures by multiplying the number of plants, N(SIC, Size), by P_F(Power). The actual number of power module failures is drawn from a Poisson distribution with this mean value. This method is entirely analagous to that derived above for the equipment failures.

Next, this submodel treats the surviving plants, those of the orignal N(SIC,Size) that did not suffer power module failures. The model samples a Poisson distribution with mean equal to the product of the number of survivors and P_F(Common) to determine the number of facilities that fail due to failures of the common module.

Those plants that survive the power and common module "cuts" are then examined one by one. For each of these plants we determine, again by sampling a Poisson distribution, the number of lines that fail. The expected number (or mean of the distribution) is the product of the number of lines in the distributed module and P_F(Line). For each plant the computer program determines whether the randomly generated number of lines that fail is equal to half or more of all the lines in the plant. If so, the plant is counted as "failed." This is repeated for all the survivors to determine the distributed module "cut."

The sum of all plants that failed due to power module failures, common module failures, and failures of more than half the lines in the distributed module yields the number of plants shut down due to carbon fiber impact. The computer program then turn to plants of the next SIC number. These methods constitute a calculation that generates a considerable increase in the variance relative to the Phase I methodology.

Cost Impact of Business/Industry Closings

The Monte Carlo submodel described above yields the number of plants in each SIC, size group that are shut down as the result of each simulated accident. In order to compute the impact of those plant closings in dollar terms we first estimate the fraction of the industry shutdown at the location

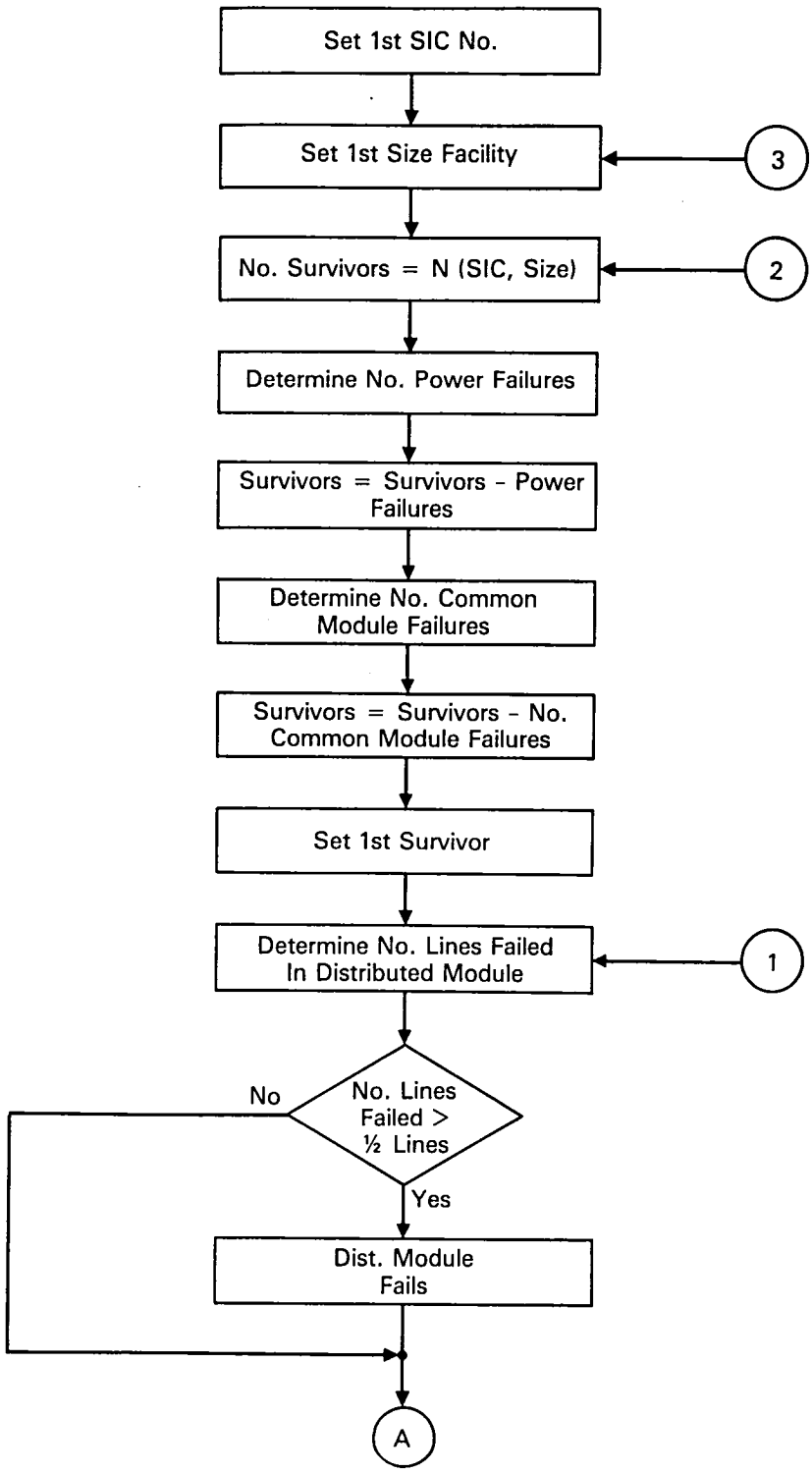

FIGURE 7.3 FLOWCHART FOR COMPUTING BUSINESS/INDUSTRY FACILITY CLOSINGS

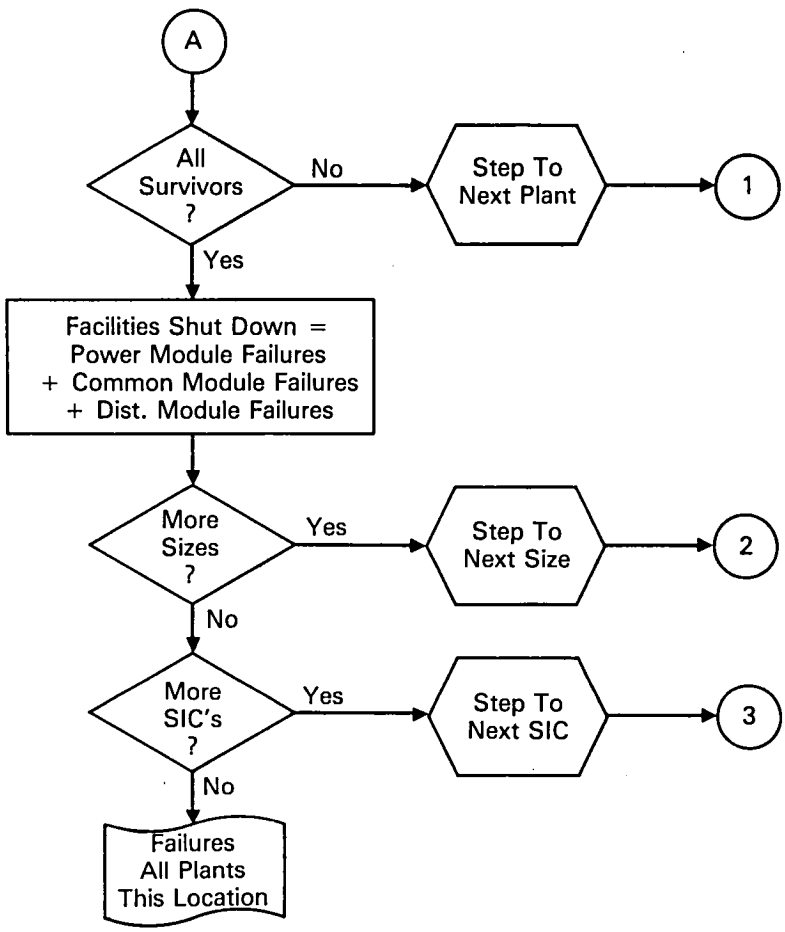

FIGURE 7.3 CONCLUDED

that is affected. This is done by using an employee weighted fraction of production lost. The expression used in the computer model is equivalent to:

$$(F.C.)_{SIC} = \frac{\sum_{Size} (\text{Employees})_{SIC,\ Size} \quad (\text{No. of Plants Shut})_{SIC,Size}}{\sum_{Size} (\text{Employees})_{SIC,Size} \quad (\text{No. of Plants})_{SIC,Size}} \qquad (7.9)$$

Equation (7.9) provides an estimate of the loss in capacity or output in an industry identified by one SIC number. The numerator is the number of employees in those facilities that are shut down in one SIC catetory; the denominator is the total number of employees in the same SIC category at the same location.

The ORI risk assessment model estimates the impact of plant closings due to carbon fiber-related equipment failures by using the Gross Domestic Product allocated to a particular business-industry segment. The Gross Domestic Product (GDP) is equal to the Gross National Product (GNP) debited by the value of foreign production of American companies and credited with the value of production by foreign companies in the United States. In this sense it measures the value of goods and services associated with particular business and industrial sectors in the United States. The GDP measures more than value of production alone and is therefore the most useful readily available economic indicator for our use. GDP estimates are published at the 3-digit SIC code level on a national basis by the Department of Commerce. In order to allocate the GDP to the local level we used county-based payroll data, published in the County Business Patterns for individual SIC numbers. The ORI model tacitly assumes that local productivity is essentially equal to the national average productivity, on an industry-by-industry basis. The GDP allocable to one industry in a particular county is estimated by:

$$\frac{(\text{County Payroll})_{SIC}}{(\text{National Payroll})_{SIC}} (\text{GDP})_{SIC} \qquad (7.10)$$

The economic impact (not the GDP lost) is estimated by the product of the expression (7.10) and FC_{SIC} defined by Equation (7.9). One further adjustment is required. Since the GDP data are usually annualized and the payroll data used for a common time interval it is necessary to multiply a factor that is the ratio of the length of time (say in number of days) a plant or

business facility is shut down to the number of business days in a year (defined as K). We generally assume that a closing of the type contemplated here would last one day. We therefore have

$$\text{Cost} = K \sum_{SIC} \frac{(\text{Local Payroll})_{SIC}}{(\text{National Payroll})_{SIC}} (GDP)_{SIC} (F.C.)_{SIC} \qquad (7.11)$$

As indicated above, county data appearing in County Business Patterns were used for the employee and payroll information. National data from the Department of Commerce provided the required GDP inputs.

HOUSEHOLD IMPACT

The method used in Phase II is essentially the same as that employed in Phase I. We estimated the fraction of households in an area that are air conditioned (FAC) and use the methods previously described to estimate the failure probability of vulnerable equipment in air conditioned and non-air conditioned households. The latter calculation includes both the failure and ventilation parameters. Transfer functions for households appeared in Table 5.2. If the fraction of time that a unit is operating is T, then the number of failures of one type of equipment is

$$\begin{aligned} &HH \times (\text{No Equip/HH}) \times T \times FAC \times P_{F,\ AC} \\ &+ HH \times (\text{No Equip/HH}) \times T \times (1\text{-}FA) \times P_{F,\ NAC} \end{aligned} \qquad (7.12)$$

where HH is the number of households and $P_{F,\ AC}$; $P_{F,\ NAC}$ are the failure probabilities for the equipment in air conditioned and non-air conditioned households respectively. If the repair cost for this equipment is RC dollars, then the total estimated cost to repair all damaged equipments of a particular class at all households at a location characterized by a single exterior explosure value, is given by:

$$\begin{aligned} &RC \times HH \times (\text{No Equip/HH}) \times T \times \\ &\quad \left(P_{F,\ AC}\ FAC + P_{F,\ NAC}\ (1\text{-}FAC)\right) \end{aligned} \qquad (7.13)$$

The locations and numbers of residential units were obtained from the Bureau of Census publication, County and City Data Book. Based on the latest experimental evidence our attention was limited to household television and

high fidelity equipment. Failure parameters ($\overline{E}$) for both were set equal to 10^8 fiber seconds per cubic meter; the repair costs were estimated to be $50 per television set and $100 per high fidelity set. Updated Phase II ventilation data were incorporated in the calculation (cf Table 5.2). It was further assumed that each of these equipments would be operated about half of the time. The equipment failure parameters and repair costs may be considered typical of a wide range of household appliances, so that any two appliances may be considered treated, rather than the television and high fidelity sets.

AIRCRAFT VULNERABILITY

Problem Definition

In Phase I it was concluded that key airport operations were essentially invulnerable to carbon fiber incidents due to the many designed redundiancies in the system. The Phase I analysis did not, however, cover the risk to aircraft on the ground at the time of the accident. Because of safety-of-flight, as well as other factors, it was decided that an investigation should be made of the risk to aircraft on the ground, at passenger gates and maintenance locations. This was initiated in Phase II, and focussed on failures of avionics equipment.

In a cooperative effort the aircraft manufacturers analyzed data to determine the number of aircraft expected to be at passenger boarding gates and at maintenance locations on the airport by day and night. This was done for the nine airports previously selected to represent the entire United States (accounting for about one third of U.S. operations with a bias toward the larger airports). The results of the airframer data collection effort, based on current operations, were extrapolated to the 1993 time frame for the ORI risk assessment. The results are shown in Table 7.2.

For the principal aircraft types the airframers reviewed all onboard electrical and electronic equipment. For the L-1011 Tristar, for example, 600 types of equipment were surveyed, and 258 components and assemblies were identified for detailed vulnerability review. After examination of all pertinent characteristics, 84 types of equipment were identified as susceptible to CF-induced damage. All of these types of equipment were assigned failure parameters based on available experimental data, extrapolated where necessary. A few examples from the L-1011 are shown in Table 7.3. The table reveals another

TABLE 7.2

ESTIMATED NUMBER OF AIRCRAFT EXPOSED ON THE GROUND - 1993

AIRPORT	A/C SIZE	DAY		NIGHT	
		GATE	MAINT	GATE	MAINT
O'Hare/ Chicago	SMALL	12	3	5	6
	MED	36	0	18	11
	LARGE	39	8	18	20
Kennedy/ New York	SMALL	12	2	3	5
	MED	49	0	21	65
	LARGE	41	8	23	32
Lambert/ St. Louis	SMALL	5	1	2	1
	MED	8	0	1	0
	LARGE	2	0	2	0
La Guardia/ New York	SMALL	5	0	4	6
	MED	0	0	0	13
	LARGE	3	0	4	0
Logun/ Boston	SMALL	4	1	5	4
	MED	12	0	4	0
	LARGE	9	0	5	4
Phila. Int'l./ Philadelphia	SMALL	2	0	3	0
	MED	6	0	1	0
	LARGE	6	0	8	0
Washington National/ Washington, D.C.	SMALL	2	0	3	0
	MED	6	0	1	0
	LARGE	6	0	8	0
Hartsfield/ Atlanta	SMALL	9	3	8	5
	MED	32	11	23	13
	LARGE	16	8	16	12

TABLE 7.2

ESTIMATED NUMBER OF AIRCRAFT EXPOSED ON THE GROUND - 1993 (Continued)

AIRPORT	A/C SIZE	DAY		NIGHT	
		GATE	MAINT	GATE	MAINT
Miami	SMALL	6	1	9	2
International/	MED	34	0	43	26
Miami	LARGE	24	12	20	24

TABLE 7.3

EXAMPLES OF VULNERABLE EQUIPMENT ABOARD L-1011 TRISTAR

EQUIPMENT I.D. NO.	USE	NO. PER AIRCRAFT	LOCATION ON AIRCRAFT	Failure Parameter ($\bar{E}$: Fiber sec/m^3)
L12	Radio Communication	2	Avionics Center	10^8
L13	Radio Communication	3	Avionics Center	10^8
L32	Electric Power	1	Flight Station	10^8
L65	Navigation	2	Avionics Center	1.5×10^7
L69	Navigation	1	Flight Station	10^8
L78	Airborne Auxiliary Power	1	Passenger Cabin	10^8

important factor in the analysis, to be discussed later: similar equipments may be installed in different parts of the aircraft. There are several different possible paths for fiber-laden air from the exterior to the different onboard equipment locations.

In order to consolidate the equipment data the airframers defined an avionics "suit" for a typical aircraft in each size category. Equipment type classifications were made on the basis of failure parameter and repair cost primarily, so that it was possible to reduce the total number of types of equipment considerably by appropriate aggregation. In this way generic types of avionics equipment were identified with onboard locations indicated for each one, as well as mean-exposure-to-failure values, and repair costs. Table 7.4 summarizes the equipment input data prepared by the airframers: the number of the aircraft, the failure parameter ($\overline{E}$), and the repair costs.

As indicated above, avionics equipment is operated in several locations on the aircraft; this factor together with the possibility of various doors and hatches being open or shut resulted in the definition of different ventilation modes for each equipment-aircraft combination. Here again, an independent analysis by the airframe manufacturers provided values of the different transfer functions and the fraction of time (during day and night) that each would be expected to prevail. These results are summarized in Table 7.5.

Computer Methods

Figure 7.4 is a flow chart illustrating the computer submodel that computes avionics failures and resulting costs. The first step in the computation is the determination, on a stochastic basis, of whether the simulated accident took place during the day or night. The conditional probability for this event is based on the analysis of the airframer aircraft accident data base. The calculation proceeds through each aircraft size in turn. For each size aircraft the program "looks up" the number of aircraft at the predefined gate and maintenance locations (for the airport being simulated). At each location in-turn the number of each type of equipment in aggregated; on a random basis the model determines the number in each of the predefined ventilation modes (i.e., finds the applicable transfer function). With the value of the transfer function and the exterior exposure for the particular location the model computes the failure probability for the equipment, using the input

TABLE 7.4

AIRCRAFT AVIONICS EQUIPMENT CONFIGURATIONS WITH FAILURE AND COST INPUTS

Aircraft Size	Avionics Equipment ORI I.D. No.	Number on Aircraft	$\bar{E}$ (Failure Parameter*)	Repair Cost ($)
Small	1	38	10^8	100
	2	7	1.5×10^7	100
	3	6	10^8	450
	4	2	1.5×10^7	450
	5	1	10^8	300
	6	18	10^8	50
Medium & Large	7	26	1.5×10^7	215
	8	24	10^8	220
	9	153	10^8	175
	10	4	10^8	250
	11	22	10^8	210
	12	43	10^8	385
	13	3	10^8	530
	14	2	10^8	1295
	15	4	10^8	1665

*In fiber-seconds per cubic meter.

TABLE 7.5

VENTILATION FACTORS (T.F.) AND ASSOCIATED PROBABILITIES FOR AVIONICS EQUIPMENT ABOARD PARKED AIRCRAFT BY LOCATION AND TIME OF DAY

Equip. No.	Gate				Maintenance	
	Day		Night		Day & Night	
	Prob.	T.F.	Prob.	T.F.	Prob.	T.F.
1 -	.99	.70	.70	.70	.23	.70
4	.01	1.0	.30	1.0	.77	1.0
5, 6	.99	.70	1.0	.70	.96	.70
	.01	.0025			.04	.0025
7	.95	.0025	.20	.0025	.79	1.0
	.01	1.0	.50	.01	.14	.01
	.04	.01	.30	1.0	.07	.0025
8	1.0	.01	1.0	.01	1.0	.01
9, 10	.99	.01	1.0	.01	.96	.01
	.01	.0025			.04	.0025
11 -	.95	.0025	.20	.0025	.78	1.0
15	.01	1.0	.50	.01	.14	.01
	.04	.01	.30	1.0	.08	.0025

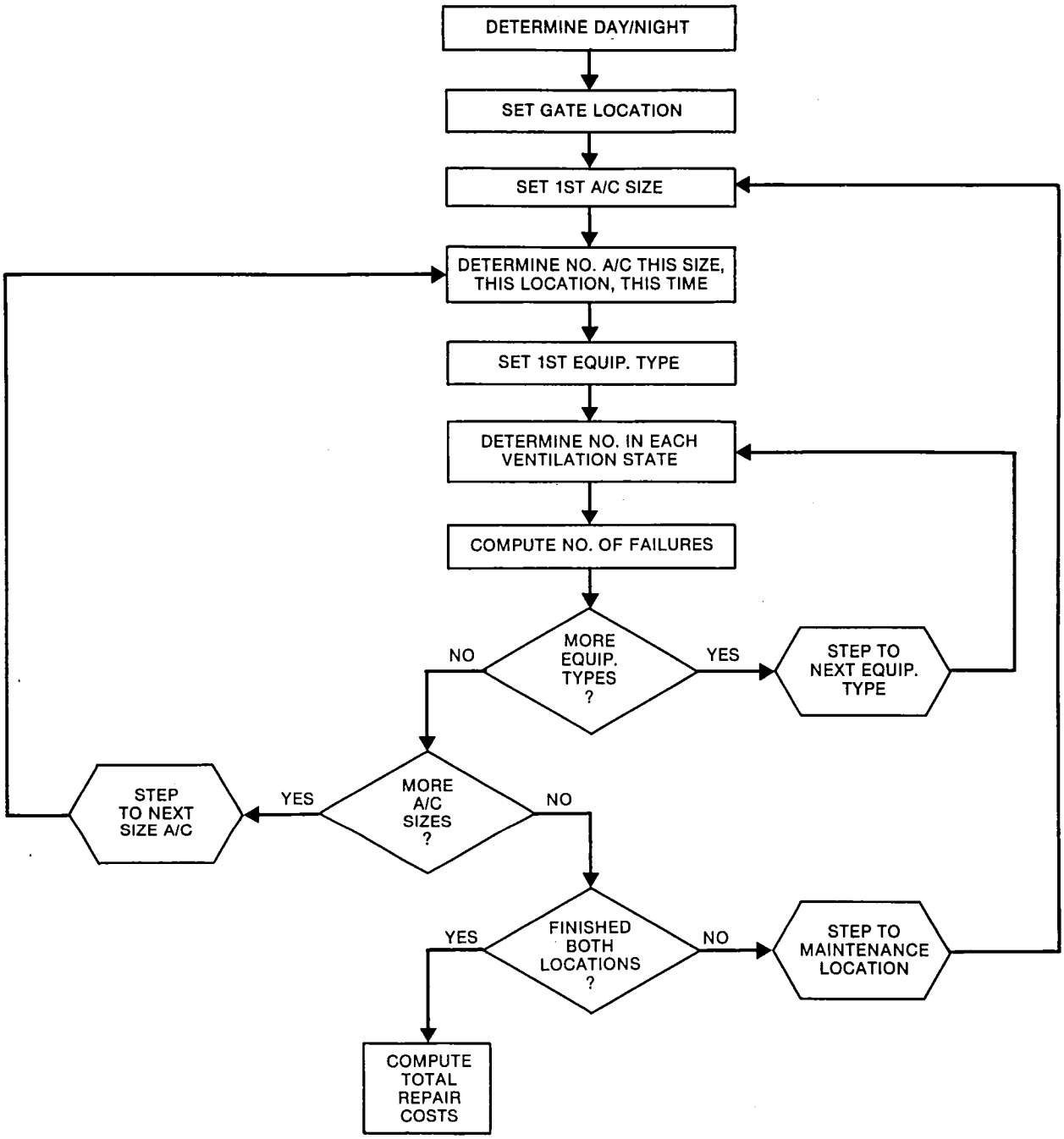

FIGURE 7.4 FLOWCHART FOR COMPUTING AVIONICS FAILURES AND ASSOCIATED COSTS

value of $\overline{E}$. Using a Poisson distribution the actual number of failures is obtained in a random draw. Using the input repair cost for the equipment the computer model then determines the total repair cost. This procedure is repeated for each type of equipment on one size aircraft, then done for the other size aircraft, then repeated at the next location.

COSTING SUMMARY

The input requirements for the business/industry impact cost model are summarized in Table 7.6. All counties within 50 miles of the airport are defined by a set of geographical coordinates. At one geographical location the model computes business-industry impact as the sum of costs of equipment repair, facility cleanup, and business disruption. At those locations defined as residential centers the model computes the total cost due to household equipment failures. At the airport itself the model computes costs required to repair failed avionics equipment. Summary results for each simulated accident present the total of costs in each of these three major categories, obtained by adding the costs over all geographical locations affected by the simulated accident.

TABLE 7.6
SUMMARY
BUSINESS/INDUSTRY IMPACT COST MODEL
INPUT REQUIREMENTS

Level	Descriptor	Input Definition
National	SIC Number	Payroll Gross Domestic Product
County	SIC Number	Local Payroll No. of Establishments by Size
Facility	SIC Number & Size	No. of Equipments by Type Plant Configuration Cleanup Cost
Equipment	Standard Type	Repair Cost Mean Exposure-to-Failure

VIII. INDIVIDUAL AIRPORT RESULTS

The simulation model was run for a large sample of accidents at the following nine airports previously examined in Phase I:

O'Hare/Chicago

John F. Kennedy/New York City

Washington National Airport/Washington, D.C.

Lambert/St. Louis

LaGuardia/New York City

Logan/Boston

Hartsfield/Atlanta

Miami International/Miami

Philadelphia International/Philadelphia.

SAMPLE ACCIDENT

To set the stage for interpreting the airport simulation statistics we present detailed output for one random accident generated at Kennedy Airport. The basic geometry is shown in Figure 8.1; the airport and accident location are indicated. Randomly generated weather data are: wind from the south at 2 meters per second and stability class 6. The accident, based on

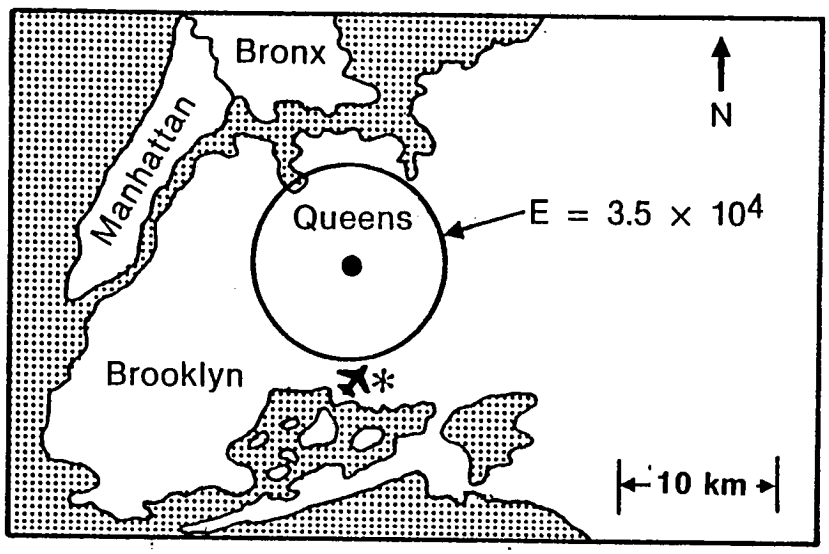

Figure 8.1 Basic Geography Associated With One Random Accident At Kennedy Airport in New York. Airplane shows airport location; asterisk indicates accident location. The circle represents Queens County for modelling purposes.

randomly-selected factors involved a large jet (type 16) with 3000 kilograms of composite aboard; 1.3×10^{10} fibers were released in a take-off accident, with the plume formed during the fire limited to a height of 100 meters by an inversion. As a result the mean exposure in Queens County is 3.5×10^{4} fiber-seconds per cubic meter; no other neighboring counties were significantly affected.

The results for this one accident include the computed cost of repairs to household equipment in Queens of $533. The impact on business comprises $5,600 in equipment repair costs and $31,577 due to business closings and cleanup as the result of equipment failure.

SIMULATION OUTPUTS

A typical set of runs includes approximately 2500 simulated accidents, each generating data of the type presented above for one accident. The computer program summarizes the data from all simulated accidents to provide the following outputs:

- Characteristics of the ten most costly accidents
- Probability distribution of annual costs for household, industrial, and avionics, as well as the mean, standard deviation, and risk profile
- Probability distribution of costs per accident for household, industrial, and avionics impacts to provide: mean, standard deviation, and risk profile
- Distribution of number of accidents per year (replication).

Available options permit printing out the details associated with each accident, as presented above. A standard printout for a sample (annual replications) results for 34,000 replications at Kennedy Airport appears in Figure 8.2. The results indicate that, for example, in 7 runs the total cost was greater than $100, and less than $178, as shown in the column headed "TOTAL COUNTS." The class intervals were selected to be equal on a logarithmic scale to facilitate computing the risk profiles, essentially cumulative probability distributions. The risk profiles for annual household avionics failures, and business-industry impact plotted from these output data appear in Figure 8.3.

JFK 1993 GF RISK ANALYSIS

SAMPLE RESULTS

COST RANGE UPPER LIMITS ($1000)	HOUSEHOLD COUNTS	INDUSTRY COUNTS	AIRPORT COUNTS	TOTAL COUNTS
0.100	33958	33957	33993	33938
0.178	13	0	0	7
0.316	10	2	3	3
0.562	11	0	1	7
1.000	3	1	1	3
1.778	2	0	1	1
3.162	3	5	0	4
5.623	0	14	1	13
10.000	0	6	0	9
17.780	0	10	0	6
31.620	0	1	0	2
56.230	0	3	0	3
100.000	0	0	0	0
177.800	0	1	0	1
316.200	0	0	0	0
562.300	0	0	0	0
1000.000	0	0	0	0
1778.000	0	0	0	0
3162.000	0	0	0	0
5623.000	0	0	0	0
10000.000	0	0	0	0
17780.000	0	0	0	0
31620.000	0	0	0	0
56230.000	0	0	0	0
100000.000	0	0	0	0
177800.000	0	0	0	0
316200.000	0	0	0	0
562300.000	0	0	0	0
1000000.000	0	0	0	0
1778000.000	0	0	0	0
3162000.000	0	0	0	0
5623000.000	0	0	0	0
TOTAL	34000.	34000.	34000.	34000.

RISK PROFILE

COST RANGE EXCEEDING ($1000)	HOUSEHOLD RISK	INDUSTRY RISK	AIRPORT RISK	TOTAL RISK
0.100	0.001235	0.001265	0.000206	0.001824
0.178	0.000853	0.001265	0.000206	0.001618
0.316	0.000559	0.001206	0.000118	0.001529
0.562	0.000235	0.001206	0.000088	0.001324
1.000	0.000147	0.001176	0.000059	0.001235
1.778	0.000088	0.001176	0.000029	0.001206
3.162	0.0	0.001029	0.000029	0.001088
5.623	0.0	0.000618	0.0	0.000706
10.000	0.0	0.000441	0.0	0.000441
17.780	0.0	0.000147	0.0	0.000176
31.620	0.0	0.000118	0.0	0.000118
56.230	0.0	0.000029	0.0	0.000029
100.000	0.0	0.000029	0.0	0.000029
177.800	0.0	0.0	0.0	0.0
316.200	0.0	0.0	0.0	0.0
562.300	0.0	0.0	0.0	0.0
1000.000	0.0	0.0	0.0	0.0
1778.000	0.0	0.0	0.0	0.0
3162.000	0.0	0.0	0.0	0.0
5623.000	0.0	0.0	0.0	0.0
10000.000	0.0	0.0	0.0	0.0
17780.000	0.0	0.0	0.0	0.0
31620.000	0.0	0.0	0.0	0.0
56230.000	0.0	0.0	0.0	0.0
100000.000	0.0	0.0	0.0	0.0
177800.000	0.0	0.0	0.0	0.0
316200.000	0.0	0.0	0.0	0.0
562300.000	0.0	0.0	0.0	0.0
1000000.000	0.0	0.0	0.0	0.0
1778000.000	0.0	0.0	0.0	0.0
3162000.000	0.0	0.0	0.0	0.0
5623000.000	0.0	0.0	0.0	0.0

****

	HOUSEHOLD ANNUAL COST	INDUSTRY ANNUAL COST	AIRPORT ANNUAL COST	TOTAL ANNUAL COST
AVERAGE	0.001	0.014	0.000	0.015
SIGMA	0.027	0.787	0.022	0.805
MINIMUM	0.0	0.0	0.0	0.0
MAXIMUM	2.665	121.689	3.910	123.695

FIGURE 8.2 Annual Result Output, for 34,000 Annual Replications - Kennedy Airport - 1993

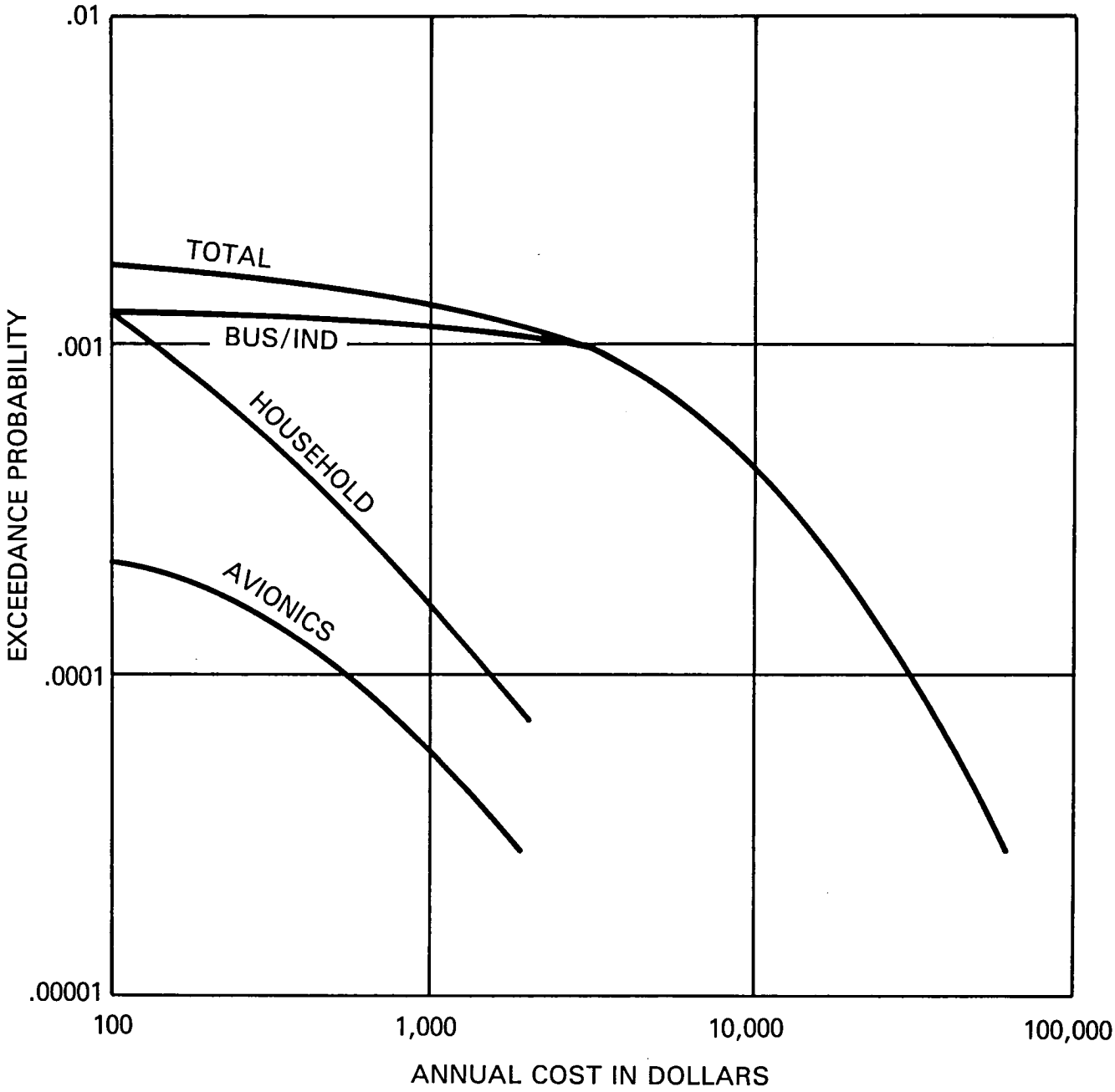

Figure 8.3 Annual Risk Profiles for Kennedy Airport - 1993: Business/ Industry, Household Equipment, and Avionics Equipment Impacts; and Total Impact.

COMPARISON OF DIFFERENT AIRPORTS

In this section representative results are summarized for the nine airports listed above. For each airport the number of samples (replications) was selected so that at least 2500 accidents were simulated. Computer time is directly proportional to the number of accidents being simulated, and comparability of results for different airports required a common basis. Results presented below show the impact of changing this number.

Table 8.1 summarizes the results of all the single airport accident simulations. The table presents accident data as contrasted with annual data. The probability of more than one accident per year is so small, however, that the average of results over all accidents is essentially equal to the average of results over all simulated years. In each set of runs the program presents detailed information about the ten worst (highest cost) accidents. The average of the ten highest-cost accidents at each of the airports also appears in the table. At each airport these ten accidents (0.4 percent of all simulated accidents) comprise the highest cost.

The results in Table 8.1 show that, typically, the costs resulting from business and industrial impact are considerably greater than the household impact costs and the avionics failure costs. All mean costs appear relatively small. To present some idea of the range of these results we note here that the maximum cost in each of the three categories and the airport at which it occurred are:

- Households: $2,665 at Kennedy Airport, New York
- Business-Industry: $274,000 at Logan Airport, Boston
- Avionics: $3,910 at Kennedy Airport, New York.

As indicated, these represent results from 2500 accident simulations at each airport, so that these extreme values were experienced with an empirical frequency of 4 in ten thousand. The extreme values quoted here are actually the maxima from a sample of approximately 9x2500 or 22,500 accidents. The likelihood of an accident with fire in any year is quite low; the extreme values reported for Kennedy airport and Logan airport would have occurred only once in 34,000 years and once in 67,000 years, respectively.

TABLE 8.1 — 1993 RESULTS FOR SIMULATED ACCIDENTS AT NINE AIRPORTS (1976 DOLLARS)

Airport/City	Mean Cost			Mean of 10 Worst
	Household	Bus/Ind.	Avionics	
Atlanta	1	70	2	14,218
Boston	2	152	0	35,818
Wash. Nat'l.	5	310	0	62,497
Kennedy	11	199	3	32,544
LaGuardia	11	373	0	56,186
Miami	2	28	1	7,566
Chicago	6	162	1	32,510
Philadelphia	7	192	0	28,971
St. Louis	2	67	0	13,779

NOTE: Approximately 2500 accidents simulated for each airport.

The computer simulation model also generates all the results needed to plot the risk profiles, as shown previously in the sample printout appearing as Figure 8.2. The risk profile is typically presented on an annual basis. Figure 8.4 shows the annual risk profiles for O'Hare Airport, Chicago, Lambert Airport, St. Louis, and Hartsfield Airport, Atlanta. O'Hare/Chicago, the Nation's busiest airport, has a risk profile that shows that the probability of exceeding $10,000 per year in total CF-related impact is approximately .0004. For St. Louis, the corresponding probability is approximately .0001 (one in 10,000). These three airports constitute a sample of different combinations of annual commercial operations and surrounding population, as summarized here:

O'Hare (ORD): High population, heavy air traffic

Hartsfield (ATL): Low population; high traffic level

Lambert (STL): Low population, low traffic level.

This stratification is reflected in the annual risk profiles. The O'Hare risk is highest, St. Louis lowest.

The Phase II computer program was modified to generate statistics on a per-accident basis as well as the customary per-year basis. Figure 8.5 shows the accident risk profiles for the same three airports. The risk is greatest for O'Hare, due to the relatively high concentration of business and industry; the St. Louis and Atlanta risk profiles are quite similar, indicating that their separation in Figure 8.4 was due to the difference in accident incidence (i.e. in our model, the difference in number of operations). The accident risk profiles may be considered conditional probabilities. For example, given that a CF-built aircraft crashes and burns at O'Hare Airport the probability is 1 in a hundred (.01) that the impact will exceed one thousand dollars ($1,000); for $100,000 the probability is 2 in one hundred thousand (.00002), by extrapolation from Figure 8.5.

STATISTICAL CONFIDENCE LIMITS

In Phase I ORI shows that the simulation runs for one airport may be considered a set of Bernoulli trials. As a result we derived the following

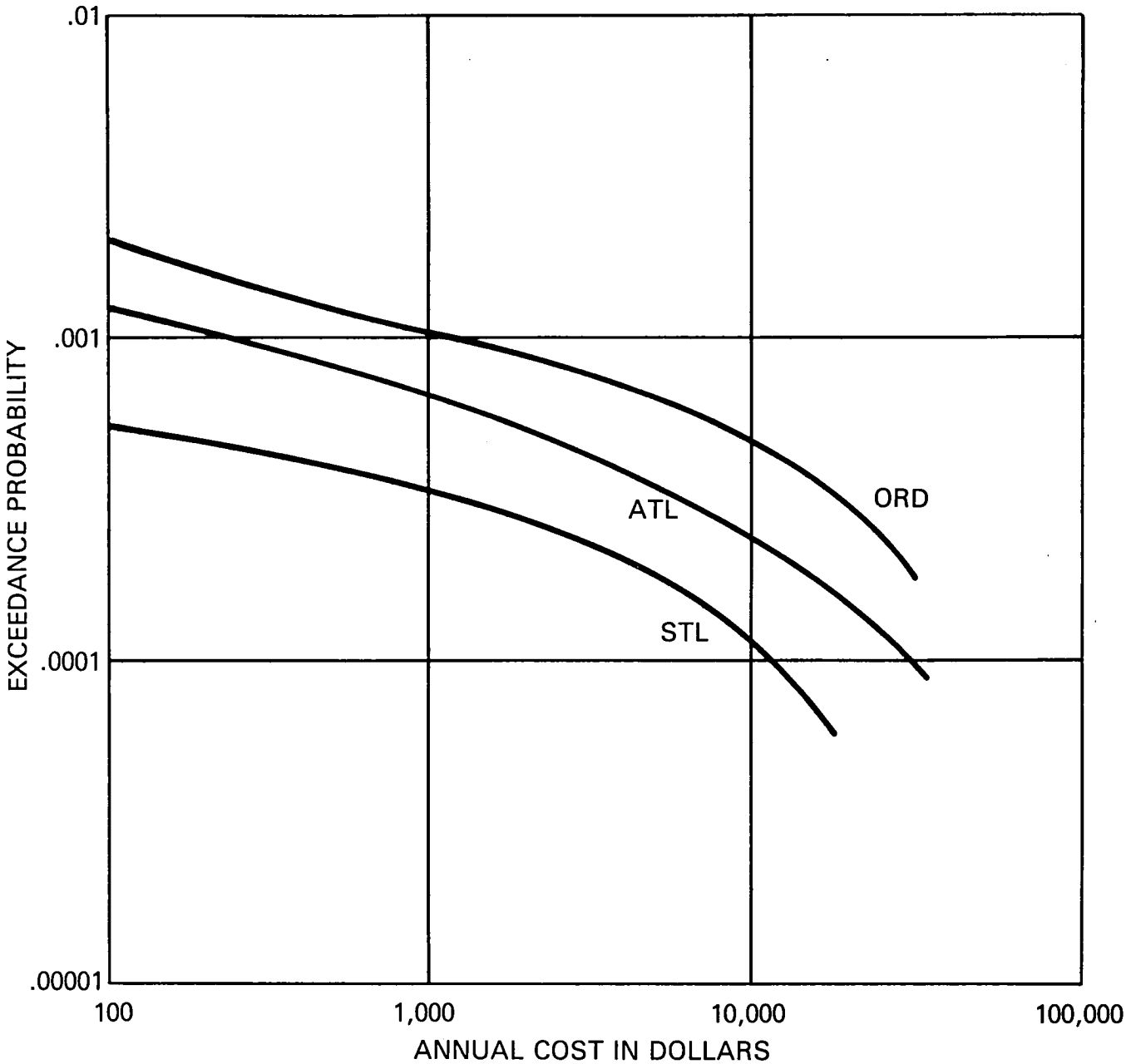

Figure 8.4 Annual Risk Profiles - 1993 Scenario - for O'Hare/Chicago (ORD). Hartsfield/Atlanta (ATL) and Lambert/St. Louis (STL)

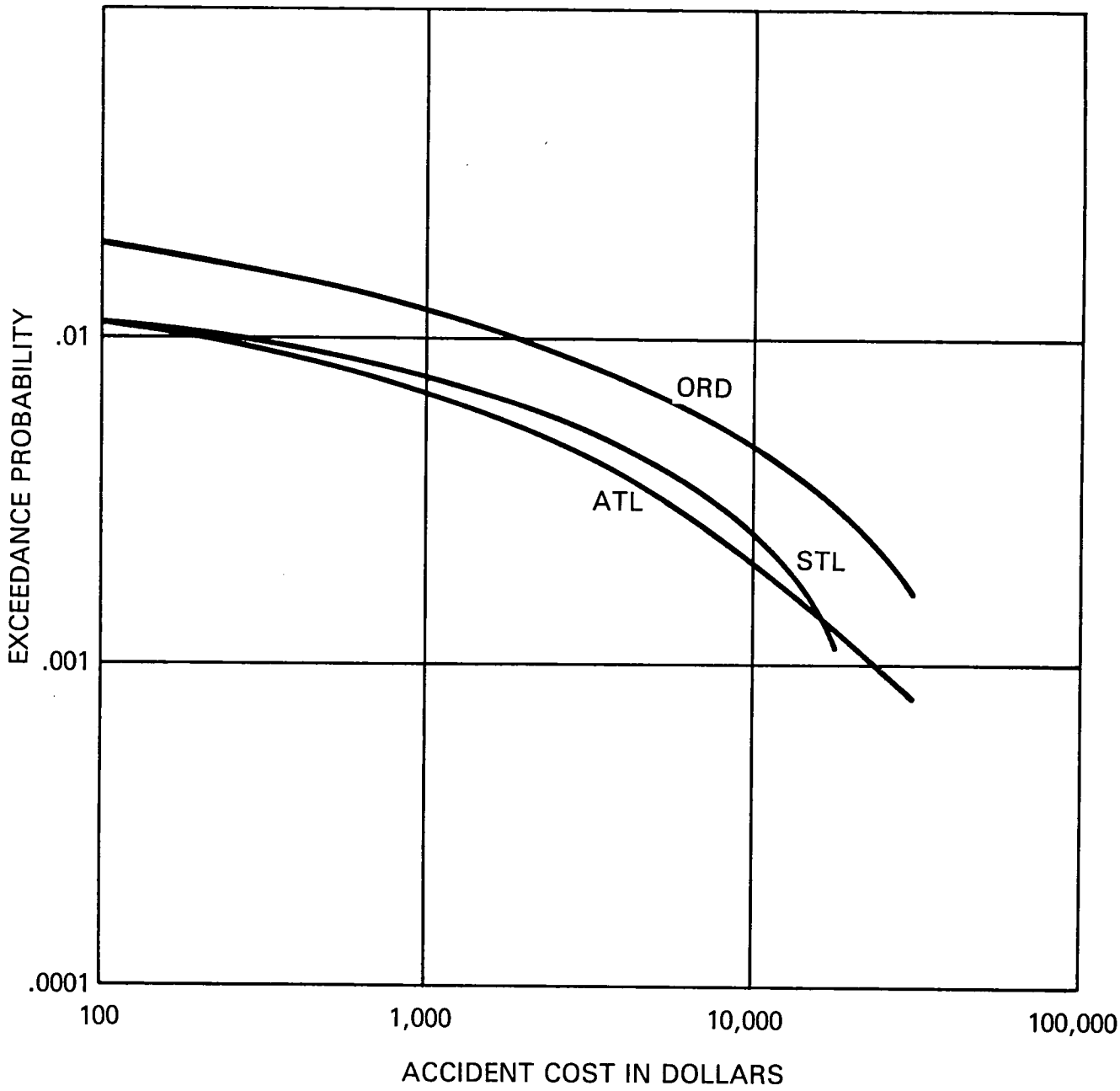

Figure 8.5 Accident Risk Profiles - 1993 Scenario - for O'Hare/Chicago (ORD), Hartsfield/Atlanta (ATL) and Lambert/St. Louis (STL).

expression for the 95% statistical confidence limits:

$$p \pm 2 \sqrt{\frac{p(1-p)}{n}}$$

where p is the computed exceedance probability after simulating n samples. Figure 8.6 shows the Washington National Airport risk profile with the 95% confidence limits. The confidence limits apply to the purely statistical nature of the simulation, and not to the impact of errors in input data. The results do show that conclusions based on the risk profiles need not be altered because of inherent statistical uncertainty. The confidence limit bars shown on the graph appear to not be of equal size above and below the curve due to fact that the results are plotted on a logarithumic scale.

ADEQUACY OF SAMPLE SIZE

In a major simulation modelling effort of the type reported here one of the important questions is whether enough runs have been made. This is related to the stability of the model and variance in the input data. Rather than invoke sophisticated statistical arguments it is more convenient to let the results "speak for themselves." In effect we compared the results for two different numbers of simulation runs.

The O'Hare Airport/Chicago simulation was run for 22,000 and 44,000 annual samples, resulting in 2537 and 5038 accidents respectively. It is not possible to compare the two risk profiles on a graph using a scale convenient for this report, since they would be too close to one another. We are therefore limited to the results summarized in Table 8.2. A significantly larger-cost accident occurred in the 44,000-sample run than in the 22,000-sample run which is typical of extreme-value statistics. In this case the contribution of the larger accident results in the mean values being somewhat different. The risk probabilities are, however, quite similar. It is also interesting to note that five of the ten highest-cost accidents in the 44,000-sample run occurred in "second half", i.e., in samples after number 22,000.

SENSITIVITY TESTS

To demonstrate the flexibility of the ORI Carbon Fiber Risk Assessment Model, as well as to provide insight into the physical mechanisms at work, several input parameters were varied and the impact of the variation on the output examined. These results are described in this section of the report.

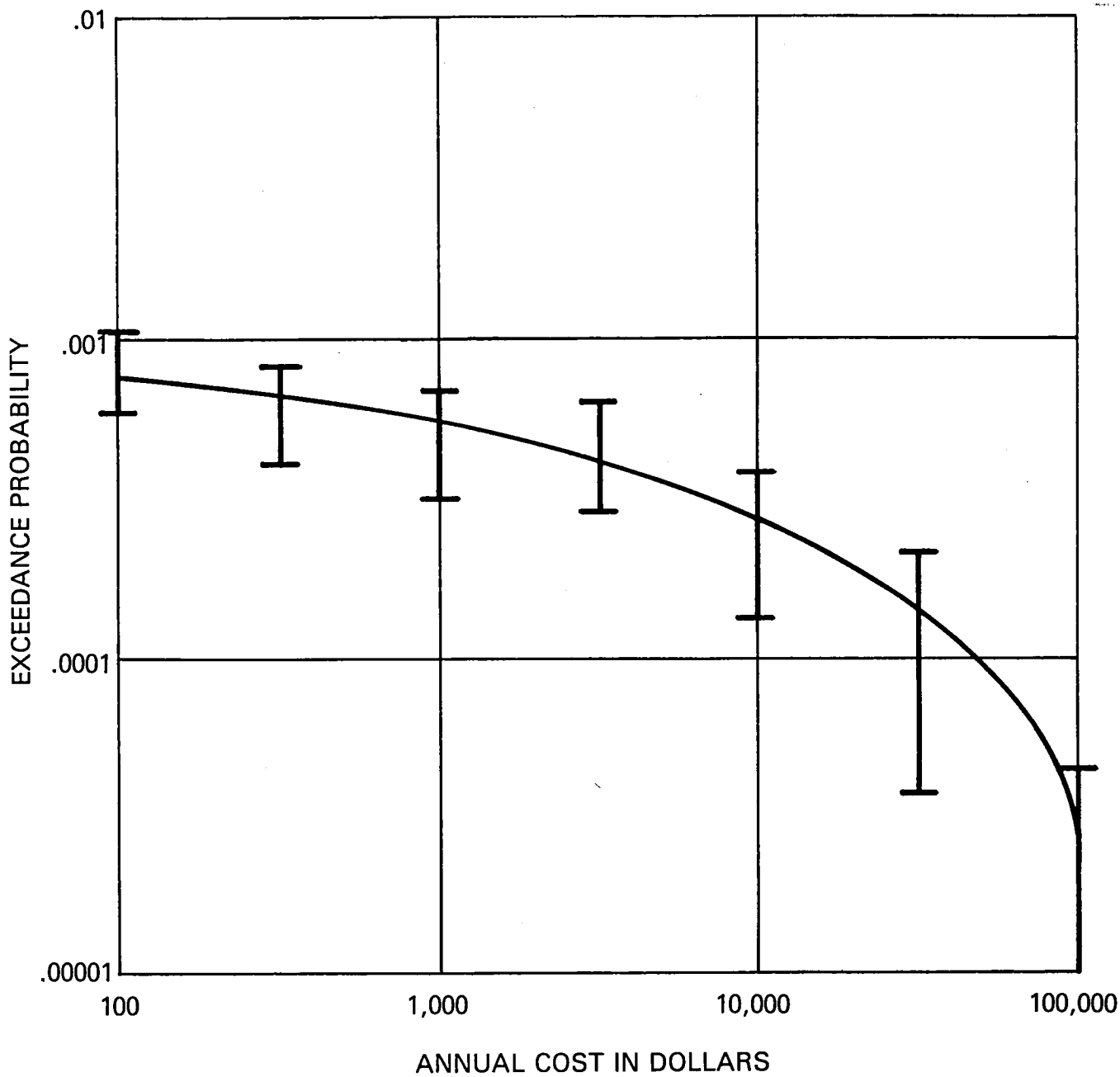

Figure 8.6 1993 Washington National Airport Annual Risk Profile Showing 95% Statistical Confidence Limits.

TABLE 8.2

1993 CHICAGO/O'HARE COMPARISON OF DIFFERENT SETS OF SIMULATIONS

Measure	22,000 Samples	44,000 Samples
No. of Accidents	2537	5038
Mean Accident	$147	$166
Worst Accident	$54,000	$110,299
P (Annual Cost >$1000)	.000955	.00111
P (Annual Cost>$10,000)	.000545	.000545

Inversion "Punch Through"

It is assumed in the results reported so far that the plume does not penetrate the inversion. For one set of Washington National Airport simulations we permitted the plume to "punch through" the inversion. This was a relatively simple program modification to introduce, since the standard model includes a test comparing the computed plume height with the inversion height. If the initially-computed plume height is greater it is reduced and set equal to the inversion height for the remainder of the calculation. In the sensitivity test reported here this comparison was bypassed and the computed plume height was used, regardless of its magnitude relative to the height of the inversion.

The results for Washington National Airport indicate risks so low compared to the base case that no risk profiles were drawn. It is only necessary to cite a few values to make the point. In the test case, with punching through permitted, the probability of exceeding $100 per year in CF - impact costs was .000045 compared to the 1993 Washington National Airport base case (no punch-through) value of .003, roughly a difference by a factor of twenty. For exceeding $1000 per year the corresponding probabilities are .000015 (punch through) and .00048 (no punch through). In the test cases the mean annual accident cost is reported as zero (actually less than 50¢) compared to $12 in the standard case. Another way of reporting these results is that, of 2590 random accidents generated in the "punch-through" runs, only three had associated CF-related costs of more than $100.

One interesting result relates to the stability class associated with the ten most costly accidents. In the base case these are all class 6 or class 5, - the most stable atmospheric conditions; these stability classes are characterized by a 100-meter inversion height. In the standard simulations this was also the height at which the plume was stopped. For the "punch-through" runs the ten most costly accidents are associated with stability class 6 although the average plume height was 437 meters; the average cost incurred in these ten costliest accidents was $571, compared to $62,497 (cf. Table 8.1) in the base case.

Random Inversion Height

In other results presented in this report the inversion height is linked to the stability class by a one-to-one relationship for each airport.

This is, in each of the airport accident simulations the random selection of the atmospheric stability category automatically determines the height of the inversion (cf. Section IV). As called for in the Phase II contract ORI tested the effect of this approach by devising a methodology to provide for a random selection of the inversion height. This was done by first associating the different stability classes with the period of the day during which each is most likely to occur. For example, stability classes 4, 5, and 6 usually prevail during the night. The previously developed values of the inversion height were selected as the values prevailing at the midpoints of each of the appropriate time intervals and were then connected by straight line segments. The actual inversion height was then determined by a random selection from that part of the continuous inversion height-time relationship appropriate to the randomly-selected stability class.

The resulting risk profiles are compared in Figure 8.7 for the 1993 Washington National Airport scenario. The standard, fixed inversion height per stability class case is characterized by a somewhat higher risk, showing that the method previously used is relatively conservative. The annual mean impact is $12 for the fixed inversion height case and drops to $5 in the variable inversion height case. The corresponding average impacts of the ten worst accidents are $62,497 and $28,994, respectively. It also turned out that, in the variable inversion height runs, the ten worst accidents were associated with stability classes 5 and 6, the most stable, although the inversion height was not always set at 100 meters as it is in the standard runs for these stability classes.

O'Hare Airport "Worst Case"

In order to examine the impact of a drastic change in the underlying assumptions the O'Hare Airport 1993 scenario simulations were run with the inputs changed so that all aircraft operations involved aircraft "loaded" with CF. In order to do this conveniently the inputs were adjusted so that all aircraft operating at O'Hare in 1993 with CF in their structure were our previously defined type number 19 (cf. Table 2.2). This is a large jet with the most CF composite of any plane expected be in the 1993 fleet; the total onboard is 15,600 kilograms. The average amount of composite aboard all 1993 aircraft is only about 2,800 kilograms per aircraft with composite while the range is from

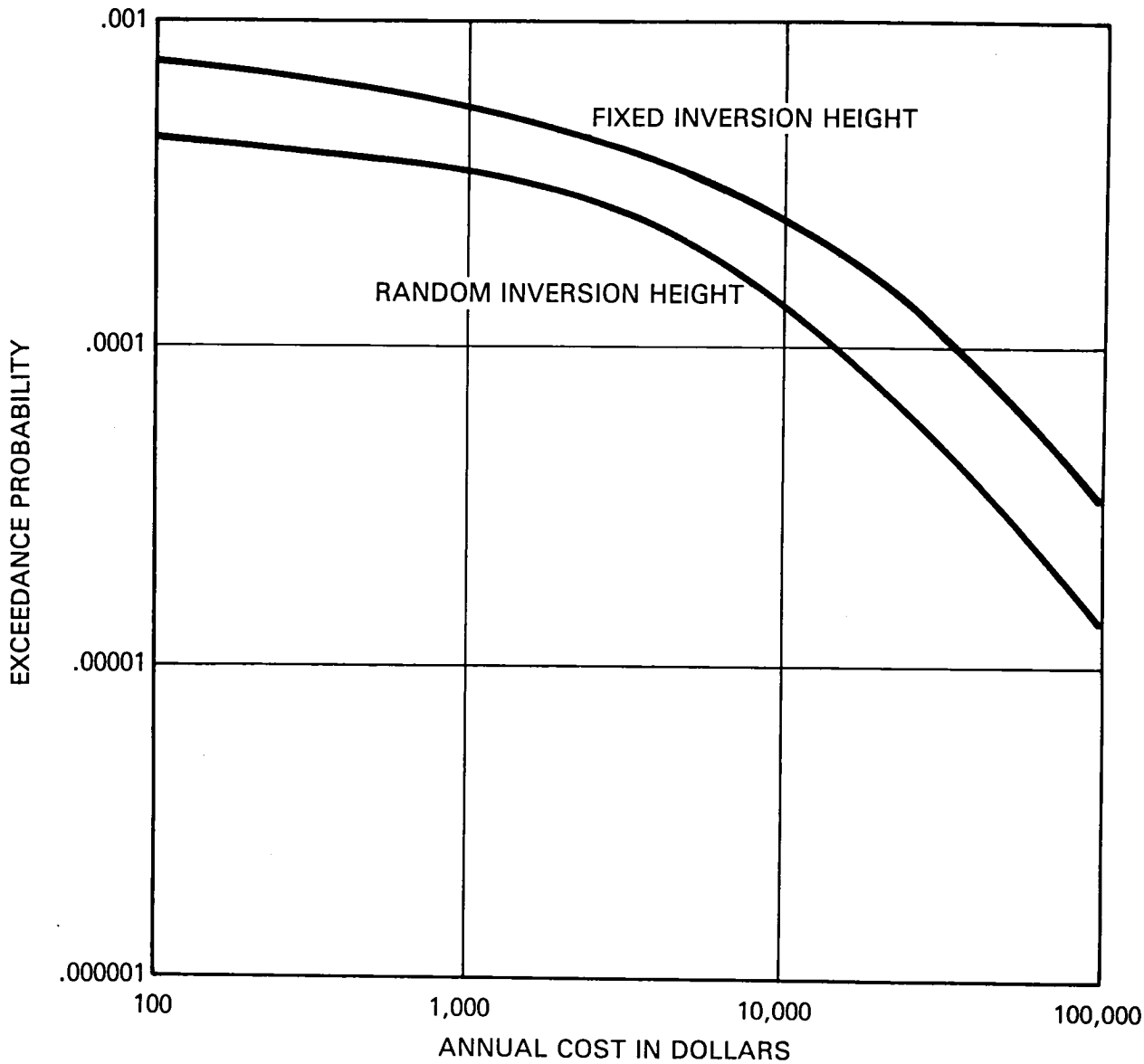

Figure 8.7 1993 Washington National Airport Annual Risk Profiles Showing Effect of Random Selection of Inversion Height.

65 to 15,600, for the aircraft with composite. The worst-case scenario effectively increases the amount of carbon fiber liberated in an accident by a factor of approximately five, on the average. Several of the output results from the two sets of simulation runs are compared in Table 8.3. The interesting result is that the mean annual impact and the mean accident cost each increase by a factor of approximately ten due to the average increase in CF-release of a factor of about five. In the case of the ten most costly accidents the ratio of the mean impacts is approximately 2.5. The average amount of composite released in the ten most costly accidents for the worst-case scenario is about 5.8 times the average for the corresponding best-estimate cases.

The results for the probabilities shown in Table 8.3 indicate that the effect of the increase in the average amount of fiber per aircraft is to shift the peak of the frequency distribution of accident impact to the right; the most trival accidents have been eliminated and this causes the larger shift in the mean values. In the standard runs the standard deviation of annual impact is equal to about 40 times the annual mean impact; in the worst case this ratio is about 15. The best-estimate 1993 O'Hare annual risk profile is compared with worst case in Figure 8.8. The comparison shows the significant impact of the increased carbon fiber. However, the probability of exceeding $10,000 in annual damages is only about .005 (five in a thousand), which is also indicated in Table 8.3.

TABLE 8.3

COMPARISON OF SELECTED OUTPUTS: O'HARE AIRPORT, 1993, BEST-ESTIMATE AIRCRAFT MIX AND ALL AIRCRAFT "LOADED"

Result Measure	Standard Average A/C: 2800 kg CF	Worst-Case All A/C: 15,600 kg CF
Mean Annual Impact	$17	$172
Mean Impact per Accident	$147	$1408
Mean of Ten Most Costly Accidents	$28,842	$68,383
Prob of Annual Impact > $10,000	.0005	.0045
Prob of Accident Impact > $50,000	.0002	.0066

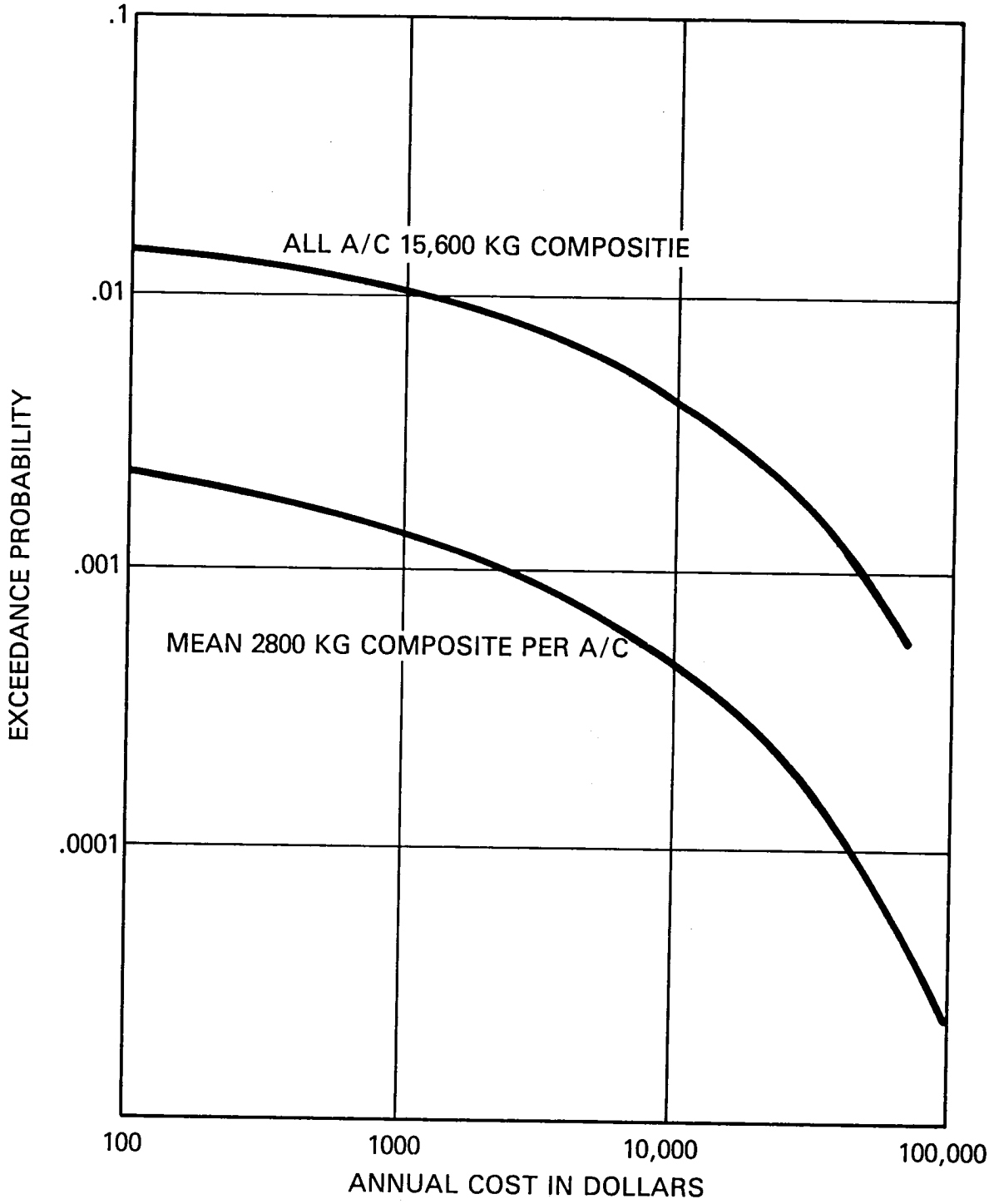

Figure 8.8 1993 Chicago/O'Hare Annual Risk Profile Compared to "Worst Case."

IX. NATIONAL RISK

In Phase I ORI used a mathematical technique called a convolution to generate the national risk profile. This method used as its input the final results of the airport simulations: the risk profiles, or probability distributions. In Phase II a somewhat more straightforward approach was used, which takes as its input the individual accident results generated for each of the airports. The method is described in more detail below, followed by a presentation of the results.

METHOD

The airports previously treated, and listed in Section VIII, account for approximately one-third of the Nation's commercial air traffic. To compute the national risk it is assumed that these airports can be used with suitable adjustment to represent the entire United States, at least as far as commercial aircraft-related CF risk is concerned. Since these are predominantly large, busy airports near large metropolitan areas, this method may be expected to overestimate the national risk; for our purposes this constitutes a conservative, and therefore desirable, result.

We have already discussed our method of estimating the average number of accidents in the U.S. in one year involving commercial aircraft with CF aboard in a fire (cf section II). In conducting a national simulation

we assume that the actual number of accidents in a year obeys a Poisson distribution with mean equal to 2.6. The ORI national risk model then draws a number of accidents at random from this distribution. The method is illustrated in Figure 9.1. Each of the accidents in a year (one replication) is assigned to one of the airports previously examined. The probability that the accident takes place at one airport is simply the ratio of the number of operations at that airport to the total for all nine airports. This again biases the results in favor of the relatively busy airports we examined previously, and this errs in the conservative direction. The important concept in this method is that the details of the individual aircraft accidents previously simulated at all nine airports are saved and used here. Figure 9.2 is a conceptual representation of the file for one airport's simulated accident. In the national calculation we simply draw one of these accidents at random off the list for the airport to which the national model has allocated the accident. This process is repeated for all accidents in the replication (i.e., simulated year). The sum of costs over all accidents in one year's sample is a conservative estimate of the total national impact.

RESULTS

The results of the calculation, using outputs from the individual airports, and the weighting factors described above, indicate a maximum annual impact on business and industry of $274,000, with a mean of $466. For avionics impact the results are $3,900 and $2, respectively. The method is entirely analogous to that used for the single airports in the sense of being Bernoulli trials, and, therefore, our previous method of computing confidence limits can be used. In this case we typically simulated about 10,000 "national years."

The national risk profile with the 95% statistical confidence limits is shown in Figure 9-3. The risk profile indicates that the probability of exceeding $10,000 per year in CF-related impact is about 1 in a hundred (.01). The statistical confidence limits indicate that the probability is .95 that the actual probability in this case is between .0133 and .00867. The sensitivity tests reported previously for one airport indicate that, with relatively drastic worst-case inputs the results do not change dramatically, thus increasing our overall confidence in the national results presented here. In Figure 9.4 the Phase I and Phase II results are compared, showing that the new Phase II inputs

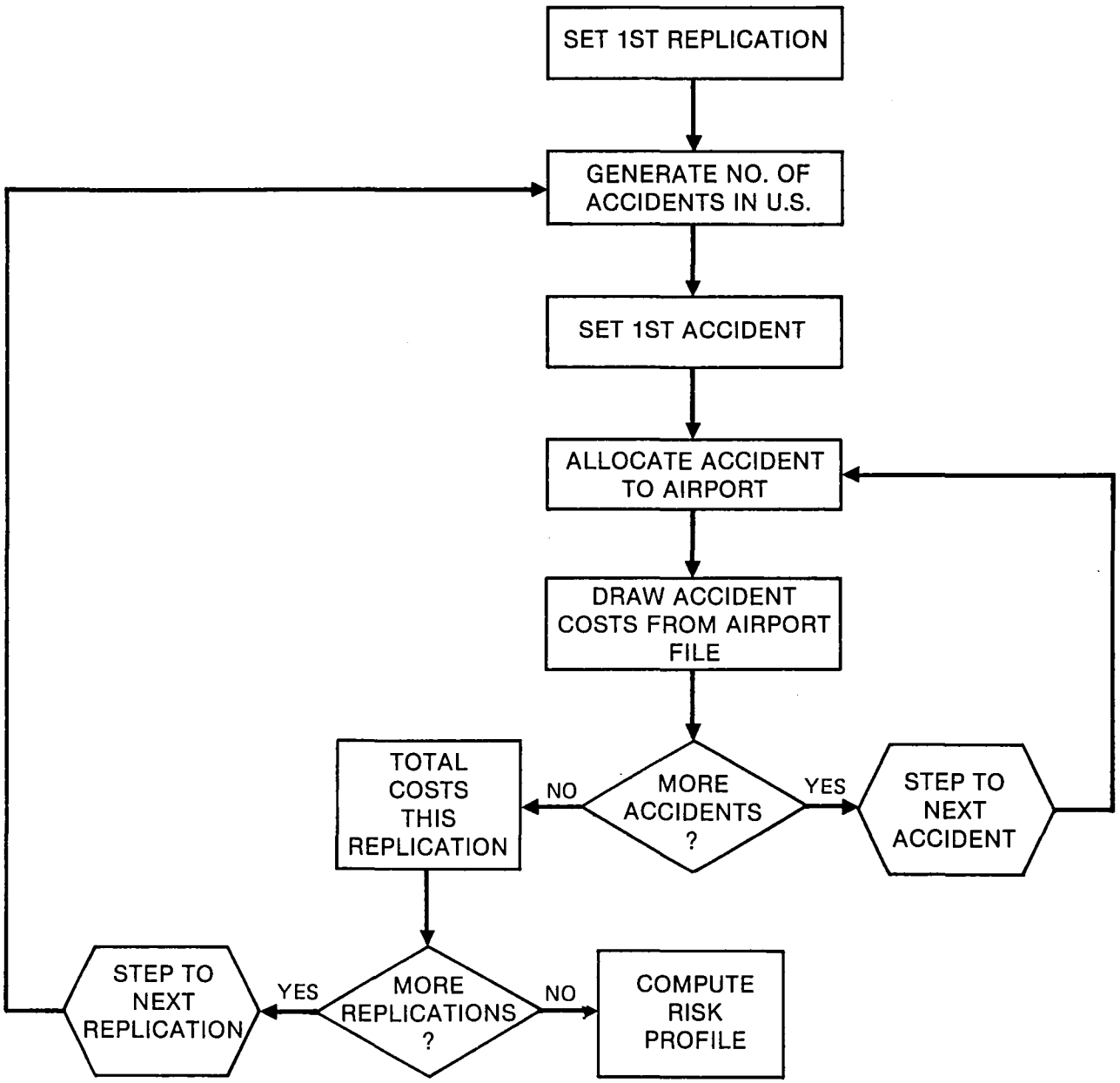

FIGURE 9.1 FLOWCHART FOR NATIONAL RISK ASSESSMENT MODEL

SAMPLE NUMBER	ACCIDENT NUMBER	AIRCRAFT CATEGORY	ACCIDENT TYPE	WEATHER	FAILURES	CONSEQUENCES	COSTS

FIGURE 9.2 CONCEPTUAL TABULAR ARRAY OF DETAILED RESULTS OF SINGLE AIRPORT SIMULATION RUNS

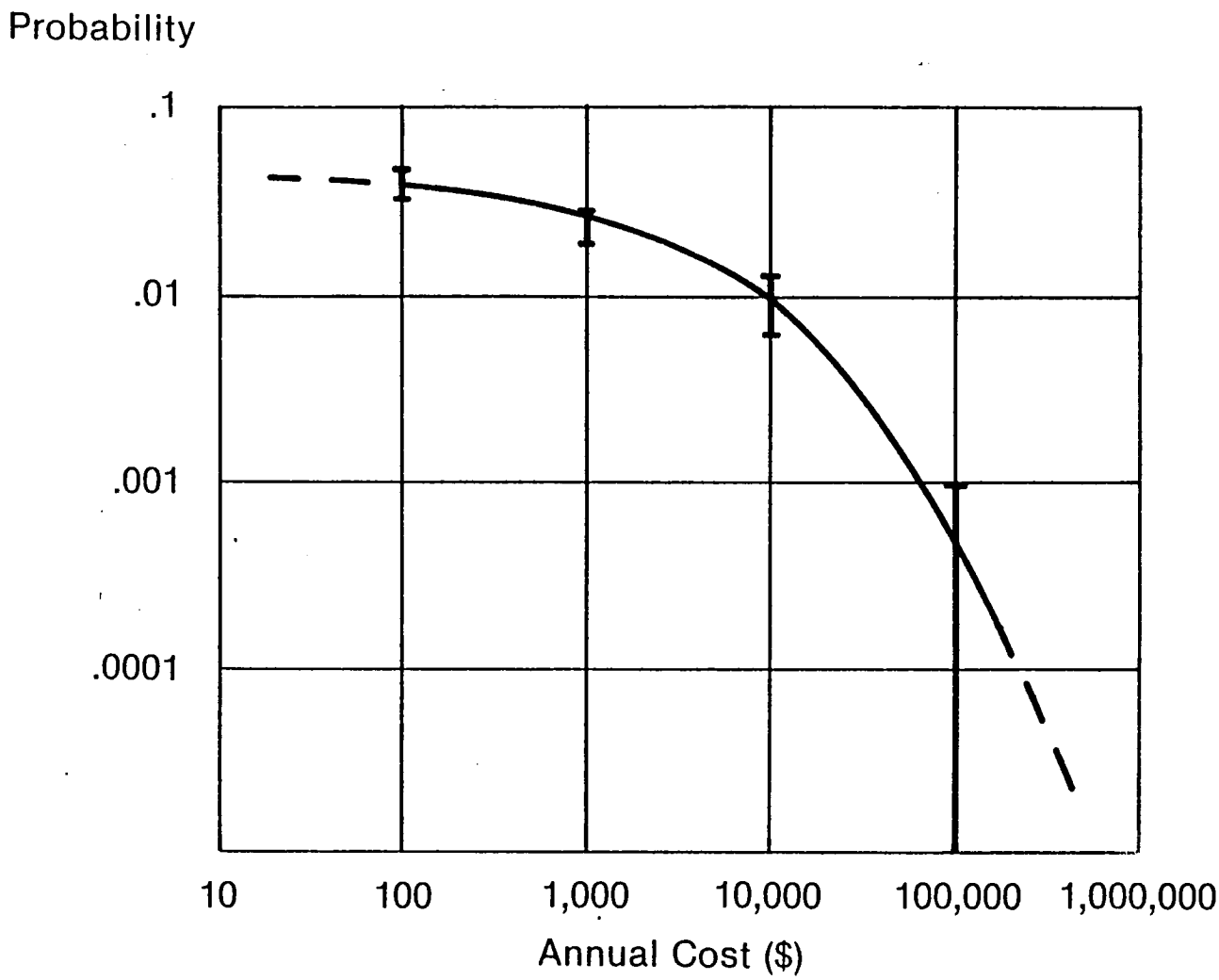

FIGURE 9.3 1993 NATIONAL RISK PROFILE WITH 95% STATISTICAL CONFIDENCE LIMITS

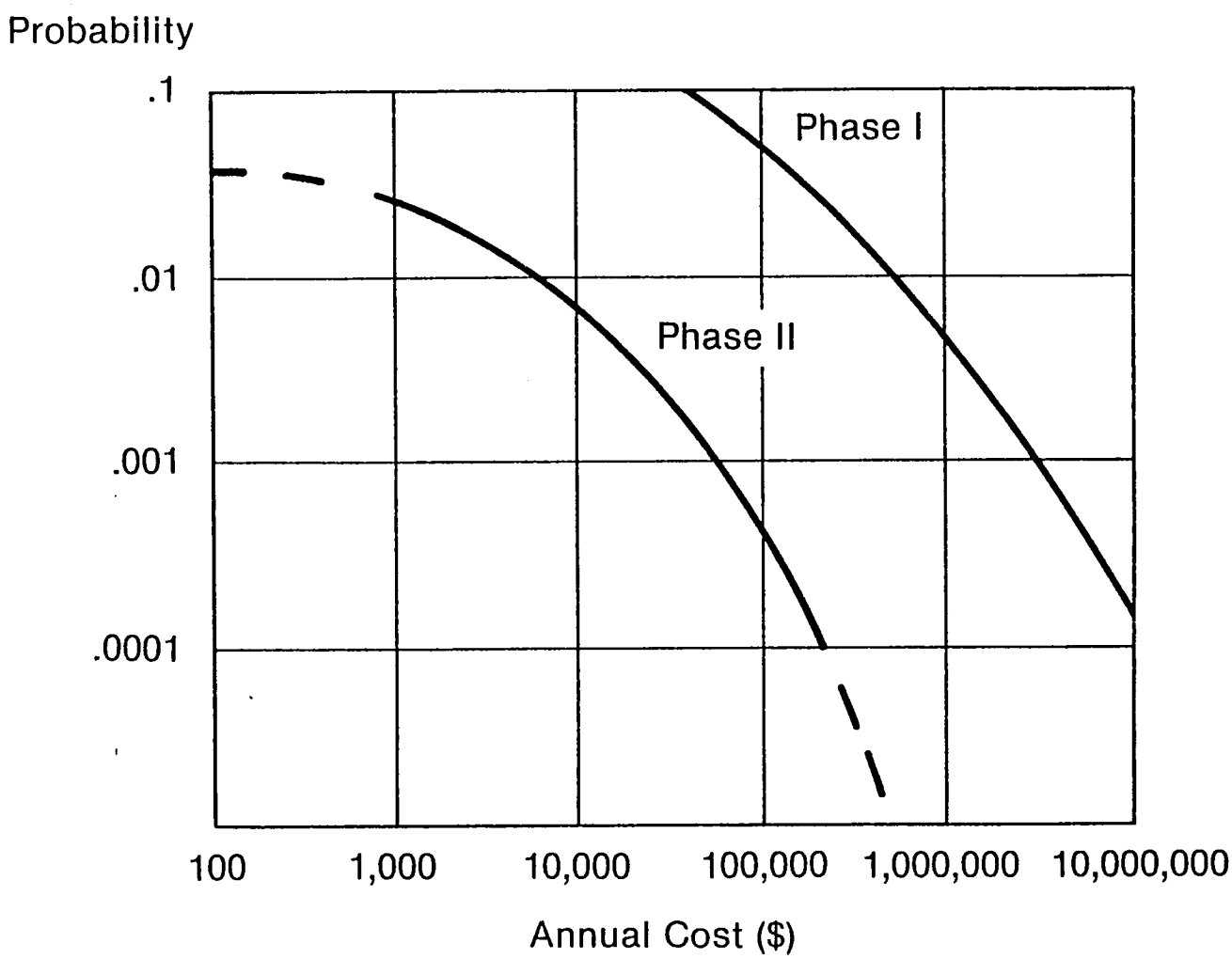

FIGURE 9.4 COMPARISON OF PHASE I AND PHASE II NATIONAL RISK PROFILES

result in a greatly reduced estimated risk, despite the fact that the Phase II model is considerably more likely to generate results with a large variance (extreme values).

X. SUMMARY AND CONCLUSIONS

ORI, Inc., has developed and demonstrated a general stochastic risk assessment model. This model has been applied to the assessment of the risk associated with proposed applications of carbon fiber composite materials in commercial aircraft structures. The airport risk model replicates key elements of the accident scenario (i.e. fire, plume, diffusion and transport, transfer, equipment failure, and economic impact) in a logic structure that supports the calculation of statistical measures of the risk. The national risk is designed to use the results from several individual airport-city calculations.

One of the principal changes from Phase I to Phase II has been the availability of improved input data, particularly for key parameters associated with the amount of fiber in a projected aircraft, the fraction of carbon fiber released in a burn, and the vulnerability of electronic equipment. Where sound experimental data is not available we have always taken a conservative approach; that is, the inputs are selected so as to maximize the estimated risk. Experimental data indicates that the exponential law tends to overestimate the probability of equipment failure for low values of carbon fiber exposure. We have used the exponential law, since it is relatively simple, and is conservative.

The model has been subjected to a variety of tests all showing its inherent stability. We have developed statistical confidence bounds about our

risk probabilities. The model outputs have been subject to a variety of sensitivity tests; these have shown that even when drastic unrealistic shifts in the input data are introduced the resulting annual risk increases by less than a factor of ten.

The national model was run using nine relatively busy airports heavily weighted toward those with large concentrations of business and industry, and thus overestimates the national risk. Even in that case, the chance of exceeding an annual economic impact of more than $100,000 due to aircraft-fire accidents and subsequent carbon fiber release is less than one in a thousand. A worst-case analysis of the possible impact of such accidents on the electric power distribution system showed that the expected number of outages would be negligible compared to outages due to other causes.

Our conclusion, based on the results presented earlier in this report, and summarized briefly above is that:

The risk due to accidental release of carbon fibers following an accident and fire involving civil aircraft is quite small.

APPENDIX A

THE EFFECTS OF CARBON FIBER EXPOSURE ON ELECTRIC UTILITY SYSTEMS

A Worst Case Analysis and Historical Outage Review

APPENDIX A

THE EFFECTS OF CARBON FIBER EXPOSURE ON ELECTRIC UTILITY SYSTEMS

INTRODUCTION

Objectives

This study assesses the expected impacts of the exposure of an electric utility system to carbon graphite fibers in response to the combined requirements of Tasks 8E and 9 of the scope of work:[1/]

- Task 8E - "is directed toward the assessment of the likelihood of failures of the electric power distribution system due to carbon fiber release accidents. Information is available that relates failures of individual critical components of the system to different levels of carbon fiber exposure."
- Task 9 - "In order to properly assess the possible impact of carbon fiber incidents on the national power supply system, it is necessary to develop a historical perspective on previous breakdowns of the system."

Scope

Based on a review of literature and visits to operating electric utilities, for Task 8E we have defined typical electric power distribution

---

[1/] Certain measurements in this Appendix are in English Units. The following factors may be used to convert these measurements to SI Units: (1) kilometer = 0.62 mile; (2) square kilometer = 0.3861 square mile.

systems in the 2.4KV-38KV range, using actual distribution circuits to the maximum extent possible. Using CF exposure failure threshold ($\overline{E}$) values provided by Westinghouse Electric Company for various types of insulators and bushings, expected customer outages due to CF are estimated for the typical distribution circuits.

Using published information and visits to electric utilities and to selected industrial facilities, for Task 9 we have estimated the frequency and duration of failures to power systems and described the protective measures taken by both the utilities and by business and industrial users. This information is used as a baseline against which to assess the expected outages due to exposure to carbon fibers.

Background

Tests which have been performed by the U.S. Army Ballistics Research Laboratory and by the Westinghouse Electric Company indicate that the effects of carbon fibers on electrical systems operating in excess of about 38KV can be neglected. Likewise, the effects of carbon fiber exposure on the secondary side of distribution transformers serving industries, businesses and residences are addressed as a part of the general NASA assessment of carbon fiber risks, described in the main body of this report. There is a need to analyze the potential risks due to CF exposure primary distribution circuits which operate in the 2.4KV to 38KV range.

Tests have been performed by Westinghouse Electric Company on various types of insulators and bushings operating at 7.5KV, 15KV, and 34.5KV and exposed to various lengths of carbon fiber. These tests which are summarized in the final section of this Appendix provide the basic inputs to this analysis.

Rationale

The risks are defined in terms of outage frequencies with and without exposure to carbon fiber. All effects of carbon fiber exposure are estimated on the basis of 3mm-length fiber segments. Power systems, typical distribution systems, and some protective measures are first described. General reliability considerations together with outage data, are then discussed. Finally, estimates of the effects of CF exposure are made on the basis of a typical circuit in the 7.5KV range and an actual 23KV circuit.

DESCRIPTION OF POWER SYSTEMS (References 1, 2, 3, 4)

Illustrative Power System

Figure A.1 is an illustrative power distribution system consisting of transmission circuits, subtransmission circuits, and primary feeders. Stations A, B, and C are bulk power stations interconnected by a transmission network. The distribution system is that portion of the power system which interconnects the customer service connections with the bulk power sources. In Figure A.1, this includes the subtransmission network, Station D, and the primary feeders. In some systems radial subtransmission circuits may be used or a loop arrangement, in which the transmission circuit connects (loops to) several distribution stations and returns to the bulk station, may be used. Often the primary feeders are connected directly to a bulk station without use of intermediate subtransmission voltages. It should also be noted that major power users such as large industrial plants may be fed directly from transmission or subtransmission circuits rather than from primary feeders. In this case, the industrial plants' substations are equivalent to the distribution substation.

Circuit breakers are usually located as shown except that the breakers on the high voltage side of a transformer bank are often omitted because of the high reliability of transformers. Bus tie breakers such as those at Station A are used where bus sectionalizing in the event of a fault is justified. Bulk power outages are usually due to interruptions in the transmission network except for events such as tornadoes that affect large portions of the distribution system. Failures due to CF exposure are expected to occur mainly at the primary feeders; however, in some systems the subtransmission circuits operate at voltages below 38KV and might also be susceptible.

Illustrative Distribution Networks

As mentioned above, the distribution system generally consists of distribution stations connected to bulk sources via subtransmission circuits and connected to the customers by primary feeders. Subtransmission circuits may be radial, loop or network configurations. Likewise, the primary feeders may be radial, loop, or network configurations. The distribution transformers may be 3 phase for industrial or commercial establishments or may be single phase-to-ground to supply residential circuits. Secondary voltages are usually

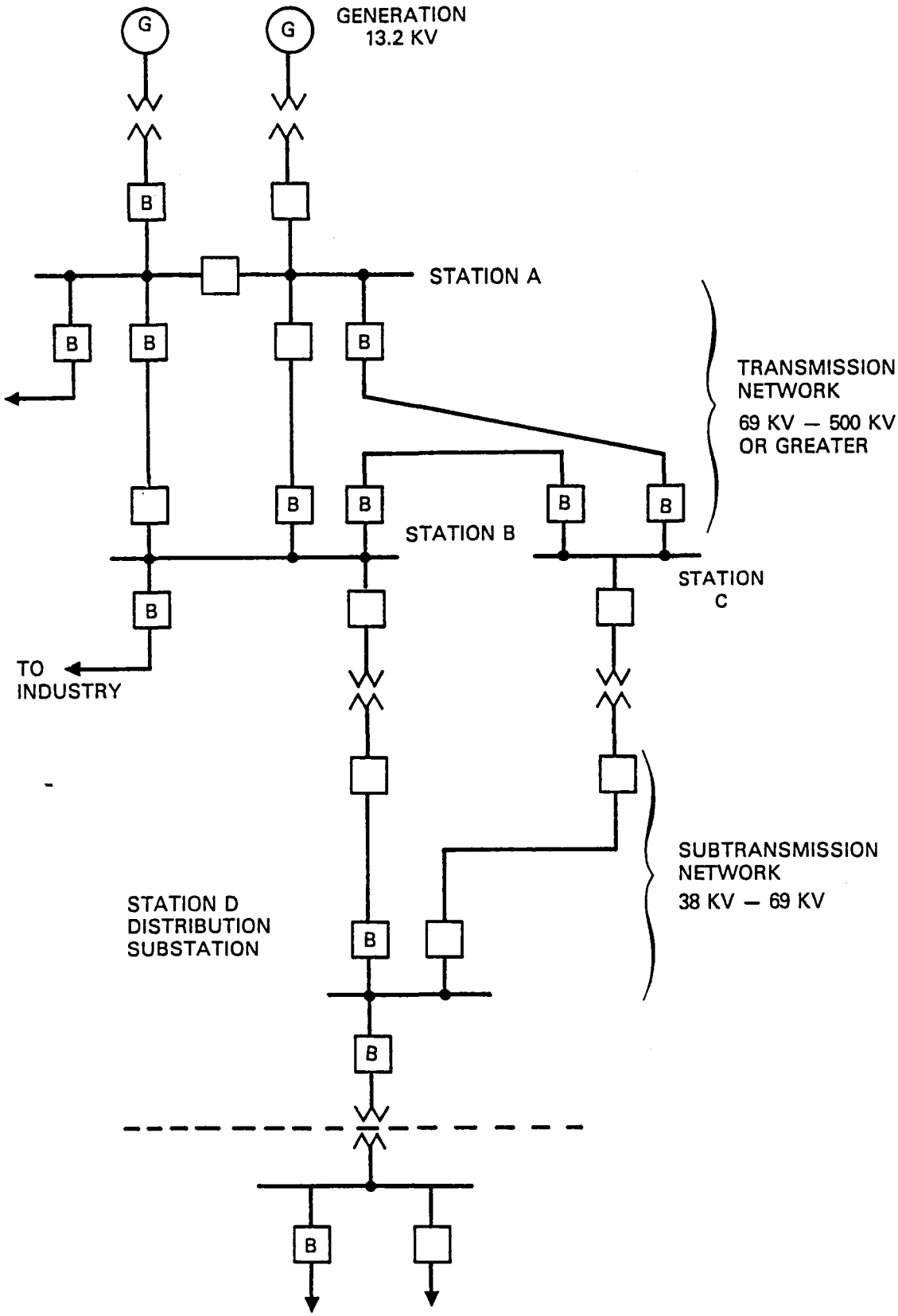

FIGURE A.1. ILLUSTRATIVE POWER SYSTEM

230/115V and are not considered in this analysis. Figure A.2 shows a typical radial distribution feeder in some detail (from Reference 4).

A fault due to CF exposure on a primary feeder can be expected to open the feeder at the nearest protective device (fuse or breaker) toward the source (or sources), thus cutting off all loads downstream from the fuse or breaker.

Figure 3 shows a typical distribution circuit for single family residences in an urban or suburban area. A single phase 230/115V, 3-wire secondary circuit is fed from a three-phase primary feeder by a distribution transformer at each end of an isolated secondary circuit. Each distribution transformer is connected to the primary feeder through a fused disconnect. The isolated secondary circuit may be extended to include other distribution transformers connected in the same manner. Other single phase isolated secondaries will be connected to other phases of the primary feeder in order to balance the loads between phases.

In some residential areas, each isolated secondary is supplied by a single transformer and often in rural areas a distribution transformer will supply a single residence. A common distribution system for commerical areas uses three-phase transformers supplying each establishment directly from the primary feeder, as shown in Figure A.3.

Insulators and Bushings

A flashover due to carbon fibers on any insulator or bushing will cause a failure to the entire circuit associated with that insulator or bushing. The circuit in this case is defined as that portion of the system protected by an associated fuse or circuit breaker. For the case of a primary feeder, a fault on any phase will fail all three phases. For the case of a single-phase fused lateral circuit, a fault will only affect the particular single phase faulted.

A count of the number of distribution transformers, disconnects, etc. in a distribution circuit is available from distribution circuit maps; however, a count of the actual number of pin insulators is not usually directly available (poles are usually not shown). The number of bushings can

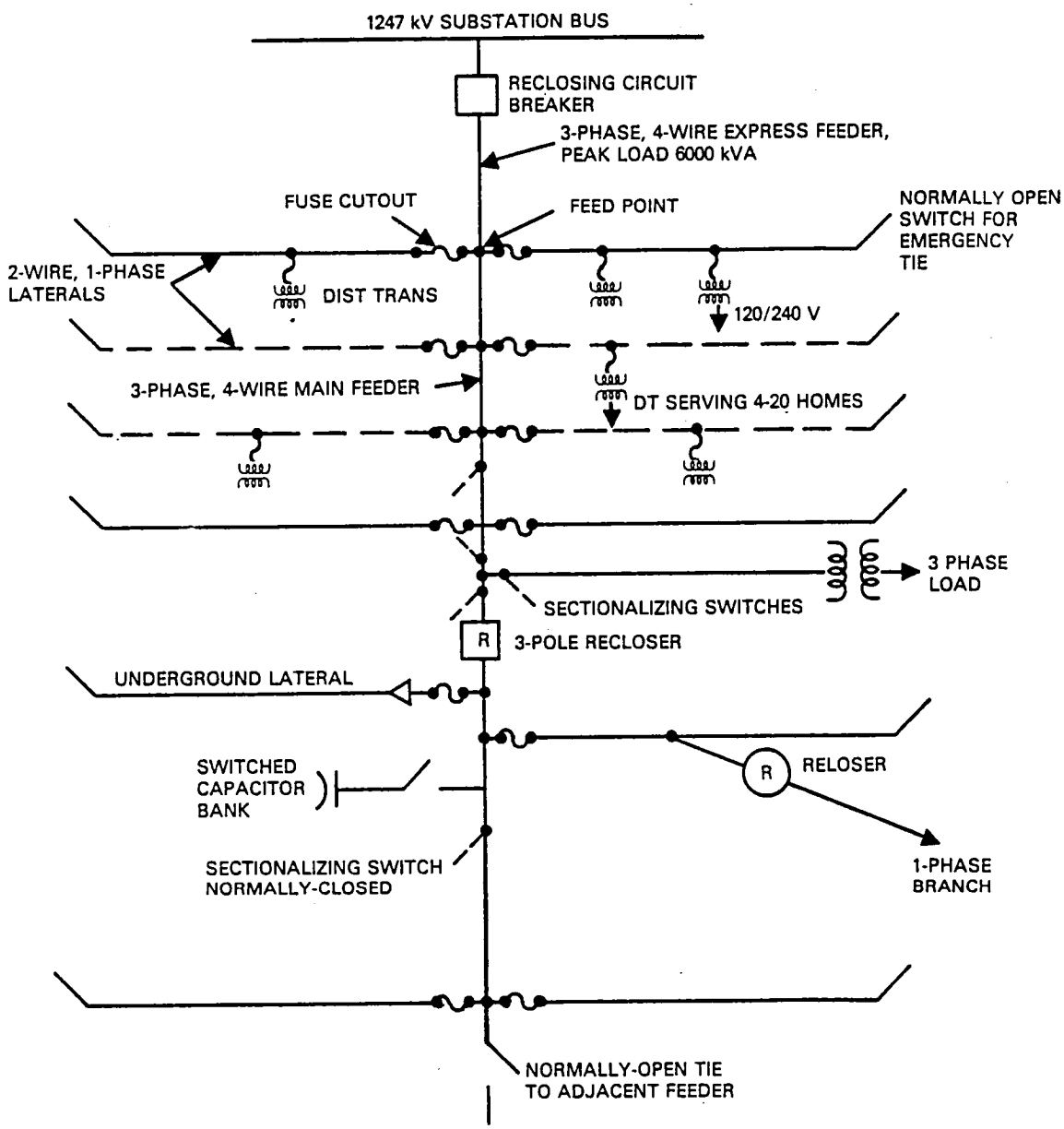

RESIDENTIAL AREA: APPROX. 1,000 HOMES/SW MILE
FEEDER AREA: 1-4 SQ MILE DEPENDING ON LOAD DENSITY
15-30 SINGLE PHASE LATERALS PER FEEDER
150 TO 500 MVA SHORT-CIRCUIT AVAILABLE AT SUBSTATION BUS

FIGURE A.2. ONE-LINE, SYMBOLIC SKETCH OF TYPICAL PRIMARY DISTRIBUTION FEEDER

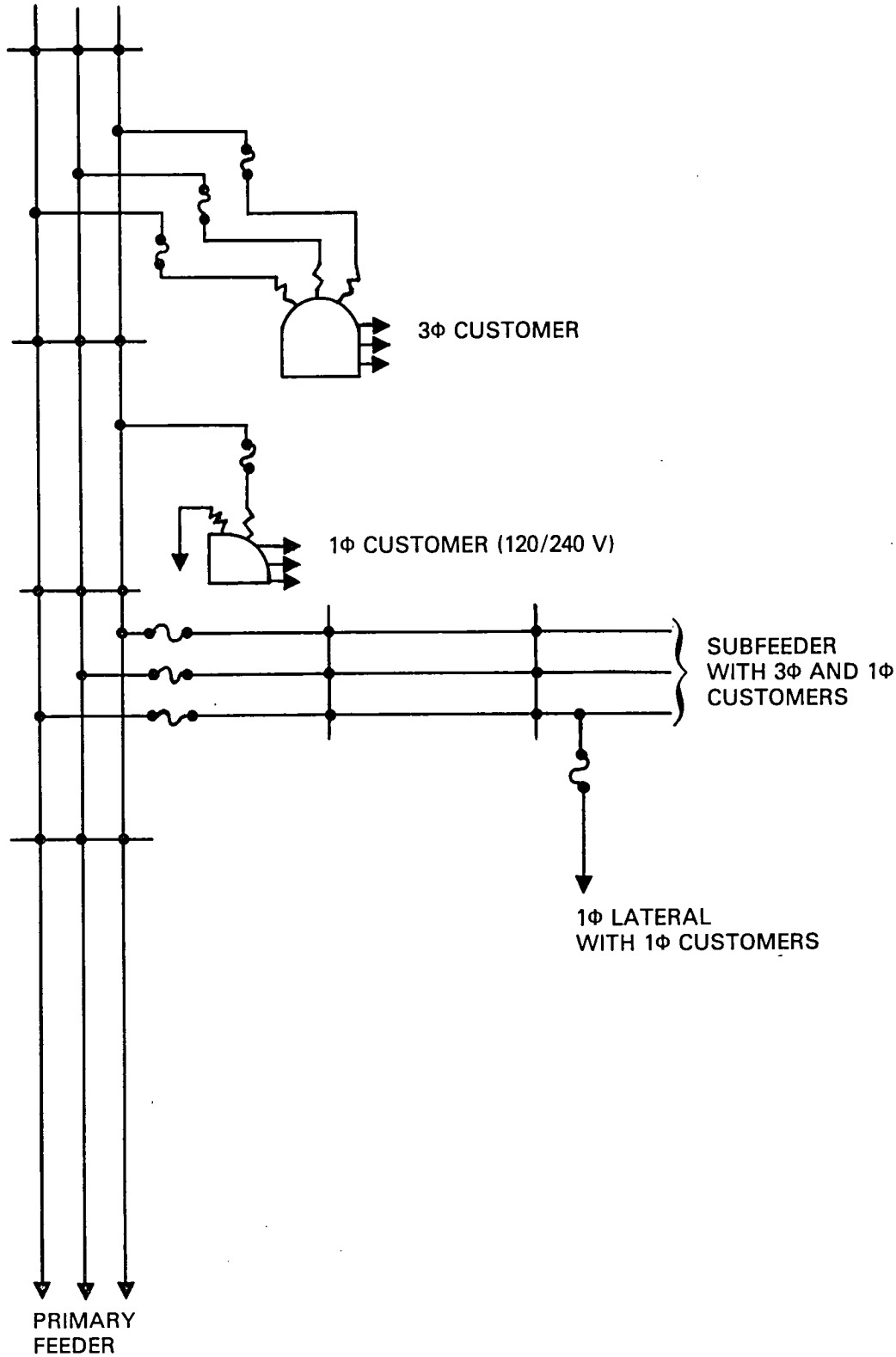

FIGURE A.3. TYPICAL DISTRIBUTION CIRCUIT ARRANGEMENT

be obtained from the number of transformers and line capacitors, while the number of post type insulators can be obtained from the number of disconnect switches and fuses.

The number of pin (or line-post) insulators is proportional to the number of poles, which can be estimated with sufficient accuracy for this study on a per mile basis. The following visual observations have been made in the Washington, D.C. area for urban, suburban, and rural primary feeders owned by PEPCO, VEPCO, and Baltimore Gas and Electric Company:

- In urban areas there are about 60-80 poles per mile and in suburban areas there are about 30-40 poles per mile with pole spacings dependent on the location of customers and street intersections. In rural areas the poles average about 20-30 per mile, depending on design span widths.
- Each pole has 1 pin insulator (or line-post) per phase of primary feeder. Each distribution transformer has 1 vertical bushing per phase plus 2 post insulators for fused cut-outs. Each capacitor bank has 2 vertical bushings per capacitor and each disconnect switch has 2 post insulators per switch.

PROTECTIVE MEASURES

The protective measures include devices and procedures used by both the utility and its customers. These measures are of interest to this problem to the extent that they affect the probability of an outage given a failure, the duration of the outage, and the impact of an outage of given duration.

Generation/Transmission Systems

Protective measures at this system level are only of background interest to this analysis. Faults due to CF on distribution circuits in the 2.4KV-38KV range will normally be cleared at the distribution level and will not affect the generation/transmission system. Note that high load/long duration outages affecting the generation/transmission system are included in the bulk outage data discussed later.

Protection measures at the bulk level include automatic operation of breakers to disconnect faults, load shedding and generator dropping practices, schemes for bringing spinning reserves onto line, means for obtaining emergency start up in the event of system outages, etc. The automatic opening and closing of breakers is the "first line of defense" in the event of unexpected faults and is of more interest to this study than other protective measures.

Some automatic generation/transmission system protective measures are described below for background purposes:

- Generators are protected from internal faults by means of percent differential (current balance) relays which insure that all secondary Ø-Ø + Ø-G currents are equal. Generators are also protected for overspeed, overload, anti-motoring, loss of field, and high temperatures.
- Power Transformers are protected by Ø-Ø + Ø-G differential, overcurrent, and thermal relays.
- Station Buses have percent differential protection to protect against Ø-Ø and Ø-G faults anywhere on the bus.
- Transmission lines are protected by directional overcurrent relays and impedance (distance) relays at the station at each end. These relays also provide backup in the event of a failure to clear faults at adjacent stations and lines. Breakers are normally programmed to open in about 5 cycles and reclose in about 15 cycles in order to clear lightning strikes without power interruption.

Distribution System

Subtransmission lines which carry high distribution loads at relatively high voltages will be protected by means similar to the bulk transmission lines. When a single radial subtransmission line feeds a distribution station, the breaker at the distribution station end of the line may be omitted with protection provided by the breaker at the supply end only. This breaker will open for any faults on the upstream side of the primary feeder breaker and will provide backup to the primary feeder breakers. Primary feeder breakers are controlled by overcurrent relays for each phase and for phase-to-ground currents.

Three automatic reclosures followed by a lockout (in the event of a sustained fault) is common.

Fuses in subfeeders and laterals are usually designed to open prior to operation of the primary feeder breaker while fuses on the distribution transformers are designed to open prior to damage to the lateral fuses, etc. Therefore, insulator or bushing flashovers due to carbon fibers will affect only that portion of the feeder protected by the next protective device toward the source from the fault.

Customer Response to Power Outages

Tables A.1 and A.2 from Ref. (5) summarize types of responses of residential, commercial, and industrial customers to electric utility power outages based on experience in the Pacific Northwest.

ORI surveys of businesses and industries showed a wide variety of protective measures. Facilities in which power continuity is absolutely necessary (e.g., hospitals, air traffic control centers, many chemical plants, radio stations, etc.) have auxiliary generators for backup. However, other industries we surveyed provided no backup power even though power outages lasting more than a few minutes would be costly. Examples include a large truck engine plant, publishing companies, etc. The rationale for this is the extremely high utility reliability that these facilities have experienced in the past coupled with the high cost of auxiliary power. In one or two instances in which the locations permitted, large industries were supplied by more than one primary feeder circuit.

GENERAL RELIABILITY CONSIDERATIONS AND ESTIMATES FOR A TYPICAL DISTRIBUTION SYSTEM

Reliability Measures (Ref. 5, 6)

Commonly applied measures of power systems reliability include the Loss of Load Probability (LOLP) and the Frequency and Duration measure (FAD). The LOLP accounts for the total fraction of time that a power system is expected to have a deficit without regard to the distribution of outage durations. The FAD, on the other hand, accounts for both the frequency and the duration of the outages. It is desirable to account also

TABLE A.1

SUMMARY OF POTENTIAL CONSUMER RESPONSES
TO LOWER ELECTRIC POWER RELIABILITY

Consumer	Function	Response
Residential	Heating	Firewood stored, oil or gas heat
	Refrigeration	Dry Ice
	Lighting	Candles, flashlights
	Cooking	Camp stove
Commercial	Lighting	Batteries, standby generators
	Data processing	UPS (Uninterrupted Power Supply) standby generators
	Refrigeration	Standby generators
Industrial	Electric drive	Standby generators
	Lighting	Batteries
	Space conditioning	Nonelectric heating & cooling

TABLE A.2

SUMMARY OF ESTIMATED CONSUMER RESPONSES TO LOWER RELIABILITY
LEVELS, AS A FUNCTION OF FREQUENCY AND DURATION

Total Outage	Consumer Response		
	Industrial	Commercial	Residential
144 min/ year	Emergency equipment installed	Emergency equipment	No response
288 min/ year	Non-electric equipment installed	Non-electric equipment installed	No response
1440 min/ year	Standby generator installed	Standby generator installed	Emergency equipment installed

Source: Impacts from a Decrease in Electric Power Service Reliability
Stanford Research Institute, June 1976.

for the class of customers affected (residential, commercial, industrial) and for the size of the loads lost. However, in general, data are not sufficient for this level of detail.

Analysis of Bulk Outage Data (Ref. 5, 7, 8, 9)

Bulk power outages are defined under FPC Order 331-1, as interruptions of a generating unit or electrical facility operating at a nominal voltage of 69KV or higher and resulting in a load loss of 15 minutes or longer of at least 100 megawatts. Smaller systems must report to DOE if one half or more of the annual system peak is involved. (Ref. 5, 9).

During CY 1978 there were 62 bulk outages reported (Ref. 9). These involved a loss of about 12,155 MW and 65,000 MWH to about 3.1 million customers. The distribution of outage duration by number of outages, customers affected, customer-hours lost, and loads are summarized in Table A.3. Figure A.4 shows the percent distribution of customers affected by various duration times. These reflect outages only, not counting load reduction measures. When ranges of outage times were given, a midpoint value was used.

If it is assumed that all 63.4×10^6 households and 4.1×10^6 commercial business establishments are utility customers, then about 4.6% of all customers were affected by bulk outages in 1978. This neglects the fact that some customers were affected by more than one bulk outage during 1978. Reference 9 reports the following distribution of bulk outages by customer types:

Residential	55%
Commercial	30%
Industrial	25%

The number of feeders required in an area is primarily a function of the peak loads, with a typical feeder handling 2-3MW. Bulk outages will usually drop a large number of feeders, and the fraction of feeders dropped is roughly proportional to the fraction of loads dropped. If it is assumed that bulk outages are randomly distributed among feeders, then the annual likelihood of a particular feeder being dropped is approximately equal to the fraction of feeders dropped per year. At an average U.S. load of about 350,000MW, the 12,157MW load dropped due to 1978 bulk outages represents about 3.4% of the feeders so that the likelihood of a feeder being dropped due to a bulk outage is approximately .034 per year.

TABLE A.3. DISTRIBUTION OF BULK POWER OUTAGES CY 1978

OUTAGE DURATION (Hours-Days)	NO. OF OUTAGES	CUSTOMERS AFFECTED (Thousands)	CUSTOMER-HOURS LOST (Thousands)	LOAD LOST (MW)
0-1 Hours	35	1612	895	6879
1-3 "	13	410	465	2635
3-6 "	5	344	2217	1459
6-12 "	4	145	1722	678
12-24 "	3	72	759	183
1-5 Days	1	200	9600	323
5-10 "	1	300	43,200	Not Available
TOTAL	62	3083	58,858	12,157

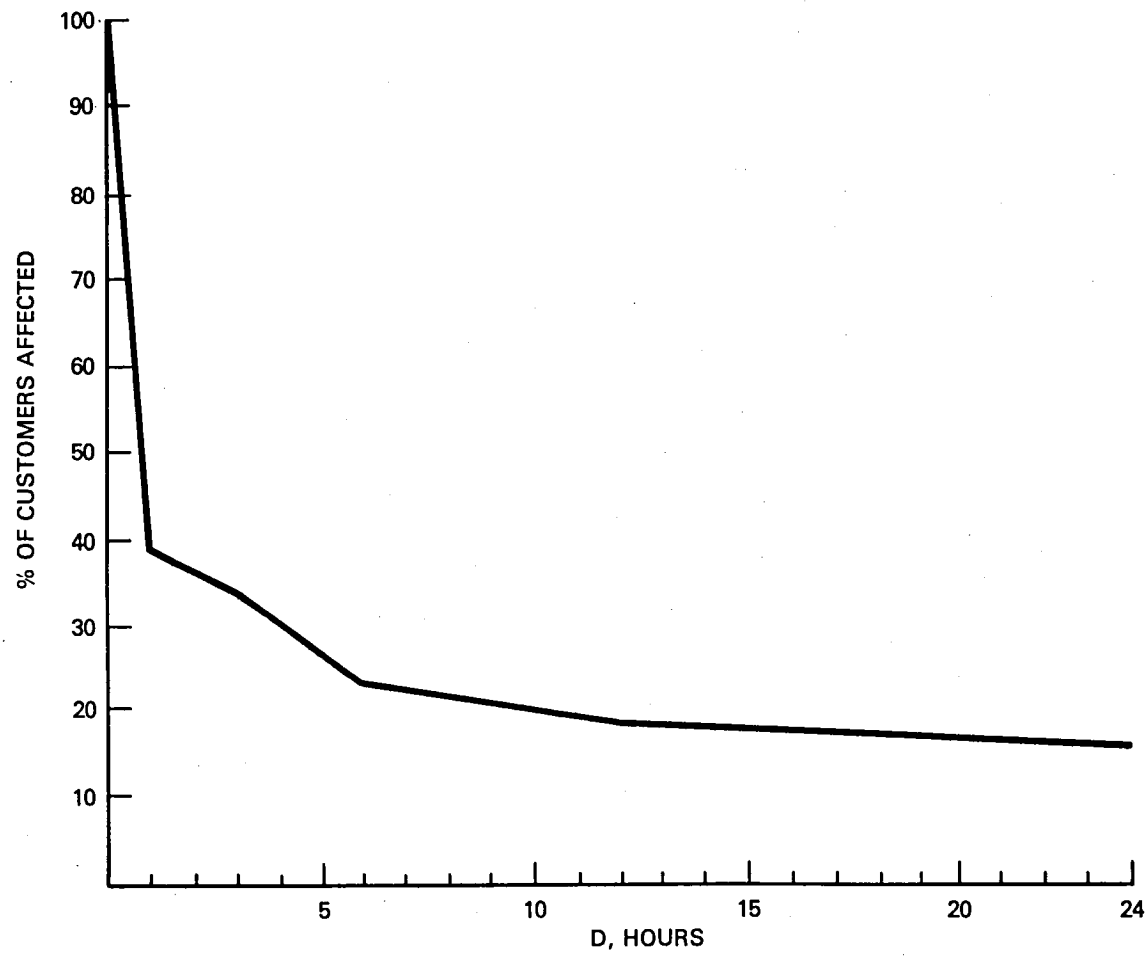

FIGURE A.4. PERCENTAGE OF CUSTOMER-OUTAGES OF DURATION D

Outages Due to Normal Equipment Failures

Estimates of outages due to normal equipment failures (not in the presence of carbon fibers) can be made by applying equipment failure data to "typical" distribution systems.

Figure A.5 shows a one-line diagram of a "typical" distribution circuit. This circuit which feeds an urban residential area consists of 3 circuit-miles of three-phase primary feeder, 16 circuit miles of three-phase subfeeders, and 8 circuit miles of single-phase lateral feeders. These circuits supply 4000 homes through 398 distribution transformers. Sectionalizing fuses are provided in each subfeeder and lateral and at the load midpoint of the primary feeder. One or more normally-open manual tie-switches permit interconnection to other feeders in the event of an emergency.

The expected outages (E_0) per customer (or per distribution transformer) can be estimated from:

$$E_0 = \sum_i E_i F_i$$

where:

E_i = outages in section i

F_i = fraction of customers (or transformers) affected by an outage of section i

and:

$E_i = \lambda_i (t)$

λ_i = failure rate of equipment in section i

t = time over which outages are estimated

The probability of an outage in section i is given by:

$$P_i = 1 - \text{Exp}(-E_i)$$

Failure rates and average outage durations are shown in Table 4 from the sources indicated. It should be noted that there are large uncertainties and variations in both published failure rates and outage durations. For example, the rates shown in Table A.4 for open line

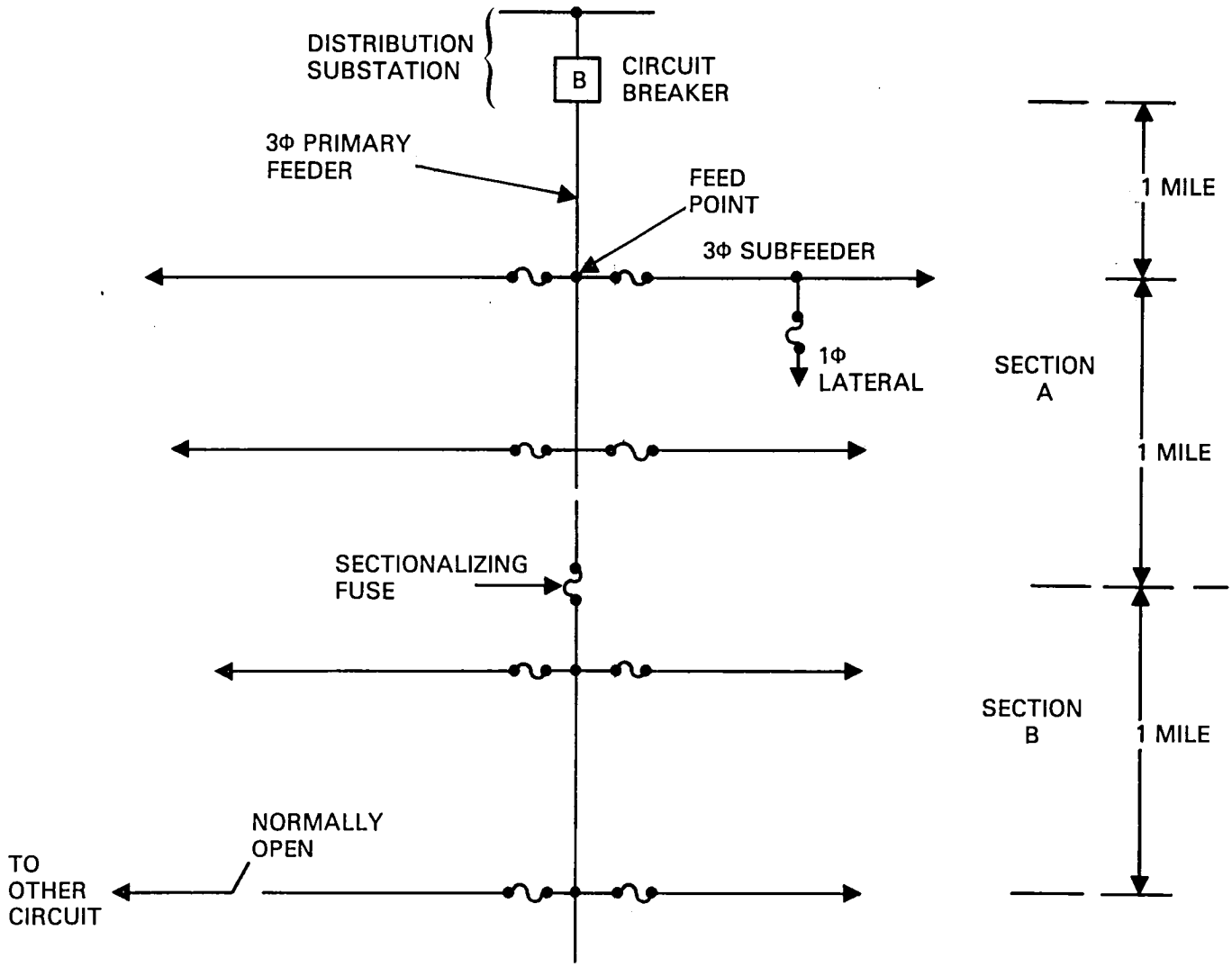

- 2500 KVA PRIMARY FEEDER — SINGLE FED RADIAL
- 4 SQ MILE RESIDENTIAL AREA, 4000 HOMES
- 16 SUBFEEDERS EACH 1 MILE LONG
- 16 LATERALS EACH 1/2 MILE LONG
- 15 — 5 KVA DISTRIBUTION TRANSFORMERS/MILE ON EACH SUBFEEDER, EACH LATERAL, AND ON PRIMARY FEEDER PAST FEED POINT.
- SUBFEEDERS, LATERALS, AND TRANSFORMERS ALLOCATED EQUALLY TO SECTION A & B.

FIGURE A.5. "TYPICAL" DISTRIBUTION CIRCUIT

TABLE A.4

FAILURE RATES OF VARIOUS DISTRIBUTION EQUIPMENTS

DISTRIBUTION EQUIPMENT	NO. FAILED	UNIT-HOURS	FAILURE RATE	OUTAGE DURATION	SOURCE
Dist. Sta. Transformer	–	–	.012/Yr	4 Hr	1, 3
Feeder Cir. Breaker	20	1870	.011/Yr	8 Hr	2, 3
Distribution Sta. Bus	35	584	.06/Yr	5 Hr	2, 3
Distribution Regulator	10	280	.036/Yr	4 Hr	2, 3
Primary Feeder	–	–	.07/Mi/Yr	3 Hr	1, 3
Lateral Feeder	–	–	.18/Mi/Yr	2 Hr	1, 3
Line Fuse	–	–	.0007/Yr	1 Hr	3
Distribution Transformer	28	290	.097/Yr	2 Hr	2

SOURCES:

1 – Power Systems Reliability Calculation (Ref. 10)

2 – Determination and Analysis of Data for Reliability Studies (Ref. 11)
- Field Data from Texas Electric Service, Co.

3 – Reliability Information for Electric Utility Transmission and Distribution Systems (Ref. 6)

feeders apparently include little if any consideration of severe wind, ice, or lightning conditions. Table A.5 provides equipment outage rates for the various equipments shown in Figure A.5.

If there were no sectionalizing fuses, all customers would be affected by all outages and the average outage per customer would be the same as the total for the circuit, 2.859/year. The annual outage probability per customer would be:

$$1 - \text{Exp}\ (-2.859) = 0.94.$$

Now if the primary sectionalizing fuse is added and coordinated so as to open for faults in Section B without interrupting customers in Section A, and if the subfeeder fuses and lateral fuses are omitted, then all customers would be affected by faults in Section A while only 50% of the customers would be affected by faults in Section B. This results in:

Section	Outages/Year	Outage Probability	Customers Affected
A	1.50	0.78	100%
B	1.36	0.74	50%

The average annual outages per customer:

$= 1.50 \times 100\% + 1.36 \times 50\% = 2.18$

The annual outage probability per customer is obtained from:

$$P_{A\overline{B}}\ (100\%) + P_{B\overline{A}}\ (50\%) + P_{AB}\ (100\%) = (.78)\ (1-.74) +$$

$$(.74)\ (1-.78)\ (.50) + (.78)\ (.74) + 0.86.$$

If fuses are now added to each subfeeder and each lateral the following allocation of failure rates, outage probability, and customer outages results:

TABLE A.5

ANNUAL OUTAGES FOR TYPICAL DISTRIBUTION CIRCUIT

DISTRIBUTION STA. TRANSFORMER	=	.012/YR
CIRCUIT BREAKER	=	.011/YR
DIST. FEEDER REGULATOR	=	.060/YR
MAIN FEED (1 MILE OPEN LINE)	=	.070/YR
SEC A PRI FEED (1 MILE OPEN LINE)	=	.070/YR
SEC A SUBFEEDERS (8 MILE OPEN LINE)	=	.560/YR
SEC A LATERALS (4 MILE OPEN LINE)	=	.720/YR
SEC A FUSES (12 TOTAL)	=	.008/YR
TOTAL SEC A	=	1.500/YR
SEC B PRI FEED (1 MILE OPEN LINE)	=	.070/YR
SEC B SUBFEEDERS (8 MILE OPEN LINE)	=	.560/YR
SEC B LATERALS (4 MILE OPEN LINE)	=	.720/YR
SEC B FUSES (13 TOTAL)	=	.009/YR
TOTAL SEC B	=	1.359/YR
TOTAL FOR CIRCUIT	=	2.859/YR

Portion of System	Outages per Year	Outage Prob.	Customers Affected
Equip. prior to Pri fuse, P	2.12	0.19	100%
Primary feeder Section B, b	.07	0.07	50%
Each subfeeder, S	.07	0.07	40%
Each lateral, L	.09	0.09	2%

The average number of annual outages per customer is:

$$.212\ (100\%) + .07\ (50\%) + 16\ (.07)\ (4\%) + 16\ (.09)\ (2\%) = .32.$$

The annual outage probability per customer is approximately:

$$1 - \text{Exp}\ (-0.32) = 0.27$$

Addition of bulk outages to equipment outages results in:

Circuit Configuration	Annual Outage Prob. per Customer $(1-R_{Bulk} \cdot R_{Equip.})$
No Fuse	0.95
Primary sectionalizing fuse	0.87
Subfeeder and Lateral fuses	0.30

Note that these values apparently understate the outages due to tornadoes, ice storms, etc.

Distribution Outage Data

Outage data at the distribution circuit level are not generally available in the published literature. Discussions with various utility companies indicate that about 5-10 outages per year per distribution circuit can be expected. The 23KV distribution circuit described later had 8 outages resulting in a total of about 3700 customer-outages in 10 calendar months.

EFFECTS OF CF ON DISTRIBUTION CIRCUITS

The exposure of electric utility distribution systems to high concentrations of carbon fibers is expected to result in flashovers across insulators and bushings. Since a large number of insulators will be exposed over a period of time, a series of interruptions can be expected

to occur. If the time between flashovers exceeds the feeder breaker reclosing cycle times (adjustable from a few seconds to about 6 minutes), a series of intermittent interruptions will occur. If a series (burst) of flashovers spans the reclosing time, the feeder breaker will lock open. In this analysis, exposure to CF is assumed to result in an interruption with a probability determined by the Weibull distribution.

The exposure values expected to result in flashovers are obtained from Westinghouse Electric Company tests which indicate that the percentage of insulators failed versus the exposure values can be approximated by the Weibull function. Some representative values from the Westinghouse data are contained in Attachment A. Note that large differences in failure characteristics result from tests on different types of insulators and different applied voltages.

In the paragraphs which follow, a typical distribution circuit at 7.5KV primary voltage and a selected actual distribution circuit operating at 23KV are analyzed. The closest applicable insulation types and voltage are selected from the Westinghouse data using the tests of 2mm fiber lengths; the exposure values at 2mm are then linearly extrapolated to values at the 3-mm fiber lengths assumed for this study.

The maximum exposure value expected to be encountered are less than 1×10^6 fiber-sec per cubic meter which yield per-insulator failure probabilities on the order of 1×10^{-8}. The insulator types which occur in small numbers in a circuit (e.g. circuit breaker bushings) can therefore be neglected. Exposure values are translated to insulator failure probabilities using the Weibull function with input constants from the Westinghouse data.

Estimates of customer outages are made based on accidents at the Los Angeles International Airport assuming (a) first that all circuits

fit the 7.5KV circuit characteristics and then (b) that all circuits fit the 23KV circuit characteristics.

Analysis of 7.5 KV Distribution System

The 7.5KV distribution system was described previously and shown in Figure 5. The failure probabilities are dominated by the pin insulators. If the effects of sectionalizing are neglected, which represents the worst case, all pin insulators can be considered in series. The total number of insulators are estimated as follows:

Primary feeder	- 2 miles x 240 insulators/mi.=	480
Secondary feeders	-16 miles x 240 insulators/mi.=	3840
Lateral feeders	- 8 miles x 80 insulators/mi.=	640
	Total	4860

Therefore 5000 insulators are assumed to be in the circuit.

Insulator failure probabilities are estimated from the Weibull function:

$$P_{FI} = 1 - EXP\left[- \left(\frac{\xi_o - \alpha_o}{\alpha}\right) \left(\frac{\mu_o}{\mu_\chi}\right)\right]^{\beta}$$

P_{FI} = Prob. of failure of a single insulator

ξ_o = Exposure value in fiber-sec per cubic meter

α_o = Cut off point on ξ_o

α, β = Welbull constant for the applicable insulator test data

μ_o = μ at fiber length in test, μ_χ = μ of desired fiber length

The probability of failure (outage) of an entire circuit with n insulators in series is equal to:

$$PFC = 1 - \left[EXP - \left(\left(\frac{\xi_o - \alpha_o}{\alpha}\right) \left(\frac{\mu_o}{\mu_\chi}\right)\right)^{\beta}\right]^{n}$$

The Westinghouse data for the wet 7.5KV pin insulator shows: α=.69 x 10^8, β=7.4, μ_o at 2mm = 5.77 x 10^7. Using linear extrapolation (see attachment A) the μ_χ a 3mm = 3.10 x 10^7. Applying the Weibull function with these

values at α_o = o results in the value of failure probability versus exposure shown in Table A.6.

Accident Scenario. There are expected to be 2.6 aircraft accidents per year which will result in fiber release. Previous ORI work has shown that a large release consists of 5×10^{11} fibers. At stability class 6 and a 5.5 meter/sec wind speed the exposure footprints shown in Figure A.6 will result from each release of 5×10^{11} fibers. Based on our earlier analyses, there conditions represent the worst case.

Los Angeles International Airport is chosen as an accident site which represents a severe case from the standpoint of downwind population densities. Data for downwind areas are shown in Table A.7. Each household, business, and industry is assumed equal to one utility customer.

The expected number of customer outages may now be obtained as follows:

$$N_o = N_a \sum_i (PC_i)\ (Di)\ (Ai)$$

where:

N_o = Number of customer outages per year

N_a = Number of accidents per year

PC_i = Probability of an outage/customer for exposure to level i

Di = Customer density in exposure level i

Ai = Area covered by exposure level i (per accident)

The values of PCi, Di and Ai are shown in Table A.8. Intersected areas were obtained by manually comparing footprints versus demographic areas from Table 7.

TABLE A.6

OUTAGE PROBABILITY VS. EXPOSURE LEVEL FOR 7.5KV CIRCUIT

EXPOSURE LEVEL	FAILURE PROBABILITY	
	1 INSULATOR	ENTIRE CIRCUIT
1×10^{3}	7.29×10^{-11}	5.00×10^{-7}
5×10^{3}	3.64×10^{-10}	2.00×10^{-6}
1×10^{4}	7.29×10^{-10}	3.50×10^{-6}
5×10^{4}	3.64×10^{-9}	1.80×10^{-5}
1×10^{5}	6.16×10^{-9}	3.10×10^{-5}
2.5×10^{5}	2.00×10^{-8}	1.05×10^{-4}
5×10^{5}	3.64×10^{-8}	1.80×10^{-4}
1×10^{6}	6.15×10^{-5}	3.03×10^{-2}
1×10^{7}	6.15×10^{-5}	2.65×10^{-1}
2×10^{7}	1.03×10^{-2}	0.9999 . . .
3×10^{7}	1.88×10^{-1}	0.9999 . . .

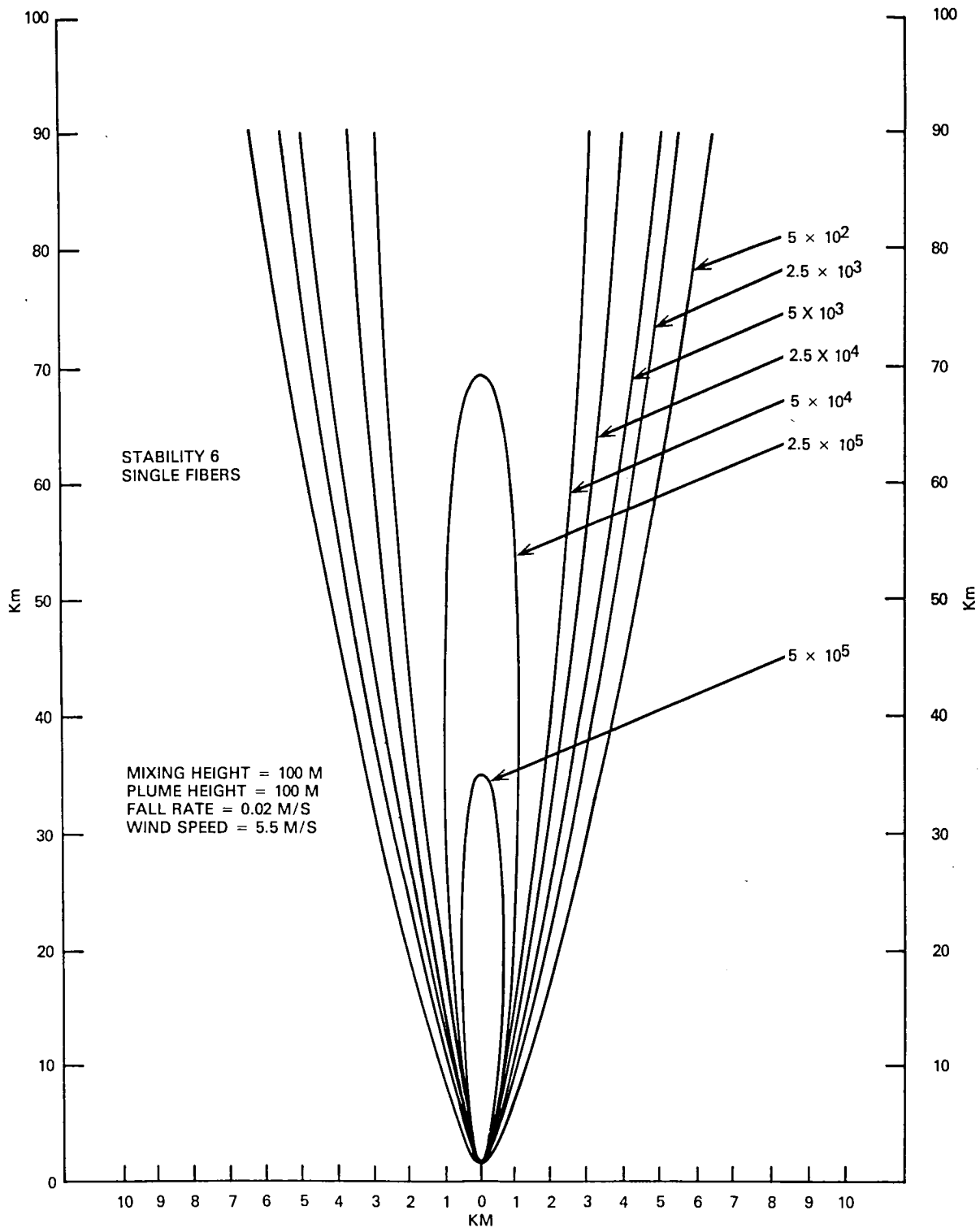

FIGURE A.6. EXPOSURE FOOTPRINTS FOR RELEASE OF 5x10" SINGLE FIBERS AND METEOROLOGICAL CONDITIONS SHOWN

TABLE A.7

DEMOGRAPHIC DATA FOR AREA DOWNWIND OF LOS ANGELES INTERNATIONAL AIRPORT

COUNTY OR CITY	AREA SQ. MI.	DISTANCE FROM A/P	DISTANCE ALONG DOWNWIND AXIS	CUSTOMERS PER SQ. MI.
Los Angeles SMSA	4069	0 Mi.	35 Mi.	650
Orange County	782	35 "	30 "	615
Riverside City	71.3	40 "	10 "	230
Ontario City	32.1	40 "	10 "	671
San Bernadino County	20,117	30 "	10 "	Urban - 370 Other - 15
Riverside County	7176	40 "	180 "	22

TABLE A.8

INTERSECTED AREAS (Ai), CUSTOMER OUTAGE PROBABILITY (PCi), AND CUSTOMER DENSITY (Di) FOR INTERSECTION OF EXPOSURE FOOTPRINTS WITH AREAS FROM TABLE 8.

EXPOSURE LEVEL Eo	FOOTPRINT SIZE (Mi.)			DEMOGRAPHIC REGION INTERSECTED	INTERSECTED AREA Ai	CUSTOMER OUTAGE PROB. PCi	CUSTOMER DENSITY Di
	L	W	Area*				
5×10^5	30	4	37	Los Angeles, SMSA	37 Sq. Mi.	1.80×10^{-4}	650
2.5×10^5	66	6	83	Los Angeles	5 Sq. Mi.	1.05×10^{-4}	650
				San Bernadino County - Urban	5 Sq. Mi.	1.05×10^{-4}	370
				Riverside City	71 Sq. Mi.	1.05×10^{-4}	230
				Riverside County	2 Sq. Mi.	1.05×10^{-4}	22
5×10^4	192	20	1093	San Bernadino County - Other	365 Sq. Mi.	1.80×10^{-5}	15
				Riverside County	728 Sq. Mi.	1.80×10^{-5}	22
5×10^3	240	36	1557	San Bernadino County - Other	519 Sq. Mi.	2.00×10^{-6}	15
				Riverside County	1038 Sq. Mi.	2.00×10^{-6}	22

*Areas are those Portions of Footprints that are Mutually Exclusive.

Applying the above relations results in the following customer outages per accident:

Exposure Level	Outage/Customer	x	Density	x Area	=	Customer Outages
$5x10^5$	$1.80x10^{-4}$		650	37		4.330
$2.5x10^5$	$1.05x10^{-4}$		650	5		0.340
$2.5x10^5$	$1.05x10^{-4}$		370	5		0.190
	$1.05x10^{-4}$		230	71		1.710
	$1.05x10^{-4}$		22	2		0.005
$5x10^4$	$1.80x10^{-5}$		15	365		0.099
$5x10^4$	$1.80x10^{-5}$		22	728		0.288
$5x10^3$	$2.00x10^{-6}$		15	510		0.016
$5x10^3$	$2.00x10^{-6}$		22	1038		0.046
			Total per accident			≃ 9.000

Total per year = 2.6 x 9 ≃ 23.40

This result compares with over 3 million customer outages due to bulk outages alone. Applying the results of the reliability analysis for the typical circuit under the same fusing conditions as above yields at least another 20 million outages per year due to normal distribution system failures.

Analysis of a Selected 23KV Distribution Circuit

Figure A.7 shows a one-line schematic of an actual 23KV distribution circuit. This circuit serves about 1800 industrial, commercial, and residential customers in an urban area of about one square mile. This circuit consists of a 3ϕ radial primary feeder with 3ϕ subfeeders and laterals together with a few 1ϕ laterals as shown. There is no automatic sectionalizing capability except for the fusing of some laterals as shown. There exists the capability to cross-tie to adjacent circuits at several points.

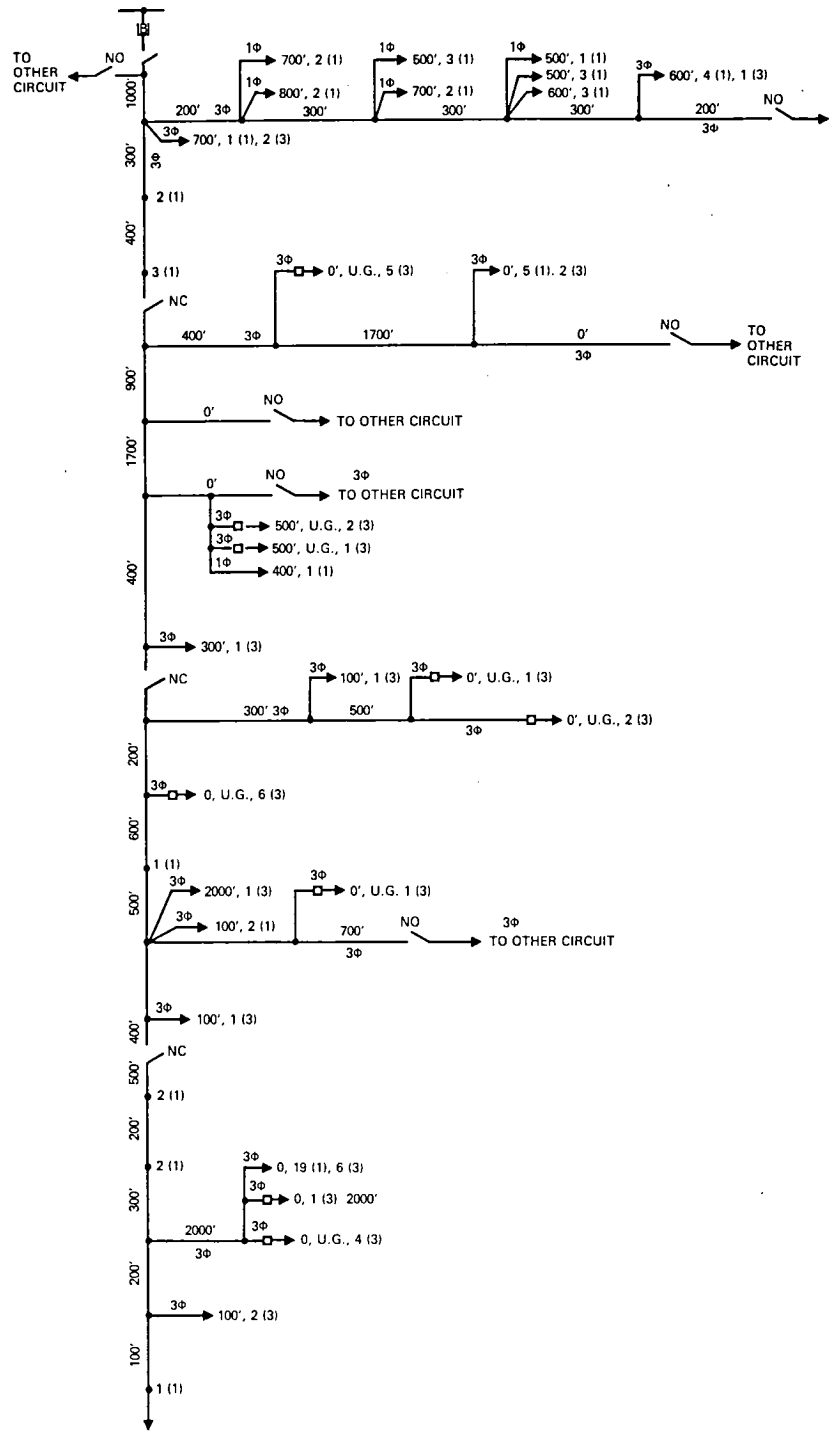

FIGURE A.7. SELECTED ACTUAL DISTRIBUTION CIRCUIT

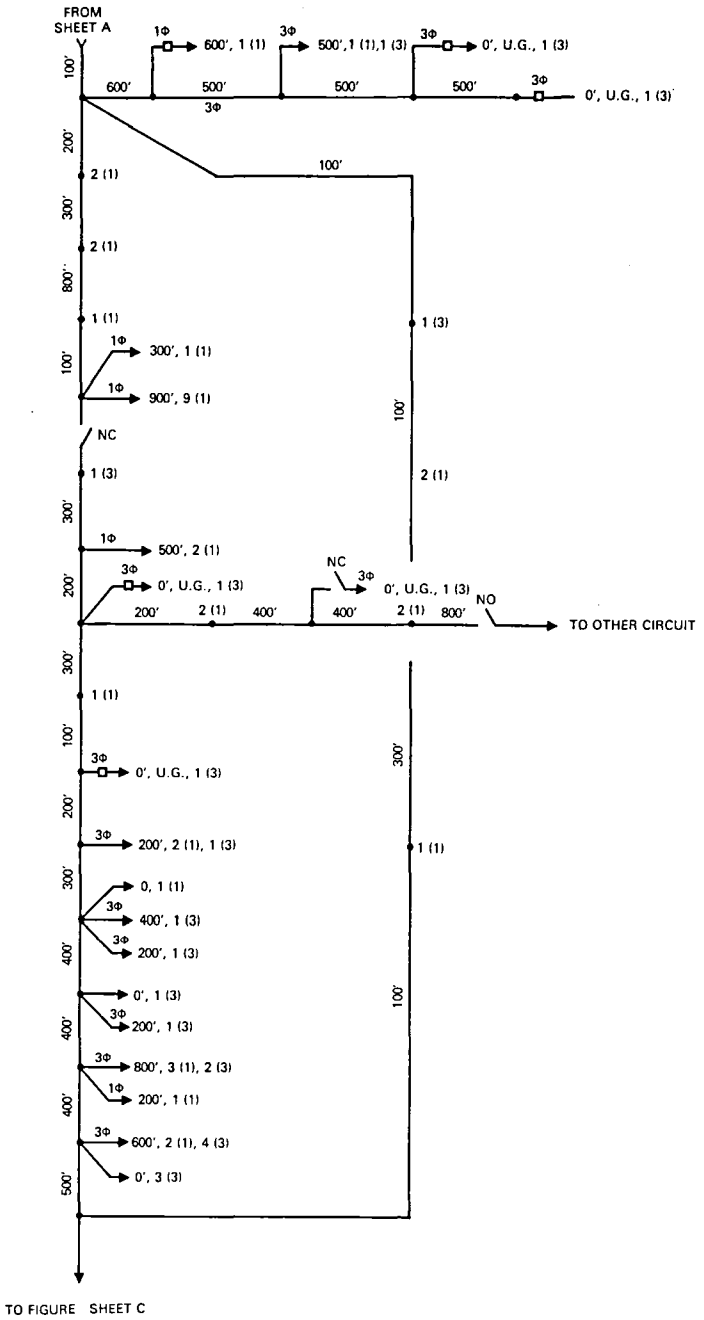

FIGURE A.7. SHEET B

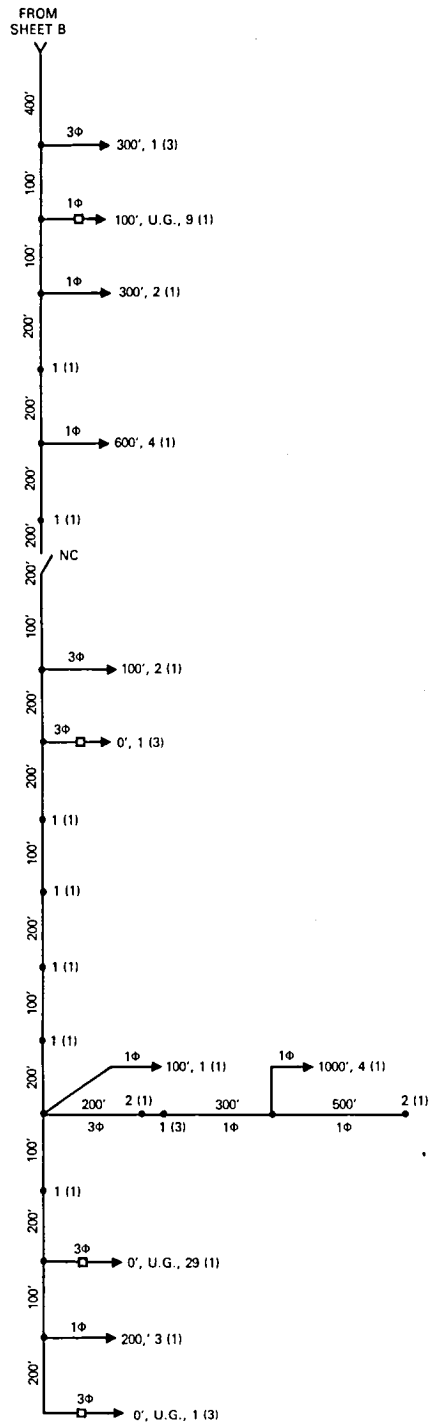

SYMBOLS

3Φ
→ 3-Phase subfeeder or lateral

X00′ is the length of the subfeeder or lateral open wire circuits

U.G. — Underground

X (3) — Number of 3Φ transformer in subfeeder or lateral

X (1) — Number of 1Φ transformer in subfeeder or lateral

X (1) — Number of 1Φ transformers located on primary feeder

NC — Normally closed

NO — Normally open

FIGURE A.7. SHEET C

Circuits and transformers are summarized below:

Total 3ϕ open lines $\simeq$ 37,000 ft.

Total 1ϕ open lines $\simeq$ 10,300 ft.

Total exposed distribution transformers

$3\phi \simeq 32$

$1\phi \simeq 116$

Total non-exposed distribution transformers (in underground vaults and in buildings)

$3\phi = 32$

$1\phi = 40$

Normal Reliability. There are about 8-10 normal outages (about 3700 customer-outages) per year on this circuit. This appears to be typical for the type of circuit (based on discussions with several utilities).

Insulator Failure Probability. The total number of insulators are estimated from:

7 miles of 3ϕ lines x 240/mile	=	1680
2 miles of 1ϕ lines x 80/mile	=	160
Total	=	1840

The 34.5KV distribution post insulators are the closest applicable insulators, used as line posts for the 23 KV open lines. The Westinghouse data for this shows $\alpha = .19 \times 10^9$, $\beta = 1.99$, M=2mm = 1.8×10^8, M=3mm (by linear extrapolation) = 1.0×10^8. Failure probabilities for a single insulator and for all insulators in series are shown in Table A.9.

Accident Scenario. The same accident scenario is applied as used previously, 2.6 aircraft accidents each releasing 5×10^{11} fibers at Los Angeles International Airport, and producing the same footprints.

TABLE A.9

OUTAGE PROBABILITY VS. VARIOUS EXPOSURE LEVELS FOR 23 KV CIRCUIT

EXPOSURE LEVEL	FAILURE PROBABILITY	
	1 INSULATOR	ENTIRE CIRCUIT
1×10^{3}	1.0×10^{-10}	1.84×10^{-7}
5×10^{3}	3.0×10^{-9}	4.60×10^{-6}
1×10^{4}	1.0×10^{-8}	1.80×10^{-5}
5×10^{4}	2.4×10^{-7}	4.46×10^{-4}
1×10^{5}	9.6×10^{-7}	1.42×10^{-3}
2.5×10^{5}	5.9×10^{-6}	1.09×10^{-2}
5×10^{5}	2.4×10^{-5}	4.26×10^{-2}
1×10^{6}	9.4×10^{-5}	.1589
1×10^{7}	9.1×10^{-3}	.9999
2×10^{7}	3.5×10^{-2}	.9999
3×10^{7}	7.8×10^{-2}	.9999

The Expected Number of Customer Outages are estimated in the same way as was done previously, producing the following results:

Exposure Level	Outage/Customer	x	Density	x	Area	=	Customer Outages
$5x10^5$	$4.26x10^{-2}$		650		37		1024.53
$2.5x10^5$	$1.09x10^{-2}$		650		5		35.43
	$1.09x10^{-2}$		370		5		20.17
	$1.09x10^{-2}$		230		71		178.00
	$1.09x10^{-2}$		22		2		0.48
$5.0x10^4$	$4.46x10^{-4}$		15		365		2.44
	$4.46x10^{-4}$		22		728		7.14
$5.0x10^3$	$4.60x10^{-6}$		15		519		0.04
	$4.60x10^{-6}$		22		1038		0.11
			Total per accident			=	1268.34

Total per year = 2.6 x 1268.34 ≃ 3298 customer outages per year

From the actual circuit outage data there were 3700 outages for 1800 customers or 2.06 outages per year per customer. For the 97636 customers within the exposure footprints, normal customer outages are expected to be about 2.06 x 97636 = 2.01 x 10^5 customer outages. The ratio of CF/normal outages is: 3298 ÷ 2.01 x 10^5 ≃ 16/1000 for those affected by CF. Over the entire U.S., the 3298 CF induced outages/year compares with over 20 million which are expected to occur normally.

CONCLUSION

The carbon fibers appear to present an insignificant problem to electrical distribution circuits, even when estimates are made using very pessimistic (worst case) assumptions.

APPLICATION OF INSULATOR TEST DATA TO POWER DISTRIBUTION STUDY

The Westinghouse Electic Company has performed tests on various types of insulators and bushings at various applied voltages and exposed to various fiber lengths. The results of these tests are summarized in Table A.10 (Westinghouse Table 3.3). Figure A.8 (Westinghouse Figure 3.3-1) shows interpolation of some of these data for various fiber lengths.

Figure A.8 has been used to scale values of $\bar{E}$ to 3mm fiber lengths for those insulators shown on Figure 3.3-1. Insulators and bushings not shown on Figure A.8 are assumed to scale to fiber length at the same rate as the 15 KV C Neck Distribution post since this is the most conservative rate indicated on Figure A.8. The results are shown in Table A.11.

The values of $\bar{E}$ at 3mm are selected for the insulator types and voltages closest to those representing the distribution systems being analyzed.

Figure A.9 shows the values of exposure-to-flashover for a wet 7.5KV pin insulator while Figure A.10 shows the values of exposure-to-flashover for 34.5KV distribution post. Thse figures and associated Weibull constants are used as the basis for failure estimates made in this study (after translation of mean values for 3mm fiber lengths).

TABLE A.1 RESULTS OF TESTS FOR SELECTED INSULATORS

INSULATOR	n	FIBER LENGTH mm	EXPOSURE		CONFIDENCE INTERVAL ABOUT MEAN 95%	MINIMUM EXPOSURE	P < MIN*	CONCENTRATION μ
			μ	σ				
7.5 kV Pin	4	2.0	2.8×10^8	1.3×10^8		1.4×10^8	44%	1.6×10^4
7.5 kV Pin (Wet)	7	2.0	5.8×10^7	2.0×10^7	$3.4 \times 10^7 < \mu < 7.4 \times 10^7$	4.8×10^7	28%	1.5×10^4
15 kV C-Neck D. Post Vert.	2	2.0	7.3×10^7	3.0×10^7		5.2×10^7	68%	1.6×10^3
15 kV C-Neck D. Post (Wet)	10	2.0	6.2×10^7	1.0×10^7		4.7×10^7	21%	1.6×10^4
34.5 kV D. Post Vert.	5	2.0	1.8×10^8	$.9 \times 10^8$		1.53×10^8	37%	1.8×10^4
7.5 kV Pin	46	4.3	4.1×10^7	4.0×10^7	$2.6 \times 10^7 < \mu < 5.7 \times 10^7$	2.8×10^7	5%	1.3×10^4
7.5 kV Stat. Post Vert.	1	4.3	$>4.0 \times 10^8$					1.5×10^4**
7.5 kV Stat. Post Hor.	1	4.3	4.0×10^8					2.1×10^4
7.5 kV Pin	15	4.3 + 9	1.7×10^7	7.6×10^6	$1.3 \times 10^7 < \mu < 2.3 \times 10^7$	3.0×10^6	14%	8.3×10^3
15 kV C-Neck D. Post Vert.	26	4.3 + 9	2.9×10^6	2.6×10^6	$2.0 \times 10^6 < \mu < 3.0 \times 10^6$	8.7×10^5	8%	6.7×10^3
7.5 kV Pin	52	9.0	4.8×10^6	2.9×10^6	$3.7 \times 10^6 < \mu < 5.3 \times 10^7$	1.6×10^6	6%	5.0×10^3
15 kV Pin Cap	14	9.0	2.1×10^6	5.9×10^5		1.3×10^6	15%	2.5×10^3
7.5 kV Stat. Post Vert.	10	9.0	1.2×10^7	1.2×10^7	$4.3 \times 10^6 < \mu < 2.47 \times 10^7$	1.6×10^6	21%	4.3×10^3
7.5 kV Stat. Post Hor.	5	9.0	3.4×10^7	2.3×10^7		1.2×10^7	37%	6.9×10^3
34.5 kV Stat. Post Vert.	9	9.0	4.9×10^7	4.7×10^7		1.3×10^6	23%	12.2×10^3
5 kV Fostoria Insulator	4	9.0	8.4×10^6	6.6×10^6		2.9×10^6	44%	2.0×10^3
5 kV Trans. Bushing Vert.	5	9.0	3.8×10^6	7.9×10^5		7.5×10^6	37%	1.2×10^3
15 kV Trans. Bushing Vert.	16	9.0	1.0×10^6	3.3×10^5		6.0×10^5	13%	1.3×10^3
5 kV Trans. Bushing Hor.	6	9.0	2.3×10^6	7.1×10^5		1.3×10^6	32%	1.0×10^3
15 kV C-Neck D. Post Vert.	15	9.0	1.2×10^6	4.0×10^5	$9.0 \times 10^5 < \mu < 1.4 \times 10^6$	5.6×10^5	14%	1.2×10^3
15 kV C-Neck D. Post Hor.	15	9.0	1.8×10^6	6.0×10^5		5.6×10^5	14%	1.6×10^3
34.5 kV D. Post Vert.	18	9.0	9.5×10^5	6.4×10^5	$5.1 \times 10^5 < \mu < 1.3 \times 10^6$	3.0×10^5	12%	9.2×10^2
7.5 kV Suspension Vert.	13	9.0	7.9×10^6	4.8×10^6		2.7×10^6	16%	2.9×10^3
7.5 kV Pin	17	9.0 + 12.0	5.0×10^6	3.2×10^6	$3.3 \times 10^6 < \mu < 6.5 \times 10^6$	2.3×10^6	13%	4.5×10^3
34.5 kV D. Post Vert.	15	9.0 + 12.0	8.0×10^5	2.8×10^5	$6.4 \times 10^5 < \mu < 9.8 \times 10^5$	3.0×10^5	14%	1.1×10^3
7.5 kV Pin	15	10.5	6.5×10^5	2.4×10^5	$5.1 \times 10^5 < \mu < 7.8 \times 10^5$	2.6×10^5	14%	8.6×10^2
7.5 kV Stat. Post Vert.	20	10.5	4.5×10^6	4.3×10^6	$2.35 \times 10^6 < \mu < 4.7 \times 10^6$	1.2×10^6	11%	4.6×10^3
15 kV C-Neck Dist. Post Vert.	15	10.5	5.2×10^5	3.18×10^5	$3.5 \times 10^5 < \mu < 6.2 \times 10^5$	2.4×10^5	14%	6.3×10^2
34.5 kV Dist. Post	16	10.5	2.2×10^5	1.2×10^5	$1.5 \times 10^5 < \mu < 2.7 \times 10^5$	1.5×10^5	13%	5.2×10^2

* Likelihood of a flashover to occur at an exposure of less than the minimum, with 90% confidence.
** This insulator flashed only after given exposure and twice rated voltage.

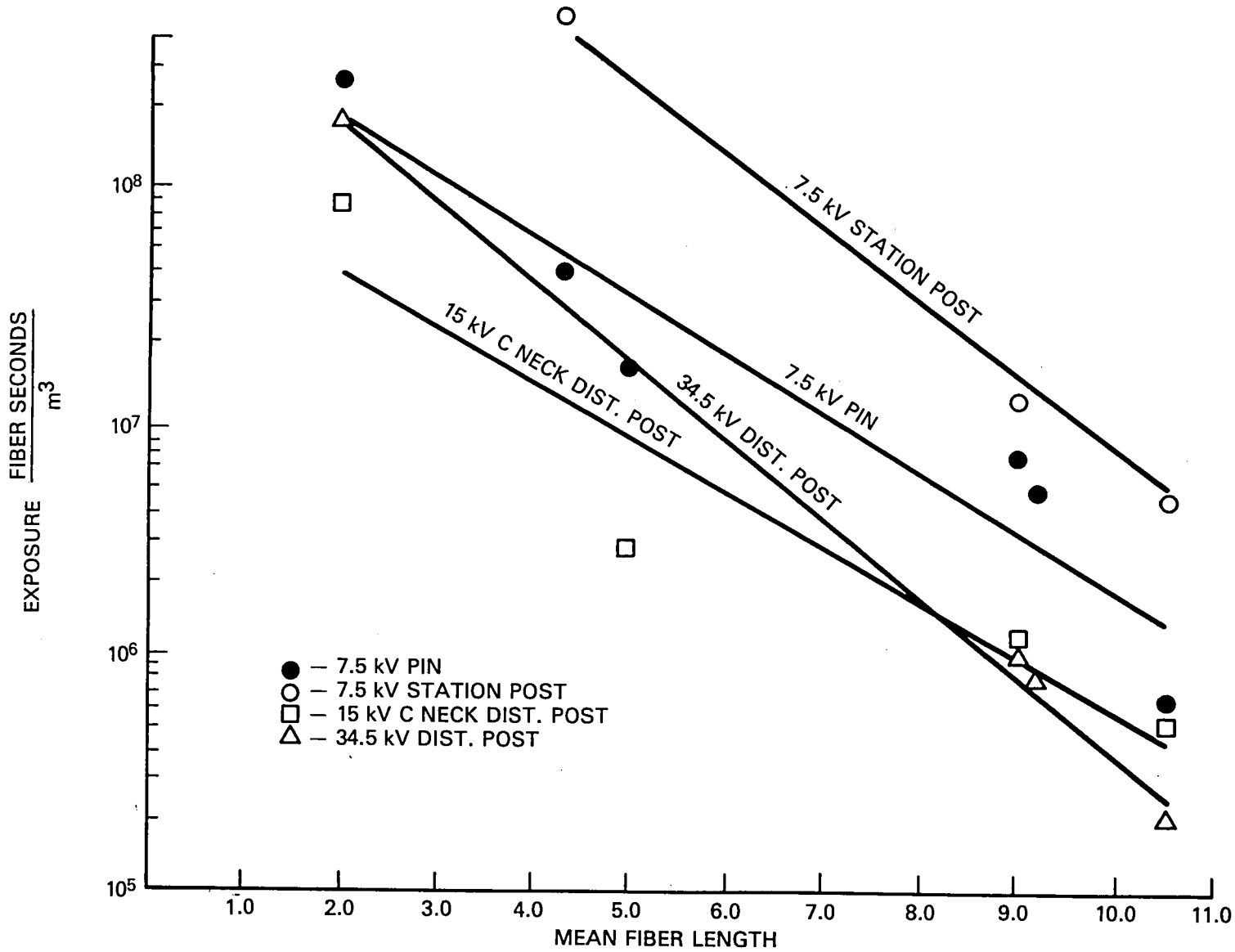

FIGURE A.8 LINEAR INTERGEOLATION OF EXPOSURE TO FIBER LENGTH

TABLE A.11

ESTIMATES OF $\bar{E}$ AT
3 MM FIBER LENGTH

INSULATOR	$\bar{E}$
7.5 KV Pin Insulator (Dry)	1.5×10^8
7.5 KV Pin Insulator (Wet)	3.1×10^7
15 KV C-Neck D. Post Vert.	2.5×10^7
15 KV C-Neck D. Post Vert. (Wet)	2.1×10^7
34.5 KV C-Neck D. Post Vert.	1×10^8
7.5 KV Station Post Vert.	4.4×10^8
7.5 KV Station Post Hor.	1.2×10^9
5 KV Trans. Bushing Vert.	9.5×10^7
15 KV Trans. Bushing Vert.	2.5×10^7
5 KV Trans. Bushing Hor.	5.8×10^7
7.5 KV Suspension Vert.	2.0×10^8

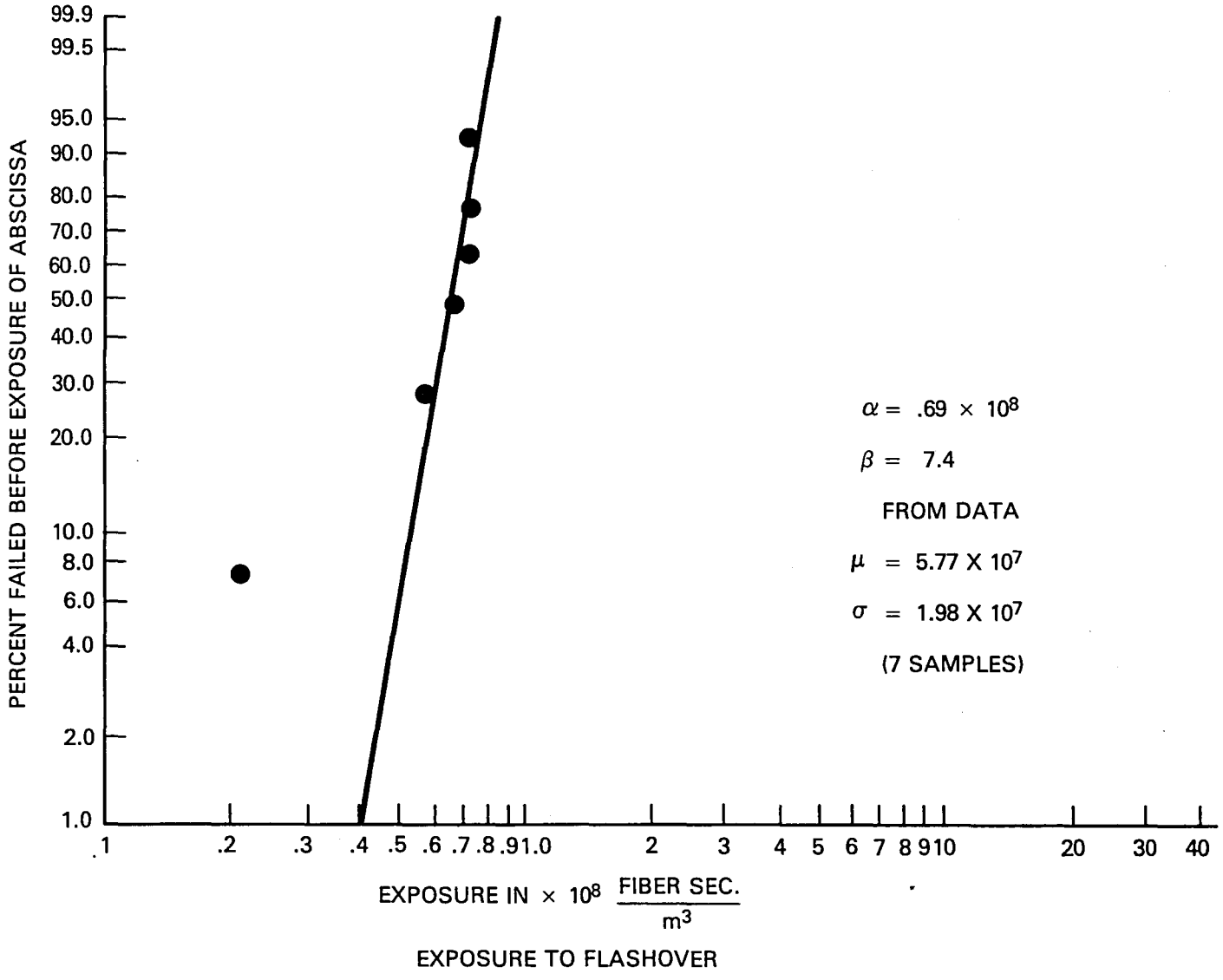

FIGURE A-9. EXPOSURE TO FLASHOVER FOR WET 7.5 kV PIN INSULATOR, 2 mm FIBERS

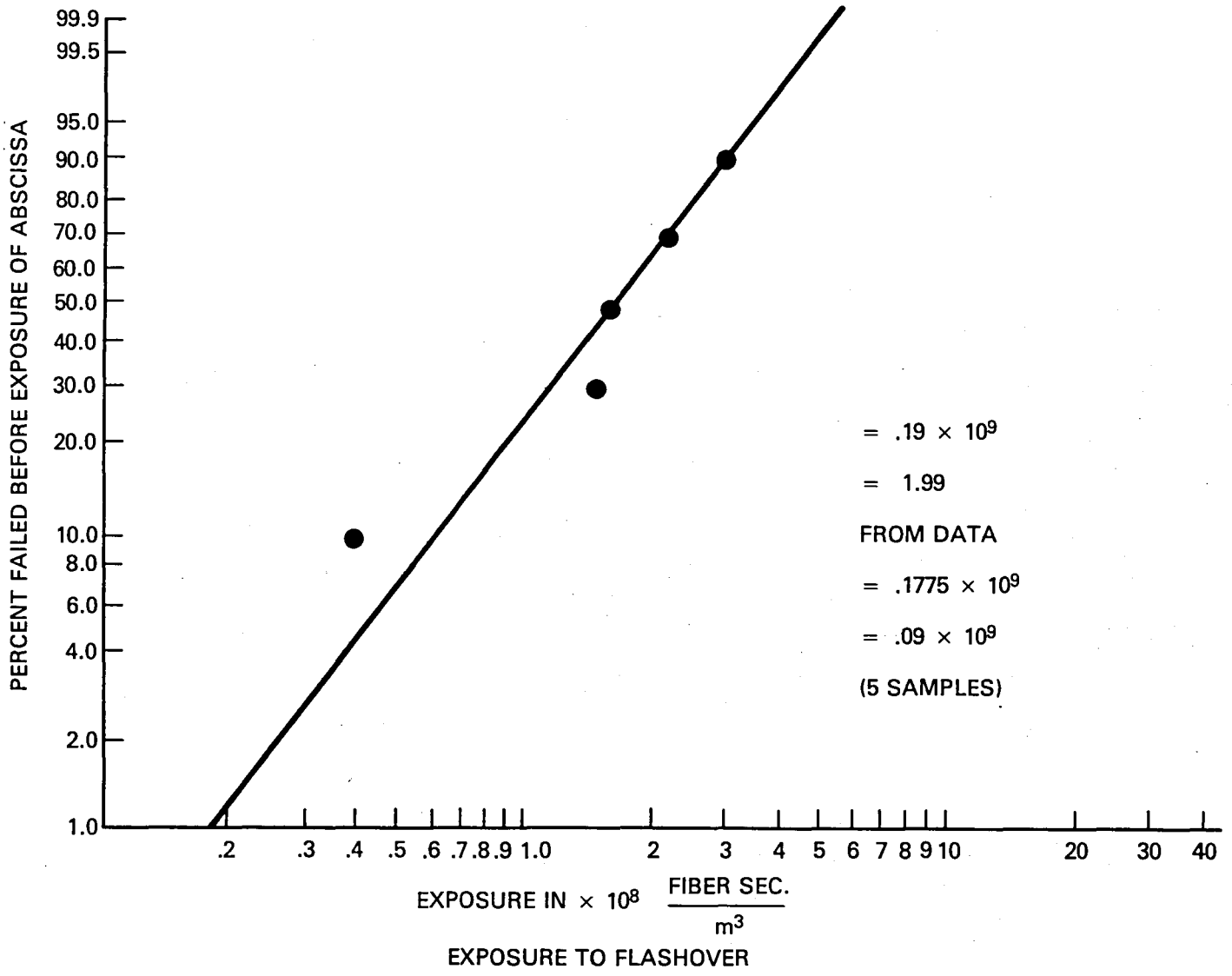

FIGURE A-10. EXPOSURE TO FLASHOVER FOR 34.5 kV DISTRIBUTION POST 2 mm FIBERS

REFERENCES

1. Electrical Transmission and Distribution Reference Book, Westinghouse Electric Company, 1950.

2. Silent Sentinals, Westinghouse Protective Relays, Westinghouse Electric Corporation, 1949.

3. Westinghouse Construction Specifications, Cat. 55-000, 57H Edition, 1978-79.

4. G.E. Power Distribution Course, General Electric Company, 1974.

5. Impacts from a Decrease in Electric Power Service Reliability, Stanford Research Institute, June, 1976.

6. Reliability Information for Electric Utility Transmission and Distribution Systems, Argonne National Laboratory, December, 1978.

7. Preventions of Power Failures, Volume I, Report of the Commission, Federal Power Commission, July, 1967.

8. Staff Report on July 13-14, 1977 Electric System Disturbance on the Consolidated Edison Company of New York, Inc. System, Federal Power Commission, August 4, 1977.

9. Bulk Electric Energy Supply System Outages and Load Restrictions (January 1978 through March 1979), U.S. DOE.

10. Power System Reliability Calculation, Billinton, Ringlee, Wood. MIT Press, 1973.

11. Determination and Analysis of Data for Reliability Studies. A.D. Patton IEEE PAS, 1968, p. 84-100.

APPENDIX B

TOTAL AIRCRAFT ACCIDENT COSTS

APPENDIX B

TOTAL AIRCRAFT ACCIDENT COSTS

ORI utilized a 1978 FAA report[1/] and historical records from the National Transportation Safety Board (NTSB) in determining the costs of major airplane accidents of the past ten years. These costs were used as the basis for a comparison of the additional risks (costs) presented by the use of carbon fibers with the accepted costs associated with major airplane accidents of the recent past.

The ORI costing methodology considered only two items: aircraft hull damage and costs of personal injuries to crew, passengers and persons on the ground. Other costs such as investigative costs, property damage to ground structures, and other incidental costs were not included.

Subsets of the entire NTSB aircraft accident file (1966-1975) were drawn in order to compare carbon fiber related costs to the costs of an appropriate population of past accidents. It was decided that this appropriate population would be those earlier accidents which were on similar scales in terms of aircraft type and accident severity as the future accidents could conceivably result in carbon fiber release. Only accidents which involved U.S. commerical transport jets of significant size were included in the analysis. These aircraft closely approximate the types of planes which will be flying with carbon fibers. All the recorded accidents involved one of the following aircraft:

1/ William L. Fallon, Cost Analysis of Aircraft Accidents, FAA Office of Aviation System Plans, June 1978.

Small Jets (150 passengers)	Medium Jets (150-260 passengers)	Large Jets (260 passengers)
BAC-111	DC-8-61	B-747
B-707	DC-8-62	DC-10
B-720	DC-8-63	L 1011
B-727		
B-737		
DC-8 (non 60's series)		
DC-9		

In addition to aircraft size and type, the severity of the accidents was taken into account. Only those NTSB file entries in which the fuselage had been labelled as being "destroyed" or having "substantial" damage were retained. This strategy was required in order to exclude minor incidents contained in the NTSB file. These less calamitous accidents may be as small as a personal injury caused during strong air turbulence and were excluded so as not to reduce the significance of the individual accidents in which partial or total fuselage destruction occurred. The restrictions these limitations produced reduced the original 1966-1975 file size from 560 accessible commercial aircraft accident files to 155 jet accidents with the proper accident severity levels (16 large jets, 0 medium jets, 149 small jets).

For hull cost computation, the selling price of an identical aircraft in the accident year was culled from printouts documenting the cited FAA study. The original source of this information was publically available records of commercial transactions such as those contained in Aviation Week. No individual consideration was given to special avionics or other equipment. One hundred percent of the replacement cost was assigned to those hulls which were "destroyed"; one third of the ocst was assigned to the substantially damaged aircraft. The FAA developed the one third factor through consultations with NTSB and industry experts.

On the subject of personal injury costs, $300,000 was selected as the the cost of a fatal injury.

The $300,000 was based on the projection of non-Warsaw Pact aircraft accident claims settlements, as reported by the Civil Aeronautics Board. The figure has been endorsed by the Associated Aviation Underwriters, and is

used by the agency (FAA) in its cost benefit work in facility establishment criteria. Serious injury is $45,000 based on actual settlement; minor injury cost is $6,000 based on recognized methodology[2/].

In all cases the injury values and aircraft replacement costs have been converted to 1974 dollars.

The following tables (Table B.1 and B.2) present the results of this analysis by jet size. The word "Significant" in the titles refers to the accident severity being substantial or worse. (Note: There are no accidents in the medium jet category which fit all the requirements.) A few cases with extremely large personal injury costs are seen to dominate the upper range of the total cost figures. These are those truly disastrous accidents in which a large number of deaths takes place.

2/ Fallon, op. cit.

TABLE B.1 SIGNIFICANT 1966-1975 SMALL JET ACCIDENT COST SUMMARY

Cost in Thousands	Number of Cases: Personal Injury Only	Number of Cases: Aircraft Damage Only	Number of Cases: Total Costs
0	73	0	0
1 - 1,000	41	11	10
1,001 - 2,000	4	52	58
2,001 - 3,000	0	43	34
3,001 - 4,000	3	11	6
4,001 - 5,000	0	6	2
5,001 - 6,000	3	4	3
6,001 - 7,000	0	7	3
7,001 - 8,000	1	2	2
8,001 - 9,000	0	0	2
9,001 - 10,000	0	1	0
10,001 - 20,000	5	2	9
20,001 - 30,000	7	0	5
30,001 - 40,000	2	0	4
40,001 - 50,000	0	0	1
Total	139	139	139

Number of Cases - 139

Worst Case (Personal Injury Only) - $34,140,000

Worst Case (Aircraft Damage Only) - $12,000,000

Worst Case (Total) - $40,390,000

Average Case (Personal Injury Only) - $2,546,000

Average Case (Aircraft Damage Only) - $2,550,000

Average Case (Total) - $5,096,000

TABLE B.2 SIGNIFICANT 1966-1975 LARGE JET ACCIDENT COST SUMMARY

Cost in Thousands	Number of Cases: Personal Injury Only	Number of Cases: Aircraft Damage Only	Number of Cases: Total Costs
0	9	0	0
1 - 1,000	6	0	0
1,001 - 2,000	0	0	0
2,001 - 3,000	0	0	0
3,001 - 4,000	0	0	0
4,001 - 5,000	0	0	0
5,001 - 6,000	0	5	5
6,001 - 7,000	0	9	7
7,001 - 8,000	0	0	2
8,001 - 9,000	0	0	0
9,001 - 10,000	0	0	0
10,001 - 20,000	0	1	0
20,001 - 30,000	0	1	1
30,001 - 40,000	1	0	0
40,001 - 50,000	0	0	1
Total	16	16	16

Number of Cases - 16

Worst Case (Personal Injury Only) - $32,502,000

Worst Case (Aircraft Damage Only) - $27,000,000

Worst Case (Total) - $49,002,000

Average Case (Personal Injury Only) $2,149,000

Average Case (Aircraft Damage Only) $8,180,000

Average Case (Total) - $10,329,000

1. Report No.	2. Government Accession No.	3. Recipient's Catalog No.
NASA CR-159210		

4. Title and Subtitle	5. Report Date
Advanced Risk Assessment of the Effects of Graphite Fibers on Electronic and Electric Equipment	February 1980
	6. Performing Organization Code
7. Author(s)	8. Performing Organization Report No.
Leon Pocinki, Merrill Cornell, Lawrence Kaplan	
	10. Work Unit No.
9. Performing Organization Name and Address	
ORI, Inc. 1400 Spring Street Silver Spring, MD 20910	11. Contract or Grant No. NAS1-15379
	13. Type of Report and Period Covered
12. Sponsoring Agency Name and Address	Contractor Report
National Aeronautics and Space Administration Washington, DC 20546	14. Sponsoring Agency Code

15. Supplementary Notes

Langley Technical Monitor: Dr. Wolf Elber
Final Report

16. Abstract

This study was performed to assess the risk associated with accidents involving aircraft with carbon fiber composite structural components. Concern was engendered as the result of evidence that individual fiber segments could cause electrical and electronic equipment to fail under certain operating conditions. The method used to compute the risk is essentially a Monte Carlo simulation model. The principal elements in the scenario that is simulated are: aircraft accident with fire; release of carbon fiber material; entrainment of carbon fibers in a smoke plume; transport of fibers downwind; transfer of some fibers into the interior of buildings; failures of electrical and electronic equipment; economic impact of failures. Risk profiles were prepared for individual airports and the Nation.

Parallel efforts investigated the vulnerability of electrical transmission equipment to carbon fiber incursion and aircraft accident total costs.

17. Key Words (Suggested by Author(s))	18. Distribution Statement
Graphite fibers Risk analysis Commercial aircraft accidents electrical effects	Unclassified - unlimited Subject Category 24

19. Security Classif. (of this report)	20. Security Classif. (of this page)	21. No. of Pages	22. Price*
Unclassified	Unclassified	165	

N-305

For sale by the National Technical Information Service, Springfield, Virginia 22161

NASA Langley Research Center
Attn: Mail Stop 185
Library
Hampton, VA 23665